Shigella Effector IpaH9.8 Interacts with Autophagy Transcription Factor ZKSCAN3 and Increases Autophagy During Infection

by

Kaitlyn Tanner

Submitted in partial fulfilment of the requirements
for the degree of Master of Science

at

Dalhousie University
Halifax, Nova Scotia
December 2014

TABLE OF CONTENTS

LIST OF TABLES

LIST OF FIGURES

ABSTRACT

Shigella spp. cause severe diarrheal disease known as shigellosis and are a major problem is countries where clean water and sanitation are lacking. *Shigella* spp. use a Type 3 Secretion System to deliver effector proteins into the cytosol of infected human cells. My thesis focuses on an effector of *Shigella flexneri*, IpaH9.8, and its role in pathogenesis. IpaH9.8 is a member of a structurally related family of enzymes called the novel E3 ligases (NELs). NEL-domain proteins are E3 ubiquitin ligases that target host proteins to alter their fate. I show that IpaH9.8 ubiquitinates ZKSCAN3, a negative regulator of genes required for autophagy, in a cell free system and induces autophagy *in vitro*. My results are consistent with a model where *S. flexneri* uses IpaH9.8 to induce autophagy resulting in degradation of host proteins to produce free amino acids and down-regulate the activity of immune complexes.

LIST OF ABREVIATIONS USED

ABIN1	A20 Binding and Inhibitor of NF-κB
ATP	adenosine triphosphate
C-terminus	carboxy-terminus
CCL	CC ligand
CD	catalytically dead
cDNA	complementary deoxyribonucleic acid
CFU	Colony forming units
CO2	Carbon dioxide
CXCL	CXC ligand
DH5α	Doung Hanahan Strain 5α
DMEM	Dulbecco's Modified Eagle Medium
DNA	deoxyribonucleic acid
dpi	days post infection
DTT	Dithiothreitol
E	enzyme
E. coli	*Escherichia coli*
EDTA	Ethylenediaminetetraacetic acid
ELISA	Enzyme Linked Immunosorbent Assay
ERK1/2	Extracellular Signal Regulated Kinase 1/2
FBS	Fetal Bovine Serum
GEF	Guanosine nucleotide exchange factor
GLMN	glomulin
GST	Gluathione Synthase Transferase
H2A	histone 2A
H2B	histone 2B
H2O	Water
HCl	Hydrogen Chloride
HECT	Homologous to the E6-AP Carboxyl Terminus
HEK293T	Human embryonic kidney 293T
HeLa	Henrietta Lacks
IBR	inbetween RING
IFNλ	interferon λ
IKKλ	I Kappa B Kinase λ
IL	interleukin
ILK	Integrin-Linked Kinase
IpaH	Invasion plasmid antigen H
IPTG	Isopropyl β-D-1-thiogalactopyranoside
IκBα	Inhibitor of κB type α
K	lysine
LB	Luria Bertani

LC3	light chain 3
LPS	lipopolysaccharide
LRR	leucine rich region
M cell	microfold cell
MAPK	Mitogen Activated Kinase
MAPKK	Mitogen Activated Kinase Kinase
mg	milligram
mL	milliliter
mM	millimolar
MOI	multiplicity of infection
Mxi	membrane excretion protein
N-terminus	Amino-terminus
NDP52	Nuclear Dot Protein 52
NEDD	Neural Precursor Cell Expressed Developmentally Downregulated Gene
NEL	novel E3 ubiquitin ligase
NF-κB	Nuclear Factor κB
NLR	NOD-like receptor
NP40	Nonidet P-40
OD600	optical density 600
Osp	Outer *Shigella* protein
PAMP	Pathogen associated molecular patterns
PBS	Phosphate buffered saline
PCR	polymerase chain reaction
PE	Phosphatidylethanolamine
PEI	Polyethylenimine
pg	picogram
PKC	Protein Kinase C
PMA	Phorbol 12-Myristate 13-Acetate
PMN	polymorphonuclear neutrophil
PRR	Pattern recognition receptors
PSB	Protein Sample Buffer
PVDF	Polyvinylidene Difluoride
qPCR	quantitative Polymerase Chain Reaction
RBR	RING inbetween RING
RCC1	Regulator of chromosomal condensation 1
RING	Really Interesting New Gene
RLD	RCC1-Like Domains
RNA	ribonucleic acid
RPL13A	Riboprotein L13A
RPMI	Roswell Park Memorial Institute
RT PCR	Reverse Transcriptase Polymerase Chain Reaction
S. flexneri	*Shigella flexneri*

SDS-PAGE	Sodium Dodecyl Sulfate Polyacrylamide Gel Electrophoresis
SQSTM1	Sequestosome 1
SspH1	*Salmonella* secreted protein H1
SUMO	Small Ubiquitin-Like Modifier
T3SS	Type 3 Secretion System
TBST	Tris Buffered Saline with Tween
TLR	Toll-like receptor
TNFα	Tumor Necrosis Factor α
TRAF2	TNF Receptor Associated Factor 2
TRAF6	TNF Receptor Associated Factor 6
TSB	Trypticase Soy Broth
U2FA	splicing factor
Ubc13	Ubiquitin Conjugating Enzyme 13
Vir	virulence protein
WIPI2	WD repeat domain phosphoinositide-interacting protein 2
WT	wild-type
YopM	*Yersinia* outer protein M
ZKSCAN3	Zinc Finger with KRAB and SCAN Domains 3
µg	microgram
µL	microliter

ACKNOWLEDGEMENTS

I would like to thank all the members of the Rohde lab for all their support. A special thanks to Angela Daurie who trained me in the mouse model of infection. As well, thanks to Dr. Jeremy Benjamin who performed the yeast two-hybrid experiment that I was able to follow up on. And thanks to Julie Ryu, Saima Sidik, Ameer Jarrar and Jeremy for all their hard work on the *S. flexneri* deletion collection, which provided me with my first *ipaH* knockout strain.

Thanks to Dr. Denys Khaperskyy for his help in all things qPCR-related. Thanks to Dr. Craig McCormick and all his help in providing me with the virus for retroviral transduction of HEK293T cells. As well I want to thank him for his help with luciferase and providing me with the pGL4.26 vector. Also thanks to Ben Johnson who provided me with the lentiviral transduction vectors. Thank you to Naoko Onodera for creation of the phylogenetic tree of the IpaH family shown in Figure 3. Thanks to Dr. Jost Enninga and his lab at the Pasteur Institute for providing me with the opportunity to work and learn in their lab for a week. Thank you to my committee members, Drs. Jim Fawcett and Roy Duncan, who have provided me with valuable insight into my experiments and helped to foster new ideas in my research. Thanks to Dr. Karen Bedard for all her help with the proper statistical analysis of my results.

A huge thanks to my supervisor, Dr. John Rohde. You have helped push me to be a better student and scientist, as well as providing great system of support and enthusiasm through this whole experience.

Lastly, I would like to thank my parents, family and fiancé for all their support and advice through my journey as a Master's student.

CHAPTER 1: INTRODUCTION

S. flexneri is a devastating gastrointestinal pathogen that causes severe diarrhea. *S. flexneri* use a Type 3 Secretion System to deliver "effector" proteins into the cytosol of infected human cells. The most abundant class of effectors is a family of closely related proteins, the invasion plasmid antigen Hs (IpaHs). IpaHs are E3 ubiquitin ligases that hijack the eukaryotic ubiquitin system. The goal of this thesis was to characterize putative substrates of the IpaHs and to determine the role of IpaHs during infection.

1.1: The Ubiquitin System, a eukaryotic-specific post-translational modification

Post-translational modifications are used to alter a protein's fate. The covalent attachment of molecules to a protein may alter its localization, stability, activity, or other aspects of the protein. In prokaryotes, most post-translational modifications are restricted to small molecules such as phosphorylation or methylation. In eukaryotes, post-translational modifications include the attachment of small proteins such as ubiquitin or ubiquitin-like modifiers such as SUMO or NEDD. Ubiquitination is largely associated with protein degradation, however there are many different regulatory roles of ubiquitin in addition to protein turnover. The addition of one or many ubiquitin moieties can regulate the cell cycle, protein expression and vesicular transport. The focus of my thesis research is on the post-translational modification ubiquitination and its ability to alter the fate of eukaryotic proteins during infection by *Shigella*.

1.1.1: E1s, E2s, and E3s: The Steps of Ubiquitination

There are three main Enzyme (E) types in the ubiquitin system: E1, ubiquitin activating enzymes; E2, ubiquitin conjugating enzymes; and E3, ubiquitin ligases (Huibregtse *et al.*, 2014). The first step in ubiquitination is the activation step where the E1 binds to glycine at the C-terminus of ubiquitin through an ATP-dependent hydrolysis reaction. In the second step the E1 transfers the ubiquitin to the E2. There are ~40 E2s expressed in eukaryotic cells. The charged E2 then interacts with one out of the hundreds of E3s expressed (Huibregtse *et al.*, 2014). In eukaryotes there are two classes of E3s, HECT-domain and RING-domain E3s, and each transfer ubiquitin from the E2 to the substrate in different manners. HECT E3s transfer the ubiquitin from the E2 to itself and act as catalytic intermediates that transfer ubiquitin to the substrate. By contrast, RING E3s interact with charged E2s, bringing it into close proximity with the substrate, where it facilitates the transfer of the ubiquitin from the E2 directly to the substrate without a catalytic intermediate (Hershko *et al.*, 1998).

1.1.2: HECT-Domain E3s

The HECT (homologous to the E6-AP carboxyl terminus) domain E3 family was discovered when proteins from rat and yeast were observed to share sequence similarity with an approximately 350 amino acid region in E6-AP from human papillomavirus (Huibregtse *et al.*, 1995). These eukaryotic proteins were shown to form thioester bonds with ubiquitin using a conserved cysteine residue within the last 32-34 amino acids at the C-terminus. Crystal structure studies revealed that HECT E3s have a bilobal conformation, where the N-terminal lobe binds to the E2, and the C-terminal lobe is

where the active site is located (Huang *et al.*, 1999). Structural analysis suggests that the hinge region connecting the two lobes is flexible and allows the lobes to come in close enough contact for ubiquitin transfer (Metzger *et al.*, 2012). In regards to the N-terminal domain, HECT family members can be classified into three groups: Nedd4, HERC and "others". Nedd4 (neural precursor cell-expressed developmentally downregulated gene 4) family members contain an N-terminal C2 domain, two to four WW domains and then the C-terminal HECT domain (Rotin *et al.*, 2009). Phylogenetic analysis of Nedd4 family members has suggested it is likely that Nedd4 is the ancestral member of the family (Yang *et al.*, 2010). The C2 domain is responsible for localization to the plasma membrane and vesicular organelles. The WW domains are able to bind PY motifs, therefore it is suggested that this is required for substrate binding. The protein structure of these family members is highly conserved across all eukaryotes, with the most striking differences being the number of WW domains (Ingham *et al.*, 2004, Yang *et al.*, 2010, Donovan *et al.*, 2013). HERC family members have regulator of chromosome condensation 1 (RCC1)-like domains (RLDs) as well as the HECT domain. RLDs can bind chromatin and guanine nucleotide-exchange factor (GEF). The "others" consists of various different domains and characteristics for protein-protein interactions (Rotin *et al.*, 2009).

1.1.3: RING-Domain E3s

Really interesting new gene (RING)-domain E3 ligases are the second class of ubiquitin ligases. The RING-domain is 40-60 amino acids in length that has a series of cysteine and histidine residues to form a cross-brace structure with two zinc ions (Lorick

et al., 1999). In contrast to HECT domain E3s, RING domains do not form thioester bonds with ubiquitin and instead function as a scaffolding protein, bringing the E2~ubiquitin conjugates in close contact to the substrate (Ozkan *et al.*, 2005). The RING domain is the site for E2~ubiquitin conjugate binding, and once bound to the RING E3, the thioester bond between the E2 and ubiquitin is vulnerable to nucleophilic attack by an amino group (usually a lysine), facilitating transfer to the substrate (Das *et al.*, 2009, Das *et al.*, 2013). While HECT E3s are always a single protein, it is not uncommon for RING ligases to be composed of multimeric and multi-subunit complexes (Tyers *et al.*, 2000). One of the most studied classes of multi-subunit RING complexes are the cullin RING ligases (CRL), consisting of a cullin protein, a small RING protein and an adaptor protein that can recognize substrates and binds to cullins and substrates (Metzger *et al.*, 2014). Multi-subunit E3s allow for increased substrate specificity as subunits can be interchangeable to meet requirements for substrate binding. In some cases, there can be multiple RING E3s within a single complex or even two RING domains within a single protein. The class known as RING 'in between RING' (IBR) RING (RBR) proteins have a first RING domain (RING1), followed by an IBR region that is cysteine rich and then lastly a second RING-like domain (RING2). Interestingly, this class has been suggested to exhibit a RING-HECT hybrid mechanism for E3 activity due to the presence of an E3~ubiquitin intermediate (Metzger *et al.*, 2014).

1.1.4: Functions of Ubiquitination

Ubiquitination dictates protein fate in a variety of ways. Single molecules of ubiquitin may be attached to a protein (monoubiquitination). In many cases the attached

ubiquitin molecule becomes a substrate for additional ubiquitin molecules that are attached to one of 7 lysine residues present on ubiquitin (polyubiquitination). Monoubiquitination is best understood as playing a role in the localization of proteins within a cell (Ramanathan *et al.*, 2012). In recent years monoubiquitination of histones has been shown to regulate their ability to form nucleosomes (Cole *et al.*, 2014). In a handful of cases, monoubiquitination of transcription factors has been demonstrated to affect their ability to function (Schnell *et al.*, 2003, van der Horst *et al.*, 2006, Ouni *et al.*, 2011, Hochrainer *et al.*, 2012). Polyubiquitination can occur in different "flavors" as well, the ubiquitin chains can be built upon specific lysine residues to dictate certain responses. The most well characterized chain is formed on lysine 48 (K48) of ubiquitin. K48-linkages on a protein usually result in targeting the protein for degradation via the proteasome complex (Xu *et al.*, 2009). The ubiquitin-proteasome system (UPS) plays a critical role in regulation of cell cycle, apoptosis, inflammation, signal transduction, transcription and protein quality control. The proteasome is composed of two major units, the regulatory particle, responsible for the recognition of ubiquitinated proteins, and the core particle, responsible for the proteolytic cleavage of recognized proteins (Finley, 2009). Other chain types include: K6, K11, K27, K29, K33 and K63. K63 linkages serve a scaffolding function and can nucleate protein interactions, particularly in immune signaling cascades (Behrends *et al.*, 2011, Chen, 2012).

1.2: Epidemiology and Pathogenesis of *Shigella*

1.2.1: *Shigella* species

The genus *Shigella* is a member of the *Enterobaceriaceae* family, characterized by rod-shaped bacteria and Gram negative staining. The *Shigella* genus is further divided into four species, *Shigella flexneri, Shigella boydii, Shigella dysenteriae*, and *Shigella sonnei*. These four species are further divided into different serotypes based on biochemical differences and O-antigen variations (WHO, 2005).

Shigellosis is a disease characterized by severe diarrhea, abdominal pain and cramping, fever and presence of blood in the stool. *Shigella* is transmitted through the fecal-oral route and is more prevalent in areas where clean water and proper sanitation infrastructure is lacking. In addition, *Shigella* species only require 10 bacteria to effectively cause infection, allowing for rapid transmission. *Shigella* species invade the colonic epithelium and cause extensive inflammation and tissue damage in the mucosa. A 1999 landmark study by the World Health Organization concluded that there were 164.7 million recorded cases of *Shigella* infections, with 69% of the cases in children less than 5 years of age (Kotloff *et al.*, 1999, WHO, 2005). In the Guidelines for the Control of Shigellosis by the World Health Organization, they state that *Shigella* has acquired widespread resistance to ampicillin, co-trimoxazole and nalidixic acid and these frontline antibiotics are no longer effective treatment options (WHO, 2005). The continued high incidence of shigellosis, coupled with increasing antimicrobial resistance, has lead to a global initiative for development of a vaccine against *Shigella* as effective antimicrobial treatment regimes decrease. A more recent study, that made use of molecular techniques and surveyed the incidence of shigellosis on the Asian subcontinent, found that while

mortality rates associated with shigellosis are declining, the burden of the disease has not subsided (von Seidlein *et al.*, 2006). They suggest that the decrease in mortality is due to the economic boost in emerging Asian countries, resulting is less malnutrition and increased availability of primary care institutions and the easy access to antibiotic regimens.

Shigella dysenteriae causes the most severe disease. Unlike the other species of *Shigella*, it produces the extremely potent Shiga toxin. Shiga toxin is a classical "AB" toxin that ribosylates host proteins and halts translation (Bergan *et al.*, 2012). In comparison to the other species, the illness associated with *S. dysenteriae* is prolonged and has a higher mortality rate (WHO, 2005). Lastly, there are higher incidences of regional epidemics of *S. dysenteriae* (WHO, 2005).

By contrast to *S. dysenteriae*, *S. sonnei* and *S. boydii* both cause relatively mild disease states. In recent years, *S. sonnei* prevalence has increased, especially within industrialized countries and is commonly reported as traveller's diarrhea (WHO, 2005). As well, many cases have been reported in daycares in the USA, consistent with children under 5 as the predominant age niche for *Shigella* infection (WHO, 2005). By contrast, *S. boydii* is less common worldwide and is associated with shigellosis in India (Levine *et al.*, 2007).

S. flexneri causes a more severe disease phenotype than *S. sonnei* and *S. boydii,* but is not as virulent as *S. dysenteriae.* It has the highest prevalence worldwide of all *Shigella* species (WHO, 2005, Levine *et al.*, 2007). Due to its high prevalence and more severe illness, it is the most commonly studied *Shigella* species in laboratories and is the

species that my research has focused on. Hereafter in my thesis *S. flexneri* will be referred to as simply "*Shigella*".

1.2.2: *Shigella* Route of Infection

Shigella is transmitted through the fecal-oral route and enters the body through contaminated food or water. Ingested bacteria pass through the gastrointestinal tract until they reach the colon (Schroeder *et al.*, 2008). The intestinal epithelial layer exists to act as a barrier from invading pathogens. To breach this barrier, *Shigella* uses M cells to facilitate its transcytosis across the epithelial layer. M cells, also known as microfold cells, are specialized epithelial cells that populate the intestine in small amounts. Their function is to sample the intestinal environment and transport suspicious materials to antigen-presenting cells, such as dendritic cells (Kraehenbuhl *et al.*, 2000). Once they have transversed through this barrier, *Shigella* are phagocytosed by macrophages and dendritic cells (Mounier *et al.*, 1992). Once inside epithelial cells *Shigella* hijack actin for their own specialized actin-based motility to move laterally through the epithelial layer (Bernardini *et al.*, 1989). Therefore, *Shigella* can spread cell-to-cell with minimal contact with extracellular space, minimizing contact with dangerous specialized immune cells.

While *Shigella* can effectively evade immune cells by hiding in epithelial cells, this does not prevent a large inflammatory response. Infection of macrophages results in induction of apoptosis, coupled with the production of interleukin-1 β (IL-1 β) and interleukin (IL-18). IL-18 can activate natural killer (NK) cells and further stimulates an immune response (Girardin *et al.*, 2003). Additionally, Nod1 pathways within epithelial cells can detect intracellular bacterial peptidoglycan from *Shigella,* leading to NF-κB

activation and subsequent expression and release of IL-8. IL-8 helps inflammation by recruiting polymorphonuclear neutrophil leukocytes (PMN) to the infection site (Girardin *et al.*, 2003). PMN must infiltrate through the epithelial cell barrier to reach the infection site, therefore creating holes for luminal bacteria to gain entry to epithelial cells. Through this, *Shigella* balances a unique combination of inflammation and immune evasion to create an ideal environment for infection.

1.2.3: *Shigella* Virulence

Shigella virulence is mediated by a ~200 kb plasmid (Sansonetti *et al.*, 1981). Known as the virulence plasmid, it encodes the proteins necessary for assembly of a Type 3 Secretion System (T3SS) (Menard *et al.*, 1996). The T3SS is composed of needle, basal body and C-ring components and is anchored in the inner and outer membranes of the bacterium, as shown in Figure 1 (Blocker *et al.*, 2001). The T3SS is widely conserved among *Shigella* species, as well as between other gram-negative bacteria such as *Salmonella* species and *Escherichia coli* (Hueck *et al*., 1995). The apparatus itself is composed of over 20 different proteins (Marlovits *et al.*, 2010). The C-ring, or base of the structure, is within the cytoplasm of the bacterium and consists of Spa33 and Spa47 (Morita-Ishihara *et al.*, 2006). Together, these "base components" function to regulate and sort the order by which effectors are transferred through the apparatus (Morita-Ishihara *et al.*, 2006, Johnson *et al.*, 2008). The basal body is composed of MxiG, MxiJ, MxiD, and MxiM and this structure spans the inner and outer membranes of the bacterium (Abrusci *et al.*, 2013). Lastly, the needle structure is made of MxiH, MxiI and capped with IpaD, IpaB and IpaC. The T3SS function is to facilitate the delivery of

bacterial proteins into the cytoplasm of a target cell. The bacterial proteins translocated through the T3SS are known as "effectors" and serve many different functions in the context of *Shigella* infection. There are two waves of effectors that pass through the T3SS, each wave targeting different aspects of the host machinery for *Shigella* survival (Parsot, 2009).

The first wave of effectors is encoded on genes found with the "entry region" of the virulence plasmid. These genes are under the transcriptional control of factors VirF and VirB and are regulated via temperature, which activate at 37°C (Phalipon *et al.*, 2007). The function of the first wave of effectors is to promote bacterial entry. These proteins are expressed prior to T3SS assembly and are associated with chaperone proteins until the apparatus is activated. Upon activation of the T3SS, IpaB and IpaC are transported into the host cell and initiate actin remodeling of the host cytoskeleton to promote the internalization of bacteria. Additional first wave effectors include: IpaA, IpgB1, IpgB2, IpgD, OspB, OspF and IcsB (Niebuhr *et al.*, 2000, Ogawa *et al.*, 2005, Parsot, 2009, Zurawski *et al.*, 2009). These effectors orchestrate actin cytoskeleton rearrangement, invasion and some immune signaling regulation. Concurrently, the chaperone IpgC formerly bound to IpaB and IpaC interacts with an AraC class transcriptional activator, MxiE, to initialize the transcription of second wave effectors (Mavris *et al.*, 2002a).

The second wave of effectors is under the control of transcription factor MxiE (Mavris *et al.*, 2002b). These effectors mainly contribute to *S. flexneri* virulence by subverting the host immune response, thereby promoting the survival and propagation of the bacteria (Kim *et al.*, 2005). Included in these effectors are OspG, OspD3, OspE1,

OspE2 and the IpaH family, which is the focus of this thesis (Phalipon *et al.*, 2007, Parsot, 2009). Many of these proteins and their functions will be further discussed in Sections 1.4 and 1.5.

1.3: Animal Models of *Shigella* Infection

Shigella species are exclusively human pathogens, which makes studying *Shigella* in an animal model difficult. There are many options available to study *Shigella in vivo*, however there is no perfect choice and the model must best fit the experiment at hand. The most widely used animal models include: rabbit ileal loop model (Schnupf *et al.*, 2012), macaque model (Kent *et al.*, 1967), Sereny test (keratoconjunctival test) (Bals *et al.*, 1961), and a variety of mouse models (pulmonary model, an oral streptomycin model, and a subcutaneous SCID-Human xenograph) (Philpott *et al.*, 2000, Zhang *et al.*, 2001, Martino *et al.*, 2005, Marteyn *et al.*, 2012). New models, such as the guinea pig intracolonic model, piglet model and the zebra fish model have recently been developed (Shim *et al.*, 2007, Jeong *et al.*, 2013, Mostowy *et al.*, 2013). Each model presents its own benefits, as well as its own specific set of challenges to account for.

The rabbit ileal loop model of infection is technically demanding. It requires highly trained individuals with great attention to detail to perform surgery on the rabbits, creating looped regions of the colon for infection (Perdomo *et al.*, 1994). It is only used for short-term infections (up to 8 hr) due to ethical issues regarding not feeding the animals (Philpott *et al.*, 2000). This model was used to confirm the site of entry of *Shigella* because loops that consisted of more Peyer's patches (where M cells associate) exhibited 3-fold more bacteria within the infected tissues (Perdomo *et al.*, 1994).

The macaque monkey model of infection portrays the most accurate depiction of shigellosis, as the primates are infected intragastrically (Fontaine *et al.*, 1988, Sansonetti *et al.*, 1991). This results in a disease similar to that observed in humans. Due to monetary and ethical constraints, this model is not used often.

The ideal model for *Shigella* infection would be in mice. Mice are cost effective, easily housed and maintained and experiments can be easily repeated. Many mouse models have been established, the most widely used being the pulmonary model. The pulmonary model dates back to the 1960s and was first described by Voino-Yasenetsky and Voino-Yasenetskaya (1962). Mice are challenged intranasally with *S. flexneri* and exhibit high mortality rates by 6 days post-infection (Voino-Yasenetsky *et al.*, 1962, van de Verg *et al.*, 1995, Fisher *et al.*, 2014). This model provided a unique tool for studying host-pathogen interactions of *Shigella.* It should be noted that the respiratory and gastrointestinal tracts are composed of different cell types and different organs and because of this, the immune response elicited with in area can vary dramatically (Phalipon *et al.,* 2007). A relatively new model that has recently been gaining in popularity and that is used within the Rohde lab is the streptomycin mouse model. The streptomycin model, as described in Martino *et al.* (2005), relies on *Shigella* colonization of the mouse colon through oral dosage of bacteria at 1 x 10^8 cfu (Martino *et al.*, 2005). As the name suggests, mice are treated with streptomycin prior to exposure to a streptomycin-resistant strain of *Shigella* in order to clear the natural gut microbiota to provide a better environment for *Shigella* colonization. While there are visible signs of illness in the mice and the presence of *Shigella* within the cecum and colon of the mice, notably absent is the recruitment of PMN leukocytes (Martino *et al.*, 2005). So while the

model has imperfections, it is still a useful tool for assessing *Shigella*-host interactions and examining pathogenesis.

1.4: *S. flexneri* Effectors and Host Modifications

As discussed previously, *Shigella* possesses a virulence plasmid encoding proteins involved in the T3SS. The effectors of the T3SS play various roles in pathogenesis, from invasion and actin-remodeling to immune evasion and regulation of the host immune response. Effectors are able to disrupt host signaling programs, most notably NF-κB by various mechanisms (as illustrated in Figure 2). By elucidating the roles effectors play during *Shigella* infection we can learn more about its pathogenesis and provide further insight into host immune responses.

1.4.1: OspI

Shigella effector OspI dampens the host immune response by suppressing the signaling cascade associated with tumor-necrosis factor (TNF)-receptor-associated factor 6 (TRAF6). OspI is a deamidase responsible for the deamidation of glutamine at position 100 of Ubc13 to glutamic acid, completely negating its function (Sanada *et al.*, 2012). Ubc13 is an E3 ubiquitin ligase and is involved in the NF-κB signaling cascade. Under normal stimulated conditions, Ubc13 would ubiquitinate TRAF6 initiating a cascade of events leading to NF-κB activation. However, when deamidated, Ubc13 is unable to ubiquitinate TRAF6 efficiently, decreasing NF-κB activation, thus dampening the immune response. The downstream effects are clearly outlined in Figure 2.

1.4.2: OspG

OspG is another effector of the *S. flexneri* T3SS and it also interferes with the activation of NF-κB. OspG is a kinase that can bind to E2 ubiquitin-conjugating enzymes to increase activity and stability (Kim *et al.*, 2005, Grishin *et al.*, 2014, Pruneda *et al.*, 2014). OspG was found to interact with multiple E2 enzymes, including those that play a role in the ubiquitination of phosphorylated inhibitor of NF-κB type α (p-IκBα), and subsequently dampens NF-κB activation (Figure 2) (Kim *et al.*, 2005). Additionally, in animal models *ospG* mutants appear to elicit stronger immune responses than wild-type strains in both rabbits and mice (Kim *et al.*, 2005, Pruneda *et al.*, 2014). In an oral mouse model of infection 30% mortality is observed with *ospG* mutant infection while no mice succumb to infection using wild-type *Shigella* (Pruneda *et al.*, 2014). Taken together these data demonstrate a role for OspG in dampening the immune response.

1.4.3: OspF

OspF is an effector from the second wave delivered into host cells by *Shigella* T3SS. Once translocated through the T3SS apparatus, it is localized in the host cytoplasm and nucleus (Zurawski *et al.*, 2006). Infections with *ospF, ospB,* and *ospC1* mutants revealed decreased recruitment of PMN leukocytes in tissues and in the PMN cell migration assay (Zurawski *et al.*, 2006, Li *et al.*, 2007, Zurawski *et al.*, 2009). OspF, OspB, and OspC1 were found to interfere with mitogen-activated protein kinase kinase (MAPKK) and extracellular signal-regulated kinase 1/2 (ERK1/2) pathways (Zurawski *et al.*, 2006, Li *et al.*, 2007, Zurawski *et al.*, 2009). The presence of OspF was associated with dephosphorylated MAPKs, which lead to decreased NF-κB response (Li *et al.*,

2007). It was further resolved that OspF acts as a phosphothreonine lyase and impairs HP1-λ (histone protein) function, thus decreasing transcriptional activation at immune genes and inactivating ERK signaling (Li *et al.*, 2007). Additional studies revealed that retinoblastoma protein (Rb) is an interacting partner for OspF and OspB. This suggests a combined role of these effectors in regulating inflammation through interactions with Rb, possibly through chromatin modifications (Zurawski *et al.*, 2009). OspF has also been shown to be required for rapid killing of dendritic cells upon *Shigella* infection (Kim *et al.*, 2008).

1.4.5: OspE

Shigella effector OspE, composed of two nearly identical proteins, OspE1 and OspE2, is involved in protein kinase C (PKC) activation and regulating focal adhesions in infected cells (Kim *et al.*, 2009, Yi *et al.*, 2014). Kim and coworkers found that OspE stabilizes infected host cell adherence to the basement membrane (Kim *et al.*, 2009). OspE interacts with integrin-linked kinase (ILK) which results in increased levels of β1-integrin on the cell surface, as well as decreased phosphorylation of focal adhesion-associated proteins involved in cell mobility (Kim *et al.*, 2009). It also contains a PDZ-binding domain that is commonly found in protein interactions and an additional protein interaction was discovered between the PDZ domain of OspE and PDLIM7 (Yi *et al.*, 2014). PDLIM7 is associated with PKC activation and when OspE is absent from *S. flexneri* infection, PKC activation is dampened (Yi *et al.*, 2014).

1.5: IpaHs (NELs)

1.5.1: IpaH Family of Effectors

The IpaHs are encoded on both the virulence plasmid and chromosome of *S. flexneri* and are secreted through the T3SS (Toyotome *et al.*, 2001, Ashida *et al.*, 2007). The family consists of 12 closely related proteins that are composed of a highly conserved novel E3 ubiquitin ligase (NEL) domain and a leucine-rich repeat (LRR) (Rohde *et al.*, 2007). A phylogenetic tree in Figure 3 illustrates the relatedness of all 12 *Shigella* IpaHs. All NEL domain proteins possess E3 ubiquitin ligase activity, which is particularly interesting as bacteria lack the ubiquitin system (Huibregtse and Rohde 2014). Even more intriguing is the fact that IpaH proteins do not share any sequence or structural homology to eukaryotic E3 ubiquitin ligases (Rohde *et al.*, 2007, Singer *et al.*, 2008, Zhu *et al.*, 2008, Quezada *et al.*, 2009).

The IpaHs consist of a catalytic NEL region on the C-terminal end and a LRR domain on the N-terminal end. The catalytic NEL domain is composed of 12 -helices and within lies a catalytic cysteine residue responsible for the ubiquitin ligase activity (Rohde *et al.*, 2007). The cysteine residue forms a thioester bond with ubiquitin, creating a catalytic intermediate, suggesting similarities to HECT-like E3s which also form a ubiquitin bound intermediate (Figure 4) (Huibregtse *et al.*, 1995, Singer *et al.*, 2008, Zhu *et al.*, 2008). The mutation of this cysteine abolishes the ubiquitin ligase activity of the IpaHs (Rohde *et al.*, 2007, Singer *et al.*, 2008, Zhu *et al.*, 2008). An essential aspartic acid resides near the cysteine. The aspartic acid residue was shown to be important in the transfer of ubiquitin to substrates by Zhu *et al.* (Zhu *et al.*, 2008). Mutation at this residue

results in the formation of a thioester bond between ubiquitin and the E3 but is deficient in ubiquitin complete transfer to substrates (Zhu *et al.*, 2008).

The LRR region has seven repeats of a 21 amino acid long sequence that contains five conserved leucines and an additional two LRR with varying leucine patterns. The LRR has no effect on autocatalytic activity of the IpaH proteins *in vitro* to polymerize ubiquitin, however, *ipaH9.8* mutant lacking the LRR domain cannot polyubiquitinate Ste7, a substrate identified by in yeast (Rohde *et al.*, 2007). Furthermore, when the LRR domains of IpaH9.8 and SspH2 (IpaH family member from *S.enterica*) were exchanged, it revealed that the LRR domain mediates substrate recognition (Haraga *et al.*, 2006). In addition to mediating recognition of substrates, the LRR domain is also important in autoinhibition of IpaHs (Figure 4) (Chou *et al.*, 2012). The autoregulatory activity of the NEL enzymes is thought to down regulate catalytic activity to help bacteria evade host detection, as the presence of untethered ubiquitin chains elicits an immune response (Xia *et al.*, 2009). Currently, only one example of NEL-substrate interaction has been fully identified. Keszei *et al.* observed the substrate, PKN1, interacts with the LRR of SspH1, interrupting the LRR-NEL interaction and promoting E3 ligase activity (Keszei *et al.*, 2014).

1.5.2: IpaH9.8

The structures and activity of the IpaHs have been well defined, while the identification of substrates has not. A major goal of the Rohde lab has been to identify the substrates of these enzymes and specifically IpaH9.8. In a report by Okuda *et al.*, U2AF, a splicing factor, was the first potential substrate for IpaH9.8 (Okuda *et al.*, 2005). They showed a

decrease in expression of mRNAs of inflammation-associated genes in HeLa cells infected with wild-type *S. flexneri*, thus a putative role for IpaH9.8 in mediating the immune response. Years later, two additional substrates were identified: MAPKK Ste7, which was targeted for ubiquitination and degradation in a *Saccharomyces cerevisae* surrogate system; and NEMO/IKK λ, which was identified using yeast-two hybrid screening (Rohde *et al.*, 2007, Ashida *et al.*, 2010). IpaH9.8 was shown to attenuate NF-κB immune response via polyubiquitination and destruction of NEMO in an ABIN-1-dependent fashion (Figure 2) (Ashida *et al.*, 2010). There are likely many more additional substrates for IpaH9.8 yet to be determined.

1.5.3: IpaH7.8

The first IpaH effector to be implicated in virulence was IpaH7.8 (Fernandez-Prada *et al.*, 2000). A mutant *ipaH7.8 S. flexneri* strain has a strong phenotype associated with infection of monocytic and macrophage cultured cells. During infection and treatment with chloroquine, *ipaH7.8* mutant strain has a large build-up of bacteria within endocytic vacuoles, suggesting that IpaH7.8 facilitates vacuolar escape in monocytes and macrophages (Fernandez-Prada *et al.*, 2000). More recently, a target for IpaH7.8 has been identified. Glomulin (GLMN), a Cullin ring ligase inhibitor, was identified through yeast-two hybrid experiments as an interacting partner of IpaH7.8 (Suzuki *et al.*, 2014b). They found that *S. flexneri*-induced macrophage cell death occurs in an IpaH7.8-dependent manner and that this is due to decreased levels of GLMN activating inflammasome formation (Suzuki *et al.*, 2014b).

1.5.4: IpaH4.5

IpaH4.5 is encoded on the *S. flexneri* virulence plasmid in the MxiE regulon (Bongrand *et al.*, 2012). In *S. flexneri* strains with mutant *ipaH4.5*, murine lung infection results in a stronger immune response with high levels of proinflammatory cytokine production (Wang *et al.*, 2013). Additionally, bacterial colonization of the mutant strain compared to wild-type was greatly decreased. To investigate the cause of these phenotypes, Wang *et al.* performed a yeast-two hybrid screen and identified the p65 subunit of NF-κB as an interactor (Wang *et al.*, 2013). *In vitro* luciferase assays revealed that interactions between IpaH4.5 and p65 results in dampened NF-κB response (Figure 2) (Wang *et al.*, 2013).

1.5.5: IpaH0722

As with other IpaHs, IpaH0722 is regulated by MxiE and is delivered through the T3SS, despite being encoded on the bacterial chromosome (Ashida *et al.*, 2007). Like IpaH4.5 and IpaH9.8, IpaH0722 also interferes with the NF-κB signaling pathway. Screening chromosomal *ipaH* mutants for NF-κB activity revealed that presence of IpaH0722 was crucial in the inhibition of NF-κB (Ashida *et al.*, 2013). There are many diverse pathways that converge to activate NF-κB, so to provide a clear mechanism by which IpaH0722 acts cells were treated with various stimuli to decipher which induction pathway is inhibited. Ashida and coworkers observed specific decrease in activity of NF-κB from the protein kinase C (PKC) induction pathway and further deduced that IpaH0722 inhibits TRAF2 through ubiquitination and proteasomal degradation (Figure 2).

1.5.6: Non-*S. flexneri* NELs

NELs are not specific to *S. flexneri*; homologs exist in other bacteria and include SspH1 and SspH2 from *S. enterica* (Haraga *et al.*, 2006, Rohde *et al.*, 2007). Like many other T3SS effectors, the search for substrates of *S. enterica*'s SspH1 began with a yeast-two hybrid screen. This revealed that PKN1, a serine/threonine protein kinase, interacts with SspH1 and was further confirmed with co-immunoprecipitation studies (Haraga *et al.*, 2006). *In vitro* ubiquitination assays by Rohde *et al.* showed that PKN1 is ubiquitinated by SspH1 and confirmed the E3 ligase activity of SspH1 (Rohde *et al.*, 2007). As PKN1 has many roles in different pathways, it was initially thought that SspH1 targeted PKN1 for regulation of NF-κB, however this turned out to not be the case. PKN1 governs androgen receptor (AR) signaling and upon further investigation, SspH1 was found to ubiquitinate PKN1 in cells, targeting PKN1 for degradation and attenuating AR activation (Keszei *et al.*, 2014). The other *S. enterica* NEL, SspH2 does not have an identified host substrate, however localization experiments reveal its presence at the apical plasma membrane within infected cells (Quezada *et al.*, 2009). The IpaH family of effectors includes YopM from *Yersinia pestis*, a truncated version that contains only the N-terminal LRR domain (and possesses no NEL domain). YopM is encoded on the virulence plasmid of *Yersinia* and is required for full virulence during infection (McDonald *et al.*, 2003). YopM activates and associates with various PKN and RSK isoforms and forms a trimeric complex that modulates the expression of TNF- (McDonald *et al.*, 2003, Hentschke *et al.*, 2010, Hofling *et al.*, 2014). The well-studied example of YopM in virulence suggests the intriguing possibility that NEL domain

effectors may carry out important roles in virulence independent of their E3 ubiquitin ligase activity.

1.6: *Shigella* and Macrophage Interactions

1.6.1: *S. flexneri*-Induced Pyropotosis

As described in Section 1.1.2, *Shigella* transverses through the epithelial layer of the colon, where bacteria can be detected and phagocytosed by macrophages. *Shigella* escapes phagocytic vacuoles and propagates within the cytoplasm of the cell. In infected macrophages, *Shigella* induces a specialized proinflammatory form of programmed cell death, pyroptosis. Pyroptosis is dependent on caspase-1 activation, which stimulates a proinflammatory response (Fink *et al.*, 2005). In contrast, apoptosis is not associated with caspase-1 activation and no inflammatory response is associated with apoptotic cell death. Interestingly, there is a divide as to whether pyroptosis is beneficial for the bacteria or the host. In cells infected with a high MOI (>50) pyroptosis seems to benefit *Shigella*, whereas lower MOIs (<10) appear to benefit the host and assist in bacteria clearance (Suzuki *et al.*, 2007, Willingham *et al.*, 2007, Miao *et al.*, 2010).

Following phagocytosis and vacuolar escape, *Shigella* controls the induction of pyroptosis by the release of effector IpaB, which binds and activates inflammasome formation via NLRC4 (NLR family CARD domain containing 4). MxiI, the rod component of *Shigella* T3SS, is recognized by immune sensor protein NAIP2 (NLR family apoptosis inhibitory protein 2) which induces the formation of the NLRC4 inflammasome (Kofoed *et al.*, 2011, Zhao *et al.*, 2011, Suzuki *et al.*, 2014a). The inflammasome is a multi-protein complex that activates caspase-1, which mediates the

proteolytic cleavages of pro-IL-1 β and pro-IL-18 to their mature forms, initiating a proinflammatory response, as well as mediating pyroptosis (Hilbi *et al.*, 1998, Fink *et al.*, 2005). Caspase-1 and regulation of IL-1 β and IL-18 is very important during *Shigella* infection (Zychlinsky *et al.*, 1994, Sansonetti *et al.*, 2000). In the murine pulmonary model of shigellosis, caspase-1 deficient mice had higher mortality, as well as increased bacterial burdens (Sansonetti *et al.*, 2000). Interestingly, treatment with IL-1 β in caspase-1 null mice resulted in an even more severe phenotype, while IL-18 treatment resulted in a phenotype similar to wild-type mice. This shows the high amount of regulation involved in maintaining the perfect environment for *Shigella* infection. IpaH7.8 has also been implicated in inflammasome activation in infected macrophages (Suzuki *et al.*, 2014b). Recently it has been proposed that IpaH7.8 targets host glomulin for degradation via ubiquitination and subsequently activate inflammasome-mediated pyroptosis (Suzuki *et al.*, 2014b). While the mechanism and role of glomulin has yet to be elucidated, Suzuki *et al.* clearly demonstrate depletion of glomulin leads to macrophage cell death and increased cytokine production (Suzuki *et al.*, 2014b).

In addition to the induction of pyroptosis, *Shigella* can also induce a caspase-1 independent form of macrophage cell death, termed pyronecrosis. Rapid cell death was observed in macrophages lacking caspase-1 therefore indicating that another mechanism of cell death initiated by *Shigella* exists (Suzuki *et al.*, 2005). Cryopyrin (also known as CIAS1 and NLRP3) is a key component of the NLRP3 inflammasome and therefore is involved in caspase-1 and IL-1 β activation. Mutations in cryopyrin result in necrosis-like death in macrophages. Willingham *et al.* examined the role of cryopyrin in *Shigella* infection and found cryopyrin-dependent necrosis, similar to that observed in the mutants

(Willingham *et al.*, 2007). Further investigation determined this necrotic cell death independent of caspase-1 and IL-1 β, thus independent of inflammasome formation (Willingham *et al.*, 2007).

1.6.2: Immune Response

In addition to inflammasome mediated cytokine release, macrophages can detect other proteins and molecules from *Shigella* through pattern recognition receptors (PRRs) to elicit strong immune responses. PRRs include Toll-like receptors (TLRs) and Nod-like receptors (NLRs). TLRs and NLRs recognize peptidoglycan, lipopolysaccharides (LPS), proteins comprising the T3SS (such the rod and needle proteins) and many other toxins and surface proteins (Jessen *et al.*, 2014). Activating PRR leads to the production of cytokines such as IL-1 β, IL-6, TNF-α, interferon- λ (IFN- λ), CCL3, CCL4, and CCL5 (Jessen *et al.*, 2014). While this is meant to provide benefits for the host, *Shigella* is well adapted to survive and takes advantage of the tissue damage resulting from infiltrating cells to promote bacteria spread.

1.7: Autophagy Overview

Autophagy is a cellular process involved in the degradation of proteins and organelles as a response to environmental and cellular stimuli in eukaryotes. It is responsible for regenerating materials necessary for biosynthesis. The hallmark of autophagy is the formation of a double membrane structure known as the autophagosome. It begins as an isolation membrane, a c-shaped double membrane formation around the degradation target, which progresses to completely surround the

target and forms the autophagosome. Next, the autophagosome fuses with a lysosome, resulting in degradation of the inner membrane and its contents (He *et al.*, 2009).

A basal level of non-selective autophagy occurs within cells, however a selective, regulated process exists as well. Similar to ubiquitin targeting degradation via the proteasome, ubiquitin can also target cargo for autophagosomal degradation. Sequestosome 1 (SQSTM1/p62), an adaptor protein, has an ubiquitin binding motif and binds to ubiquitinated proteins. It also binds autophagy-related gene 8/ microtubule-associated protein 1 light chain 3 (ATG8/LC3). LC3 is bound to phosphatidylethanolamine (PE) embedded in the double membrane of the forming autophagosome, thus linking the p62 bound ubiquitinated cargo to the autophagic machinery (He *et al.*, 2009).

1.7.1: Autophagy and Bacteria

In addition to responding to cellular stresses such as starvation, ER stress and growth factor deprivation, autophagy is also involved in pathogen clearance. Specifically, the use of autophagy machinery in pathogen clearance is called xenophagy. Selective clearance of bacteria through xenophagy is mediated through ubiquitination. Host E3 ligases can recognize and ubiquitinate surface molecules on specific bacteria. Currently only two E3s have been implicated in xenophagy, LRSAM1 and Parkin, however it is speculated that many more exist (Huett *et al.*, 2012, Shibutani *et al.*, 2014). Autophagic adaptors responsible for selective targeting of bacteria to autophagosomal degradation have been identified and the process is outlined in Figure 5. These proteins include previously mentioned p62, nuclear dot protein 52 kDa (NDP52), optineurin (OPTN) and

neighbor of BRCA1 gene 1 (NBR1) and they act as adaptors to link ubiquitinated bacteria/bacterial remnants to ATG8/LC3 (Jo *et al.*, 2013). In autophagy deficient animals, there is higher susceptibility to bacterial infections (Shibutani *et al.*, 2014). Additionally, some bacteria, including *Shigella,* have evolved mechanisms for evasion of host autophagy machinery (Ogawa *et al.*, 2005, Shibutani *et al.*, 2014).

Shigella evades xenophagy in an IcsB-dependent manner and this has been illustrated in Figure 5 (Ogawa *et al.*, 2005, Baxt *et al.*, 2014). IcsB is secreted through the T3SS and is necessary for actin-based motility of *Shigella.* Ogawa *et al.* showed that *iscB* mutant strain of *Shigella* is unable to escape autophagy and that IscA/VirG, *Shigella* surface protein also involved in actin-based motility, is recognized by ATG5, inducing autophagy (Ogawa *et al.*, 2005). They determined that in wild-type *Shigella* IcsB binds IscA preventing binding by ATG5. Recent literature has provided further insight into the role of IscB and evasion of autophagy. IscB recruits host protein Toca-1, which effectively inhibits the recruitment of NDP52 and LC3 (Baxt *et al.*, 2014). It was also proposed that Toca-1 aids in the motility of *Shigella* within the cytosol and that through its mobility it also evades ubiquitination (Ogawa *et al.*, 2005, Baxt *et al.*, 2014).

1.7.2: Autophagy and Inflammasome Interplay

Crosstalk between autophagy and inflammasomes exists to help regulate the two cellular responses. Autophagy has been implicated as a negative regulator of inflammasome activation, while the induction of autophagy depends on the presence of inflammasome sensors (Yuk *et al.*, 2013). Autophagy regulates inflammasome activation and degrades the inflammasome complex through selective autophagy and the autophagy

adaptor p62. Inflammasome components, AIM2, NLRP3, and ASC, are sequestered to autophagosomes for selective degradation in order to prevent excessive inflammasome activation (Shi *et al.*, 2012). Dupont and coworkers observed that induction of autophagy initiated by vacuolar membrane remnants from *S. flexneri* escape decreases the inflammatory response (Dupont *et al.*, 2009). Additionally, autophagy is involved in the regulation and secretion of inflammasome-associated cytokine IL-1 β. TLR stimulation sequesters pro-IL-1 β in autophagosomes in macrophages, thus blocking the secretion of mature IL-1 β (Harris, 2011). In contrast, studies have also shown that an unconventional export pathway for IL-1 β exists that is autophagy-dependent, suggesting a positive role of autophagy in inflammasome activation as well (Dupont *et al.*, 2011).

1.8: Research Described in Thesis

The research described in this thesis focuses on the characterization of the *S. flexneri* T3SS effector IpaH9.8. To determine a role for IpaH9.8 during an oral model of infection, mice were infected with WT, Δ*ipaH9.8* (*ipaH9.8* knockout) and Δ*ipaH9.8*Δ*ipaH2* (*ipaH9.8* and *ipaH2* knockout) strains of *Shigella*. Mice infected with WT *Shigella* displayed a higher degree of illness and increased bacterial burdens. This suggests an essential role for IpaH9.8 in the survival of *Shigella* during infection. The molecular mechanism of IpaH9.8 was examined by investigating potential substrates. ZKSCAN3 was a top hit from a yeast-two hybrid experiment done by former lab member Dr. Jeremy Benjamin. I was able to confirm ubiquitination of ZKSCAN3 by IpaH9.8 in a cell free ubiquitination assay. ZKSCAN3 is a transcription factor and a negative regulator of autophagy, so I hypothesized that IpaH9.8 may interfere with autophagic regulation in

eukaryotic cells. In cell culture analysis of cells stably expressing IpaH9.8 and cells infected with mutant *S. flexneri* strains I observed an increase in autophagy marker LC3B in the presence of IpaH9.8. Additionally, I constructed an LC3 promoter controlled luciferase vector and observed that luciferase activity was decreased in cells infected with mutant-IpaH9.8 strains of *Shigella*. Lastly, I propose a mechanism of action for IpaH9.8 and ZKSCAN3. IpaH9.8 inactivates ZKSCAN3 resulting in increased autophagy. The induction of autophagy helps *S. flexneri* infection through degradation of cellular materials to provide nutrients for intracellular growth and regulation of inflammasome activation, thus preventing pyroptosis and excessive proinflammatory cytokine release.

CHAPTER 2: METHODS

2.1: Bacterial Strains and Bacteria Culture Maintenance

Shigella flexneri serotype 5a (M90T) was used as the wild-type *Shigella* strain throughout this study (Onodera *et al.*, 2012). *Shigella* was grown overnight at 37°C in 30 mg/mL trypticase soy broth (TSB) if liquid cultures were required. Cultures were maintained on solid medium consisting of 30 g/L TSB with 20 g/L agar and 0.01% Congo red. *Escherichia coli* (*E. coli*) strains DH5α and BL-21 were used for propagation of plasmids and genetic manipulations of DNA. These two strains were grown in Luria Bertani broth (10 mg/mL tryptone, 5mg/mL yeast extract and 10 mg/mL sodium chloride) with or without 20 mg/mL agar. Frozen stocks for all bacterial strains were created by the addition of 15% glycerol to overnight liquid cultures grown at 37°C and placed at -80°C for long-term storage. If necessary, antibiotics were added to the medium at the following concentrations: ampicillin 100 μg/mL, tetracycline 5 μg/mL, and streptomycin 100 μg/mL**.**

The *ipaH9.8* gene was targeted for knockout by cloning a tetracycline resistance cassette with 50 nucleotides flanking each end of the cassette matching the *ipaH9.8* gene (Sidik *et al.*, 2014). The *ipaH2::kan* Δ*ipaH9.8* double mutant was created by lambda red recombination using the Δ*ipaH9.8* mutant as a parent strain and targeting the *ipaH2* locus for replacement by a cassette encoding kanamycin resistance flanked by 50 nucleotides of homology within the *ipaH2* open reading frame using the oligos listed in Table 1. The procedure for λ red recombination is described in Sidik *et al.* 2014 (Sidik *et al.*, 2014). Briefly, the gene replacement cassette was electroporated into wild-type the Δ*ipaH9.8*

mutant that was made hyper-recombinogenic by the expression of the phage λ proteins (Datsenko *et al.*, 2000). Following electroporation, bacteria were recovered in liquid TSB at 37 °C with constant shaking at 200 RPM for 2 hours and then plated on solid media containing kanamycin to select for bacteria with the desired mutation. The deletion was confirmed through PCR using one primer that binds within the kanamycin cassette and one primer for the flanking DNA sequence (Table 1).

Table 1: Primers used for cloning and *ipaH* gene knockouts

Construct	Forward Primer	Reverse Primer
pcDNA3-ZKSCAN3 pGEX6P1-ZKSCAN3	CCCCCCGAATTCATGGC TAGAGAATTAAGT	CCCCCCCTCGAGTCACTG TGATAGGAT
pGL4.26-LC3-Promoter	TAAGCACTCGAGACAGC CACCAGGAGAGTTCC	TGCTTAAAGCTTACTCTG GCGATAGCCACTTC
ipaH9.8 knockout cassette	TCTTTTAACAAAGCCATT TGTCCACCGGCTTTAACT GGATGCCCATCATGATT CCGGGGATCCGTCGACC	GTAATTTCCTCACTGAGC TACCAGCATTTTCTGAGG GAAATAATCCCGTTATTC CGGGGATCCGTCGACC
ipaH2 knockout cassette	CTACTTATTTCTTTTAAC AAAGCCATTTGTCCATC GGCTTTAACTGAATGAT TCCGGGGATCCGTCGAC C	CAGTCCGGTCTGTGGTTT ATGCGATGTGATTATGAA TGGTGCAGTTGTGATGTA GGCTGGAGCTGCTTCG

2.2: Murine Model of *Shigella* Infection

Balb/c female mice aged 6-8 weeks were used for all experiments and were obtained from Charles River. A visual representation of the mouse infection protocol is outlined in Figure 6. The infection procedure is adapted from that reported by Martino *et al.* and described in Pruneda *et al*. (Martino *et al.*, 2005, Pruneda *et al.*, 2014). Two days prior to infection the mice were placed on streptomycin by supplementing the water supply with antibiotic at 100 μg/ml. Overnight cultures of *Shigella* strains were grown in TSB media and were grown at 37°C the afternoon before infection day. On infection day,

all food was removed from the cages and food was removed from mice 6 hours prior to infection. Prior to infection, the overnight cultures were sub-cultured at a dilution of 1:100 in TBS media and incubated for 3 hours at 37°C. Following the incubation, the OD600 of each culture was measured and recorded. Cultures were then diluted in Phosphate-Buffered Saline (PBS) to a concentration of $1x10^9$ cells/mL and contained in 1 mL syringes. The clinical scores and weights for all the mice were recorded and then the mice were orally gavaged a dose of $1x10^8$ bacteria in 100µL. Mice were monitored every 8 hours for 3 days, where weights and clinical scores were measured and recorded. Table 2 outlines the clinical scoring criteria used to assess the mice. If clinical scores reached 12, the mice were placed on two-hour watch, where they were examined every two hours until their condition improved or worsened. If mice reached a clinical score of 15 or greater they were euthanized. During the course of infection, fecal samples were collected once a day and were used to make serial dilutions in PBS, which were plated on MacConkey agar (peptone 20g; lactose 10g; bile salts 5g; sodium chloride 5g; neutral red 0.075g in 1L dH_2O) containing 100 mg/mL streptomycin and incubated at 37°C overnight. The bacterial colonies that grew on the plates were counted and recorded. Mice were euthanized on the third day of infection. They were put into surgical plane using ketamine intraperitoneally or isoflurane gas. The blood of the mice was collected through cardiac puncture. Following cardiac puncture, cervical dislocation was performed on each mouse to insure its death. Next, mice were dissected and organs were harvested for further analysis, including: the spleen, liver, cecum and colon. The contents of the cecum were serially diluted and plated on MacConkey agar to assess bacterial burden. The colon was cut into two pieces, one half was cultured overnight in DMEM

supplemented with antibiotics and the other was made into a swiss roll for histological staining. The rolled colon half was fixed in 10% formalin and embedded in paraffin with the cecum and spleen for histological analysis. Part of the spleen, as well as the liver, were homogenized using wire mesh and were serially diluted and plated on MacConkey agar to assess bacterial burden and dissemination of the infection.

Hematoxylin and eosin (H&E) staining was performed on the fixed histological samples. First, samples were deparaffinized with xylene for 10 minutes and rehydrated with 100% ethanol twice for 5 minutes. Samples were placed in 95% ethanol for 2 minutes followed by 70% ethanol for 2 minutes and then rinsed in water. Next, samples were immersed in Harris hematoxylin for 8 minutes and rinsed with water. Samples were then treated with 1% acid alcohol for 30 seconds and rinsed in water. Samples were placed in 0.2% ammonia water for 30 seconds and rinsed with water. Then samples were dipped in 95% ethanol 10 times and stained with eosin-phloxine solution for 30 seconds. Samples were dehydrated with incubation in 95% ethanol for 5 minutes followed by incubation in 100% ethanol for 5 minutes. Lastly, samples were treated with xylene for 5 minutes and mounted on glass slides.

Enzyme-Linked Immunosorbent Assays (ELISAs) were used to assess the cytokines involved during *Shigella* infections. Common pro-inflammatory molecules, IL-6 and TNF-α were assessed, as well as IL-1 β (DuoSet R&D Systems, Cat# DY406, Cat# DY410, Cat# 401). Capture antibody was diluted with sodium bicarbonate buffer (100 mM sodium bicarbonate, 500 mM sodium chloride, pH 8.3) and was used to coat the wells of a 96-well microplate. The microplate was sealed and plated at 4°C overnight. Each well was aspirated and washed with 1X Phosphate Buffered Saline with 0.1%

Tween (PBST) for a total of 3 washes. Next the wells were blocked using 0.1% Bovine Serum Albumin (BSA) in PBS for 1 hour at room temperature. Wells were aspirated and washed 3 times with 1X PBST. Supernatants collected from overnight colon cultures of infected mice and standards diluted in Dulbecco's Modified Eagle Media (DMEM) were added to the wells of the microplate and incubated overnight at 4°C. Wells were aspirated and washed with 1X PBST. Next, Streptavidin-HRP in 0.2% BSA in PBS was added to the wells and incubated at room temperature for 30 minutes. The wells were aspirated and washed with 1X Tris Buffered Saline (TBS). Next, substrate solution from the ELISA Amplification System (Life Technologies, Cat# 19589-019) was added to the wells and incubated for 30 minutes. Lastly, the amplification solution from the ELISA Amplification System was added to the wells to allow for colour development. To stop the colour from reaching saturation, 0.3M H_2SO_4 was used. Finally, microplates were read by BioTek Eon microplate spectrophotometer.

The Mouse Cytokine Array Panel A (R&D Systems, Cat# ARY006) was used to assess cytokines on a large scale. Arrary Buffer 6 (provided in the R&D Systems kit) was used to block nitrocellulose membranes containing 40 different capture antibodies for 1 hour at room temperature with gentle agitation. Pooled supernatants collected from cultured colons from infected mice were mixed with Mouse Cytokine Array Panel A Detection Antibody Cocktail (provided in the R&D Systems kit). Array buffer 6 was aspirated away from the membranes and the mixture of supernatants and dectection antibody was incubated with the membranes at 4°C overnight. Membranes were washed with 1X Wash Buffer (provided in the R&D Systems kit) 3 times. Streptavidin-HRP was added to the membranes and incubated for 30 minutes. Membranes were then washed 3

times with 1X Wash Buffer. The membranes were moved onto plastic sheet protectors and Chemi Reagent Mix (provided in the R&D Systems kit) was evenly spread onto each membrane and incubated for 1 minute. Excess Chemi Reagent Mix was removed from the membranes using paper towels. The membranes were placed in an autoradiography film cassette and were exposed to x-ray film for up to 10 minutes.

Table 2: Clinical scoring parameters for monitoring mouse health. Each parameter is assessed on a scale of 0-3, with 3 being the worst. Mice that reach a score of 12 are monitored every 2 hours until their condition either improves or worsens. Mice with a score >15 are euthanized.

Parameter	Observation	Score
Appearance	Normal	0
	Rough, lack of grooming	1
	Coat staring, nasal and ocular discharge	2
	Dark fur, discharge, urine marks	3
Food intake	Normal	0
	Slight decrease	1
	Large decrease	2
	No food intake	3
Hydration	Normal	0
	Skin less elastic	1
	Skin tents	2
	Skin tents, sunken eyes	3
Temperature	Normal	0
	±1°C	1
	±2°C	2
	±3°C	3
Behavior	Normal	0
	Slightly uncoordinated	1
	Less mobile, uncoordinated	2
	Staggering, little movement	3
Posture	Normal	0
	Abnormal posture	1
	Hunched over, less active	2
	Inactivity, labored breaths	3
Weight-loss	No change	0
	0-5% change	1
	5-10% change	2
	10-15% change	3

2.3: GST-Purification and Cloning of ZKSCAN3

Yeast two-hybrid experiments performed by former lab member Dr. Jeremy Benjamin identified potential substrates for IpaH9.8. ZKSCAN3 was recovered multiple times as an interactor of IpaH9.8. ZKSCAN3 was cloned from cDNA (primer details in Table 1) and the protein was expressed and purified from *E. coli*. ZKSCAN3 is a eukaryotic protein expressed in all human cells. RNA was extracted from HeLa cells using RNeasy Mini Kit according to the manufacturer's instructions (Qiagen Cat# 74104). RNA extracted was then used to make cDNA via qScript cDNA Supermix (Quanta Biosciences, Cat# 95048-025). Specific primers were designed to clone ZKSCAN3 from cDNA template (Table 2). Next, the PCR product was purified by using QIAquick PCR Purification Kit (Qiagen Cat#28104) followed by restriction enzyme digest in 1X New England Biolab (NEB) buffer for 1 hour at 37°C. The sample was analyzed using gel electrophoresis on 1% agarose in 1X TBE (5X Tris 54 g, borate 27.5 g, 20 mL of 0.5 M EDTA, pH 8 in 1 L H_2O) gel and ran at a voltage of 100 V for 20-30 minutes, until the bands of the 1kb DNA Ladder (New England Biolabs, Cat#N3232L) were resolved. The band corresponding to 1.5 kb was excised and purified using the QIAquick Gel Extraction Kit (Qiagen Cat# 28704). Ligation of the 1.5kb insert and restriction cut pGEX-6P1 vector was performed by incubation at 4°C overnight with T4 Ligase (New England Biolabs, Cat# M0202L) in NEB Reaction buffer. The product of the ligation was used to transform $CaCl_2$ competent DH5α *E. coli*. Bacteria were spread onto LB agar plates containing ampicillin and incubated overnight at 37°C**.** Of the resulting colonies, three were chosen for overnight culture and QIAprep Spin Miniprep Kit (Qiagen Cat#27104). Purified DNA from the QIAprep Spin Miniprep kit was sent

through Genewiz for sequencing. DNA samples with the correct sequencing were then used to transform $CaCl_2$ competent BL21 *E. coli*. Bacteria were spread onto LB agar plates containing ampicillin and incubated overnight at 37°C**.** Of the resulting colonies, three were chosen for overnight culture and QIAprep Spin Miniprep Kit. A glycerol stock of bacteria containing the plasmid was stored at -80°C.

To express the ZKSCAN3 protein, BL21 *E. coli* were induced with 1 mM IPTG to promote expression of T7 polymerase and subsequent expression from the ZKSCAN3 expression plasmid. Bacteria were inoculated into 50 mL LB broth and grown overnight at 37°C. The following morning, the IPTG was added to the media, and the bacteria were incubated for an additional 16 hours at 20°C at constant agitation. Bacteria cultures were collected by centrifugation at 5000 RPM for 15 minutes. Bacteria were lysed by sonication on ice, 15 times in 1 second bursts. Cellular debris was removed by centrifugation of the sample at 12 000 RPM for 5 minutes. Pierce Glutathione Agarose beads (Thermo Scientific Cat# 16100) were prepared as outlined in the manufacturers protocol. Next, the beads were added to the bacterial lysates and incubated at 4°C for 3 hours to overnight on an end-over-end rotator. Following incubation, the beads were spun at 700 x g for 2 minutes and the supernatant was removed and beads were washed with wash buffer (50mM Tris, 150mM NaCl, pH 8.0). The spin and wash step was repeated twice. Finally, to remove the purified ZKSCAN3 protein from being bound to the beads, two different protocols were used. One method was the addition of elution buffer (50mM Tris, 150 mM NaCl, 10mM reduced glutathione, pH 8.0) and incubation at room temperature to release the GST-ZKSCAN3 from being bound to the glutathione. The other method used was the cleavage of the GST fusion protein from ZKSCAN3 by

PreScission Protease (GE Healthcare Life Sciences Cat# 27-0843-01) by incubating the sample with 1 unit of protease per 100 μg of substrate at room temperature for 2 hours and collection of the ZKSCAN3-containing supernatant. Purified ZKSCAN3 was stored at -80°C with the addition of 20% glycerol.

To confirm the purified protein was in fact ZKSCAN3, SDS-PAGE was performed. The purified protein was mixed with 2X protein sample buffer (PSB, 0.375 M Tris-HCl pH 6.8, 6% SDS, 36% glycerol, 0.03% bromophenylol blue, 0.6 M DTT) and then boiled for 5 minutes. The sample was loaded onto a 7.5% polyacrylamide gel and a voltage of 120 V was applied through the apparatus for 1.5 hours. Once the loading front reached the end of the gel, the gel was removed from the running apparatus and placed in Protein Staining reagent (Sci-Med Inc., cat# SM001000).

2.4: Ubiquitination Assay

Ubiquitination reactions were performed in a cell free system to assess the activity of ligases and substrates. Reaction mixtures contained 0.5 μg E1 ligase (Boston Biochem), 2 μg E2 ligase (UbcH5b, Boston Biochem), 2 μg IpaH9.8 (purified by Rohde lab members), 1 μg HA-tagged ubiquitin (Boston Biochem), 1X of 5X Charging buffer (25 mM Tris-HCl pH 7.5, 50 mM NaCl, 5 mM MgCl, 4mM ATP, 0.25 mM DTT) and dH_2O. Reactions were incubated for 30 minutes to overnight at room temperature and stopped by addition of 2X PSB, followed by boiling the sample for 5 minutes. Samples were stored at -20°C or used immediately for SDS-PAGE analysis. Resulting gels were either stained via silver stain, or Sci-Med Inc. protein staining reagent, or used in Western blot analysis. BioRad silver staining kit (BioRad, Cat# 16104499) and Protein Staining

Reagent (Sci-Med Inc., Cat# SM001000) were performed as per manufacturer's instructions.

2.5: Cell Culture and Maintenance

2.5.1: HEK293T, Phoenix, and HEK293A cells

HEK293T, HEK293A, and Phoenix cell lines were all maintained in the following manner. Cells were subcultured when confluency reached 80-90% (every 2-3 days). To subculture cells, all old media was removed from the cell culture flask, briefly rinsed with PBS and then treated with trypsin (0.05% Trypsin with 0.5 M EDTA, Invitrogen, Cat# 25300-054) for 10 minutes at 37°C. Following the trypsin, cells were resuspended in growth media and seeded back at a 1:10 dilution. The growth media used was Dulbecco's Modified Eagle Medium (DMEM, Invitrogen) supplemented with 10% Fetal Bovine Serum (FBS, Invitrogen) and 100 mM HEPES. Cells were grown in an incubator at 37°C and 5% CO2.

2.5.2: U937 cells

U937 cells were subcultured every 2-3 days, when cells reached confluency. To subculture cells, all media was removed and a 1:10 dilution was seeded back into the flask (cells are in suspension). Growth media used was RPMI (Roswell Park Memorial Institute medium, Invitrogen) supplemented with 10% FBS. Cells were grown in an incubator at 37°C and 5% CO2. To activate U937 cells into macrophages-like cells (and also induce adherence), cells were pelleted by centrifugation at 500 x g for 10 minutes and then the pellet was resuspended in fresh media containing 60 pg/mL phorbol 12-

myristate 13-acetate (PMA). Cells were incubated at 37°C for 15 minutes in the PMA-supplemented media and seeded into the appropriate cell culture dishes. Cells were left overnight to mature and adhere prior to any experiment.

2.5.3: Retroviral Stable Cell Lines

Stable cell lines expressing codon-optimized IpaH9.8 WT and IpaH9.8 C337A were created using the retroviral transduction method. Codon optimized IpaH9.8 WT and C337A were purchased from Genewiz and cloned into the pBMN-IRES-PURO (here on referred to as pBMN) vector (courtesy of Dr. Craig McCormick, Dalhousie University). Next, empty pBMN, pBMN-IpaH9.8WT and pBMN-IpaH9.8C337A were transfected using the PEI protocol (see Section 2.9**)** into Phoenix cells. Supernatants from the cells were collected 2 days following transfection. The supernatants were filtered through 0.45 μm filters and polybrene was added to a final concentration of 8 μg/mL. The supernatants were then added to the media of HEK293T or HEK293A cells and left for 2 days at 37°C and 5% CO2. Following incubation with viral supernatants, media was removed, cells were briefly rinsed with PBS and fresh media was added. Cells were given one day of recovery and then puromycin was added to select for the cells with the pBMN plasmids. Cell lines were maintained by subculturing every 2-3 days when cells reached 70-80% confluency and grown in 10% FBS DMEM supplemented with puromycin at 37°C and 5% CO2. Virus stock not used for immediate transduction was stored at -80°C. A flowchart outlining the steps for viral transduction is illustrated in Figure 7.

2.5.4: Lentiviral Stable Cell Lines

To create lentiviral stable cell lines, 3 vectors are simultaneously transfected into HEK293T cells. The 3 vectors were: psPAX2 (packaging plasmid), pMD.2G (envelope plasmid) and pLJM1B* (transfer vector). The DNA inserts encoding codon-optimized IpaH9.8 WT and C337A were cloned into pLJM1B*. Using the PEI transfection protocol (Section 2.9), HEK293T cells were transfected with 2 μg psPAX2, 1 μg pMD.2G and 3.3 μg pLJM1B* in a 10 cm dish. 48 hours post transfection, the supernatants were collected and filtered through a 45 μm filter and polybrene was added. Viral supernatants were diluted 1:5 into serum free media (RPMI, Invitrogen) and added directly to U937 cells for viral transduction. 4 hours later the cells were pelleted by centrifugation (500 x g for 10 minutes), media was discarded and fresh 10% FBS RPMI media was added. Cells were in recovery for 1 day and then blasticidin (10 μg/mL) was added to the media for selection. Stable U937 cells were maintained in 10% FBS RPMI supplemented with blasticidin. Virus not used for immediate transduction was stored at -80°C. All cell lines have extra stocks in liquid nitrogen storage and are frozen in 10% DMSO 10% FBS media. Figure 7 shows a side by side comparison of lentiviral and retroviral transduction techniques.

2.5.5: Cell Culture Infections

Infections were performed on U937 cells and HEK293T/A cells. Overnight cultures of bacteria strains to be used for the infection were inoculated in TSB broth and incubated at 37°C. The following day, subcultures were made using a 1:50 dilution from the overnight cultures and bacteria were incubated at 37°C until growth reached an OD600 of 0.6. The amount of bacteria added to the cells corresponded to an MOI of 10.

To synchronize the bacteria, infected cells were spun at 500 x g in an ultra centrifuge for 10 minutes. To prevent rapid cell death due to bacteria, gentamycin was added to each well 30 minutes post infection. Samples were collected following each experiment at specified time points.

2.6: SDS-PAGE and Western blotting

For a typical HEK293T/A experiment in a 6-well plate, cells were subcultured at a concentration of 6.7 x 10^5 cells/well. Alternatively, PMA-activated U937 cells were subcultured at a concentration of 1 x 10^6 cells/well in a 6 well dish. If experiments were done in larger or smaller formats, the ratio was adjusted accordingly. Cells were given minimum one day of recovery to reattach to the plates. In some experiments, treatments (MG132) were added and incubated with the cells at various time points. All cells were harvested in the same manner. Media was removed and discarded, then cells were washed twice with PBS, and finally cells were lysed on the plate by addition of RIPA buffer (10% NP40, 1% SDS, 0.5 M Tris-HCl pH7.4, 1.5 M NaCl, 5% sodium deoxycholate, 0.01 M EDTA, dH_2O). The cell lysates were collected into tubes and cellular debris was pelleted by spinning samples at 13 000 x g for 2 minutes. The supernatants were saved, 2X PSB was added and then samples were boiled for 5 minutes. If the samples appeared thick or viscous, they were sonicated for 10 seconds. Cell lysates were either used immediately for PAGE or stored at -20°C.

For SDS-PAGE and Western blot analysis, polyacrylamide gels were made in accordance to the protocol from Sambrook and Russel (Sambrook *et al.*, 2001). Gels were placed in the running apparatus and the chambers of the apparatus were filled with

Running Buffer (Tris 30 g, glycine 144 g, SDS 10 g in 1 L dH_2O). Samples were loaded into the wells in the gel and electrophoresis was performed with an applied voltage of 120-140V for 1.5 hr (or until bromophenol blue loading front reached the end of the gel). At this point, the polyacrylamide gels could be used for Western blotting, silver staining or stained by Protein Staining Reagent (Med Sci Inc.).

For Western blot analysis, the wet transfer apparatus was used to transfer proteins from the polyacrylamide gel to a polyvinylidene fluoride (PVDF) membrane. The transfer apparatus was filled with Transfer Buffer (Tris, glycine, methanol, dH_2O) and the transfer proceeded for 1 hour at 100 V or overnight at 0.5 A. All subsequent incubation steps were performed with constant agitation on a shaker. Following the transfer, PVDF membranes were incubated in a solution of 5% skim milk powder in Tris-Buffered Saline with 0.1% Tween (TBST) for 1 hour at room temperature. Primary antibody was diluted in 5% milk TBST (see Table 3 for details) and incubated the membrane for 1 hour at room temperature or overnight at 4°C. Membranes were washed 5 times with TBST for 5 min per wash. Secondary antibody was diluted in 5% milk TBST (see Table 3 for details) for 1 hour at room temperature. Membranes were washed with TBST 5 times for 5 minutes each. Finally, membranes were developed using the Pierce ECL Plus Substrate

Table 3: Antibody dilution factors and purchasing information

Antibody	Dilution	Source
ZKSCAN3	1:2000	Sigma-Aldrich Cat# SAB2700902
LC3B	1:200	Nanotools Cat# 0231-100/LC3-5F10
IL-1 β	1:1000	Abcam Cat# AB2105
Actin	1:2000	Cell Signaling Cat# 4967
IpaH	1:1000	Gift from Régis Tournebize (Mavris 2002)
Mouse	1:2000	New England Biolabs Cat# 7076
Rabbit	1:2000	New England Biolabs Cat# 7074

kit (Thermo Scientific, Cat# 32132) and imaged using the KODAK imager (McCormick lab).

2.7: RT qPCR Analysis

RNA was collected from cells using the RNeasy Mini Kit as per manufacturer's protocol. RNA concentrations were measured using a spectrometer and 5 µg of RNA was added to cDNA qScript Supermix. The PCR cycles were set as per the kit instructions. cDNA generated from the kit was used directly as template for qPCR. Samples for qPCR were set up as follows: 12.5 µl SYBR Green (Quanta Biosciences, cat# 95073-012), 0.1 µl of 10 mM forward primer, 0.1 µl of 10 mM reverse primer, 0.5 µl MgCl, 1 µl cDNA and 10.8 µl dH_2O. The MxPro software and MX3000 was used to collect qPCR data. Primers used for qPCR are listed in Table 4. Data was assessed using the methods outlined in Livak (2001).

Table 4: Primers used for qPCR analysis

Target	Forward Primer	Reverse Primer
WIPI2	AATGTTCAACCAGGGCAGAG	CTAAGGGGCAGTCGTGAGAG
LC3B	CTGCTGAAGGTCCCTGACTC	CACTGCTGCTTTCCGTAACA
RPL13A	CCTGGAGGAGAAGAGGAAAGAGA	TTGAGGACCTCTGTGTATTTGTCAA

2.8: Immunofluorescent Microscopy

Prior to seeding cells, cover slips were treated with polylysine to increase adherence to the surface. Sterile coverslips were placed in a 50µg/mL polylysine solution for 1 hour. They were washed in cell culture media twice and then left to air dry in 12-well plates. U937 cells were seeded onto the coated coverslips and left overnight. The cells were washed once with PBS and then fixed with 4% paraformaldehyde in PBS for

15 minutes. The paraformaldehyde was removed and cells were washed twice with PBS. Cells were then permeabilized with 0.1% saponin for 15 minutes. Primary antibody was diluted in 1% BSA in PBS and incubated with the cells at room temperature for 30 minutes. Cells were washed with PBS twice and then light-sensitive secondary antibody (in 1% BSA PBS) was added for 30 minutes. Secondary antibody was washed off with PBS twice. Lastly, coverslips were treated with Prolong Gold with DAPI and mounted on slides. Slides were imaged at the Pasteur Institute using confocal microscopy.

2.9: PEI Transfection

Cells were subcultured the previous day to have a confluency of 60-70% (for HEK293Ts this equates to 6.7 x 10 5 cell/well in a 6 well dish). Plasmid DNA was prepared from Qiagen Midi prep kit and diluted to a final concentration of 500 μg/mL. For one well of a 6 well dish, 1 μg of DNA per well was mixed with Opti-MEM to a total volume of 100 μL and 3 μg of PEI (1mg/mL) was mixed with Opti-MEM to a total volume of 100 μL. The two mixtures were incubated at room temperature for 5 minutes and then the PEI mixture is added to the DNA mixture, mixed and incubated for another 15 minutes at room temperature. Cells for transfection were washed twice with SFM and then 1 mL of SFM is left in each well (half the normal amount). Next, the PEI/DNA/Opti-MEM mixture is added to the well slowly. The cells are incubated with the transfection mixture for 4-6 hours at 37°C and 5% CO_2. Following incubation the media containing the transfection mixture is removed and replaced with normal amount of supplemented media. Cells were left to recover overnight and then supplementary experimental procedures continued (harvest, luciferase assay, infection, etc.).

2.10: Luciferase Assay

To assess the activity of the LC3 promoter, LC3 promoter luciferase vectors were created. Genomic DNA was collected from HEK293T cells using Dneasy Blood and Tissue Kit (Qiagen Cat# 69504). Primers flanking the promoter region of LC3 were designed and used for PCR amplification of the promoter region. The resulting PCR product was digested with restriction enzymes and then ligated into cleaved pGL4.26 vector (provided by Dr. Craig McCormick, Dalhousie University). Following ligation, the resulting plasmid was used to transform $CaCl_2$ competent DH5α *E. coli*. The bacteria were incubated overnight on solid media containing ampicillin at 37°C. A few colonies were chosen for Genewiz sequence analysis and the positive colony was prepped via Plasmid Midi Kit (Qiagen Cat# 12143) and stored as a glycerol stock at -80°C.

To perform the luciferase assay, HEK293T cells were transfected with the pGL4.26 vector containing the LC3 promoter and a vector containing ZKSCAN3 as per Section 2.9. The following day cells were infected with *S. flexneri* strains, as per Section 2.5.5, for 2 hours and then cells were harvested with Passive Lysis buffer from the Dual-Luciferase Reporter (DLR) Assay System (Promega Cat# E1910). DLR reagents were prepared as per manufacturer's instructions and luciferase activity was measured on the Fluoroscan luminometer (Dr. Jean Marshall, Dalhousie University).

2.11: Statistical Analysis

The clinical score and bacterial burden graphs from the mouse experiments in Figure 8 were analyzed using a one-way ANOVA (with WT-infected mice designated as

the control comparison) followed by a Dunnett's test. ELISA data was analyzed using the same parameters as the clinical score and bacterial burden data, however the differences between infection strains were not significant. The Western blot optical density graphs in Figures 14, 15 and 16 were only an n=1, therefore no statistical tests were performed. In Figure 17 a one-way ANOVA was performed on both qPCR data sets, however there was no significance found. A one-way ANOVA was performed on the fold change in luciferase activity compared to uninfected cells in Figure 18 followed with a Dunnett's test. Lastly, an unpaired t-test was used to compare the number of foci per cell in control U937 cells and in IpaH9.8-expressing U937 cells in Figure 19.

CHAPTER 3: RESULTS

3.1 Mouse Model of *S. flexneri* Infection

3.1.1 Δ*ipaH9.8* strains of *Shigella* illicit decreased illness in Balb/c mice

Suitable animal models for *Shigella* infection have been difficult to identify, as *Shigella* is a human-specific pathogen (Organization, 2005). In the Rohde lab, the streptomycin mouse model of infection has seen success (Pruneda *et al.*, 2014). Mice infected with wild-type (WT) *Shigella* show signs of illness and bacteria persist throughout the course of the infection. To examine the role of *Shigella* effector IpaH9.8 and the closely related IpaH2 during infection, mice were infected with WT *Shigella*, single *ipaH9.8* knockout strain of *Shigella* (Δ*ipaH9.8*) or double knockout *ipaH9.*8 and *ipaH2 Shigella* strain (Δ*ipaH9.8*Δ*2*). Mice infected with WT *Shigella* displayed a more severe illness compared to mice infected with the two knockout strains. WT-infected mice had matted fur, excessive amounts of mucus buildup surrounding the eyes and nasal passage, decreased activity, and fecal samples that were small and wet. The mice infected with the mutant strains displayed some of the aforementioned symptoms but to a lesser severity, this was quantified in the clinical score for each mouse. The parameters used to assign clinical scores are outlined in Table 1. Figure 8A shows a graphical representation of the clinical scores for each infection group. WT-infected mice had clinical scores 2-fold higher than mice infected with knockout strains of *Shigella.* These data show that IpaH9.8 is important in creating a stronger disease state during *Shigella* infection.

3.1.2 Lower bacterial burdens in tissues of Δ*ipahH9.8* infected mice

In the search to identify the underlying cause of increased illness in WT-infected mice, the bacterial burdens of the mice were examined. Tissue from the spleen and liver were homogenized, serially diluted and plated on MacConkey agar to assess the bacterial burden and dissemination of the bacteria. Bacterial burdens of the gastrointestinal tract were measured through serial dilutions of feces and cecal contents of the mice. The bacterial burdens of mice infected with Δ*ipaH9.8* and Δ*ipaH9.8*Δ*2* strains were significantly lower in the cecum and spleen compared to WT (Figures 8B and 8C). This is consistent with results in studies done by Ashida *et al.* (Ashida *et al*., 2010). In that case, using a pulmonary model of infection, they observed lower bacteria burden in the lungs of mice infected intranasally with a Δ*ipaH9.8* strain of *Shigella*. In contrast, bacterial counts obtained from the liver showed no difference among infection groups (Figure 8D). My results suggest a role for IpaH9.8 in the dissemination of *Shigella* infection.

3.1.3 Histological Analysis of Infected Colon Tissue

Histology is a useful tool in assessing the tissue damage and or morphological changes in the cellular environment during *Shigella* infection. We examined swiss-rolled colon tissues prepared from mice infected with various strains of *S. flexneri* by microscopy. Figure 9 contains representative images of colon tissue from uninfected, WT-, Δ*ipaH9.8*- and Δ*ipaH9.8*Δ*2*-infected mice. The uninfected control mouse colon has well-structured finger-like crypts formed at the base of the submucosa. In the colon infected with WT *Shigella*, there is a large amount of infiltrating immune cells (indicated

by the blue straining) and some crypt disruption. When compared to WT infected controls the colons from Δ*ipaH9.8* and Δ*ipaH9.8*Δ*2* infected mice display increased colon destruction but smaller amounts of infiltrating immune cells. Additionally, the muscle layer in mice infected with Δ*ipaH9.8* and Δ*ipaH9.8*Δ*2* is thicker than the muscle layer of WT-infected and uninfected mice.

3.1.4 Proinflammatory cytokine levels of Δ*ipaH9.8* infected mice are similar to cytokine levels in WT-infected mice

Ashida and coworkers also examined proinflammatory cytokines in mice infected intranasally with *Shigella* and found that in mice infected with the Δ*ipaH9.8* strain there were increased proinflammatory cytokines (Ashida *et al.*, 2010). Due to the increase observed by Ashida *et al.* and the importance of proinflammatory cytokines during *Shigella* infection, I examined the levels of proinflammatory cytokines (IL-6, TNFα, IL-1β) secreted from mice through ELISA (Ashida *et al.*, 2010). The IL-6 level in blood serum appeared to be slightly elevated in some WT-infected mice, but was not significantly different from the mice infected with Δ*ipaH9.8* and Δ*ipaH9.8*Δ*2 Shigella* (Figure 10C). IL-1β secreted from colon tissue is also slightly elevated in WT-infected mice but is not statistically significant (Figure 10B). TNFα appeared to be the same across all infection groups, although it should be noted that there was greater variability in the WT-infected group (Figure 10C). Unfortunately this data was inconclusive due to the high degree of variability of cytokine levels within each infection group. Lastly, all the cultured colon media samples for each infection group were pooled together and used in a cytokine array to identify cytokine differences between the WT and knockout

infected mice. The array revealed increased G-CSF, GM-CSF, IP10, IL-6 and IL-16 (Figure 10D). However, follow-up analysis of the potential cytokines using ELISA revealed no differences between the three infection groups. While these results were inconsistent with the previous study with Δ*ipaH9.8* strains by Ashida *et al.*, the differences could be attributed to the differences in route of infection (pulmonary vs. oral) (Ashida *et al.*, 2010).

3.2 Confirmation of IpaH9.8 Substrate ZKSCAN3

3.2.1 GST Purification of ZKSCAN3

Yeast two-hybrid experiments are a common method of identifying potential protein interactions. Dr. Jeremy Benjamin, a former Rohde lab post-doctoral fellow, performed a yeast two-hybrid screen to identify mammalian proteins that interact with IpaH9.8. In this screen a catalytically dead variant of IpaH9.8 (C337A) was fused to the DNA binding domain of Gal4 and used as "bait". A normalized human cDNA library (purchased from Invitrogen) was screened to identify interactors. The top hit with high confidence was ZKSCAN3. ZKSCAN3 is a transcriptional repressor of autophagy and is transported to and from the nucleus dependent on stress conditions (Chauhan *et al.*, 2013). This was an interesting hit for us, as *Shigella* can evade autophagic machinery and IpaH9.8 can shuttle to and from the nucleus (Okuda *et al.*, 2005). To investigate if IpaH9.8 can ubiquitinate ZKSCAN3, ZKSCAN3 was purified via a GST fusion protein system and glutathione-coated agarose beads (Figure 11A).

3.2.2 ZKSCAN3 is ubiquitinated in a cell free system by IpaH9.8

The yeast two-hybrid experiment provided evidence that IpaH9.8 and ZKSCAN3 come in close contact and may directly interact but does not prove that ZSKCAN3 is a substrate for IpaH9.8. To show that ZKSCAN3 is a bona-fide substrate of IpaH9.8, IpaH9.8 must be able to act upon ZKSCAN3 with its E3 ligase activity. A cell free *in vitro* reaction containing purified proteins and reagents necessary (E1, E2, IpaH9.8, ubiquitin, and ATP) for ubiquitination of purified ZKSCAN3 to occur was performed. The reaction was incubated at room temperature overnight and stopped with the addition of 2X PSB containing 100 mM DTT. Western blot analysis of the reaction mixture with anti-ZKSCAN3 revealed an additional species present 20 kDa above the 60 kDa band associated with ZKSCAN3 (Figure 11B). In reactions without IpaH9.8 or with a catalytically inactive C337A mutant of IpaH9.8, this species is not present (Figure 11B). Ubiquitin is 8 kDa, and the ubiquitin used for the reaction was HA-tagged, therefore increasing the size to 9.5 kDa. I hypothesize that IpaH9.8 catalyzes the addition of two monoubiquitin residues, which would account for the 20 kDa increase. This is quite different in comparison to previous studies of IpaH9.8 E3 ligase activity. Ashida *et al.* showed polyubiquitination of NEMO by IpaH9.8, and Rohde *et al.* showed polyubiquitination of MAPKK Ste7 in yeast and most recently Suzuki *et al.* showed that IpaH7.8 polyubiquitinates substrate glomulin (Rohde *et al.*, 2007, Ashida *et al.*, 2010, Suzuki *et al.*, 2014b). This is the first example of IpaH9.8 acting upon a substrate without utilizing polyubiquitination. I shared the reagents that I constructed with the laboratory of Dr. Frank Sicheri and they have independently validated that ZKSCAN3 is di-

ubiquitinated by IpaH9.8 in a cell free system and their results mirror my own (data not shown).

3.3 Autophagy and IpaH9.8

3.3.3 Evidence of *in vitro* ubiquitination of ZKSCAN3 is difficult to find

Stable IpaH9.8-expressing HEK293T cells were established through retroviral transduction. Codon-optimized transcripts were designed and synthesized by Genewiz and cloned into retroviral transduction vector pBMN. The vectors were transfected into Phoenix cells and virus was collected 2 days later. The virus was then used to transduce target HEK293T cells. Transduced cells were selected using puromycin treatment. Cells were harvested and assessed for expression of IpaH9.8. Due to the autoregulatory activity of IpaH9.8, proteasome inhibitor (MG132) treatment was required to observe IpaH9.8 (Figure 12A). These data are consistent with the notion that in mammalian cells, IpaH9.8 autoubiquitinates and is degraded by the proteasome. To investigate if ZKSCAN3 is ubiquitinated by IpaH9.8 *in vivo*, cell lysates were analyzed using SDS-PAGE and Western blot. Probing PVDF membranes with anti-ZKSCAN3 antibody showed no observable differences in the expression level of ZKSCAN3 between control, WT-IpaH9.8, and catalytically dead C337A-IpaH9.8 (mutation of cysteine at 337 to alanine) cells. Additionally, the presence of background bands made it difficult to observe changes in ZKSCAN3 within the WT-IpaH9.8 cells (Figure 12B).

HEK293T cells are human embryonic kidney cells and while they are easy to grow and manipulate in the laboratory, they are not a physiologically relevant cell line for examining *Shigella* infection. Therefore, a more relevant cell line, U937 macrophage-like

cells, was examined. These cells were infected with WT, Δ*ipaH9.8,* and Δ*ipaH9.8*Δ*2* strains of *Shigella.* Cells were harvested and protein levels were examined through SDS-PAGE and Western blot. I was unable to draw any conclusions from the ZKSCAN3 Western blot due to a large amount of background (Figure 13B). In addition to examining infected U937 cells, lentivirus transduction system was used to establish U937 cells stably expressing WT-IpaH9.8 (Figure 13A). Retrovirus transduction is not effective with U937 cells, so lentivirus was used instead. The same codon-optimized version of WT-IpaH9.8 was cloned into lentiviral packaging vectors. Virus containing the gene of interest was collected following transfection of HEK293T cells with three essential lentiviral vectors: psPAX2, vector required for packaging of viral components; pMD.2G, vector encoding viral envelope proteins; and pLJM1B*, vector containing the gene of interest. Virus was then used to transduce the U937 cells and blasticidin was used to select for cells expressing our gene of interest. Cell lysates were collected and SDS-PAGE and Western blot analysis revealed that ZKSCAN3 expression in these cell lines remained unchanged as well (Figure 13A).

3.3.2 IpaH9.8-Expressing HEK293T Cells Have Increased Autophagy

Although I did not observe modification of ZKSCAN3 in IpaH9.8 expressing cells, I investigated the possibility that IpaH9.8 was inducing autophagy. I examined the levels of autophagy marker LC3B when IpaH9.8 was present. LC3B is a common indicator of autophagic levels and is also one of many proteins that are repressed by ZKSCAN3 (Chauhan *et al.*, 2013). Two species may be evident in immunoblotting, corresponding to LC3B-I and LC3B-II. LC3B-I has a smaller molecular weight than

LC3B-II, but LC3B-II is bound to PE, increasing its hydrophobicity, which makes the protein migrate further in SDS-PAGE. LC3B-II is the autophagosome-bound isoform, and is often used to measure the level of autophagy induction. Interestingly, LC3B I and II levels were increased in HEK293T cells expressing WT-IpaH9.8 (Figure 14). This suggests that IpaH9.8 increases overall levels of LC3B.

3.3.3 U937 Macrophage-like Cells Have Increased Autophagy in the Presence of IpaH9.8

There was no evidence of ZKSCAN3 modification in the presence of IpaH9.8 in U937 cells. However, due to the increase in the autophagy marker LC3B in HEK293T cells, LC3B expression was examined in U937 cells infected with WT, Δ*ipaH9.8,* and Δ*ipaH9.8*Δ*2* strains of *Shigella.* Consistent with results obtained in HEK293T cells, LC3B expression was increased in U937 cells infected with WT *Shigella* compared to cells infected with either knockout strain (Figure 15A). Moreover, additional experiments in U937 stable cell lines revealed that in the presence of WT-IpaH9.8 there was increased LC3B (Figure 15B). These data support the notion that IpaH9.8 induces autophagy.

3.3.4. Macrophage Cytokine Analysis

During the mouse infection studies I did not observe any changes in cytokines with any confidence. Therefore, I set out to identify the possible cytokine changes during infection of cultured U937 macrophage-like cells. Unlike mice, a cell culture model provides less variability and various time points can be examined to provide optimized results. Additionally, there are many variables during mouse infection studies that could

interfere with the production of reliable results. As well, the most severe effects of IpaH9.8 could be in early infection, and it could be possible that day 3 of infection is too late to see any difference.

U937 cells can secrete IL-1 β, which was of particular interest for my studies. IL-1 β is produced by macrophages as a pro-protein (pro-IL-1 β, 31 kDa) and is cleaved by caspase-1 into its mature form (17.5 kDa) and is important in mediating the inflammatory response. In addition, Ashida and coworkers (2010) observed an increase in IL-1 β in mice infected with Δ*ipaH9.8 Shigella* (Ashida et al., 2010). U937 cells were infected with WT, Δ*ipaH9.8,* and Δ*ipaH9.8*Δ*2* strains of *Shigella* for 1 hour at 37°C and then supernatants were collected and TCA precipitation was used to concentrate the proteins in the supernatant. The resulting pellet was resuspended in 2X PSB and used for SDS-PAGE and Western blot analysis. Membranes were probed for IL-1 β and there was an increase in IL-1 β (pro and mature) in samples prepared from cells infected with WT *Shigella* when compared to uninfected controls. However, there was >2-fold increase in secretion of both pro and mature IL-1 β in samples prepared from cells infected with Δ*ipaH9.8* and Δ*ipaH9.8*Δ*2* strains (Figure 16). Thus, in the absence of IpaH9.8, there is increased IL-1 β secreted. This suggests that IpaH9.8 is involved with the suppression of IL-1 β production and cleavage to its mature state. Additionally, a 27 kDa species of IL-1 β was observed in cells infected with WT *Shigella*. In the literature this has been reported to be an intermediate and there has been no functional role described for the 27 kDa IL-1 β species (Brough *et al.*, 2007).

3.4 Reverse Transcriptase Qualitative PCR Analysis of ZKSCAN3-controlled genes

Reverse Transcriptase (RT) qualitative (q) PCR was used to examine the transcript levels of autophagy-related ZKSCAN3-controlled genes. The gene encoding LC3B is repressed by the transcription factor ZKSCAN3 and so I reasoned that the observed increase in protein expression of LC3B may be due to an increase in transcript levels. Primers were designed to target three different transcripts: LC3B transcript; WIPI2 transcript, a gene that is solely regulated by ZKSCAN3 and a protein that plays a role in early autophagosome formation; and RPL13A transcript, a housekeeping gene encoding ribosomal protein L13a, part of the 60S ribosomal subunit (Chauhan *et al.*, 2013, Pietrocola *et al.*, 2013). RNA was extracted from U937 cells infected with WT, Δ*ipaH9.8,* and Δ*ipaH9.8*Δ*2* strains of *Shigella* and control uninfected cells. qPCR data was analyzed using the $2^{-\Delta\Delta Ct}$ method described by Levik (2001). Inconsistent with my hypothesis, there was no change in LC3B or WIPI2 transcript levels between cells infected with WT *Shigella* and mutant strains of *Shigella* (Figure 17A&B).

3.5 LC3B Promoter Controlled Luciferase Assay

Another method of examining promoter and transcription factor activity is through luciferase constructs. The LC3B promoter region was cloned into a luciferase vector, pGL4.26 and used to assess the activity of the transcription factor ZKSCAN3 in the presence and absence of IpaH9.8. HEK293T cells were transfected with the pGL4.26-LC3 promoter vector and an additional vector for over-expression of ZKSCAN3. Cells were infected with WT, Δ*ipaH9.8,* and Δ*ipaH9.8*Δ*2* strains of *Shigella* and luciferase activity was examined in each condition. In cells infected with the single knockout,

ipaH9.8, luciferase activity were decreased compared to WT-infected cells however the means did not differ significantly (Figure 18). In cells infected with the double knockout, Δ*ipaH9.8*Δ*2,* luciferase activity was decreased significantly compared to WT-infected cells (Figure 18). This data supports the idea that IpaH9.8 promotes autophagy by increasing autophagy components, such as LC3 at the level of transcription. Also this data reveals that there may be overlap in the functions of closely related effectors IpaH9.8 and IpaH2, as infection with the double mutant showed a significant decrease in luciferase activity within cells.

3.6 ZKSCAN3 Forms Increased Puncta in the Presence of IpaH9.8

U937 cells stably expressing WT-IpaH9.8 were differentiated into macrophages using PMA and seeded onto poly-lysine treated coverslips. Cells were fixed and immunostained, probing for ZKSCAN3. Figure 19A shows microscopy images representing what was observed. ZKSCAN3 did not appear to localize to any specific cellular compartment, however there was the presence of concentrated ZKSCAN3 puncta. The puncta were present in both control U937s and WT-IpaH9.8-expressing U937s, but there were increased puncta in the IpaH9.8-expressing cells by ~2 fold (Figure 19B). In addition, control U937 cells showed more perfuse staining than WT-IpaH9.8 U937 cells. This suggests that IpaH9.8 promotes the formation of ZKSCAN3 aggregates, potentially aiding in the inactivation of ZKSCAN3.

CHAPTER 4: DISCUSSION

4.1: The role of IpaH9.8 in an oral model of infection.

The Rohde lab has established the use of the streptomycin mouse model, as it provides physiological relevance since *Shigella* successfully colonizes the GI tract. This model has been very successful in our lab and we observe many phenotypes associated with illness in the mice, including a robust weight-loss.

I infected mice with two knockout strains of *Shigella*, Δ*ipaH9.8,* and Δ*ipaH9.8*Δ*2,* along with WT-*Shigella.* Mice infected with either of the knockout strains displayed a 2 fold-lower clinical score when compared to WT-infected. Additionally, the bacterial burdens from the cecum contents and spleen revealed lower CFUs in knockout-infected when mice compared to WT-infected. By contrast, there were no significant differences in bacterial burden from liver or fecal samples between any of the infection groups. It is possible that the disease may not have had enough time to sufficiently colonize the liver in my experimental time frame of 3 days. Additionally, many recent studies have become skeptical of the use of fecal samples as a measurement of colonization. Successful colonization also involves invasion, therefore the majority of the bacteria may be thriving within the tissue and submucosa, rather than within the colon itself. This could explain why the fecal samples did not show any differences in bacterial burden. An alternative method to measure bacterial burden could be to homogenize a portion of the colon tissue or to perform a "scrape" of the colonic epithelium upon sacrifice of the animals. In support my findings, mice infected intranasally with a Δ*ipaH9.8* strain of *Shigella* reported by Ashida *et al.* also observed decreased bacterial

burden within the lungs of knockout-infected mice (Ashida *et al.*, 2010). Another study, done by Wang *et al.* examined the effects of infecting mice intranasally with a Δ*ipaH4.5* strain of *Shigella* (Wang et al., 2013). This study observed a 3-fold decrease in the bacterial burden on mice infected with the knockout strain. Although IpaH4.5 and IpaH9.8 are not as closely related as IpaH9.8 and IpaH2, they are all coregulated, encoded by the virulence plasmid of *Shigella,* and their targets and functions may be similar or behave in a synergistic manner.

In the analysis of the histology of colon tissue from each infection group there were some differences that were observed. There was an increase in the influx of immune cells during WT-*Shigella* infection, which could compromise barrier function of the gut and aid in dissemination of bacteria. Interestingly, the crypts in the colon are disrupted and seem smaller in Δ*ipaH9.8*- and Δ*ipaH9.8*Δ*2*-infected mice. In the Δ*ipaH9.8*- and Δ*ipaH9.8*Δ*2*-infected mice there also appears to be a thickening of the muscle layer. These differences are subtle compared to infection of the intestinal tract by other Gram-negative bacteria. *Salmonella typhimurium* destroy the cells lining the crypts of the intestine, the damage done by *Shigella* appears to be quite mild in comparison. Martino *et al.* were the first to describe this model of shigellosis, and their histological analysis revealed distinct changes in the colonic tissue, such as induction of apoptosis and strong presence of infiltrating PMLs with WT *Shigella* infection (Martino *et al.*, 2005). They also observed hepatocyte death in the liver, which I did not observe. Their experiments were also performed on Balb/c mice, however they examined earlier and later time points (1 and 5 dpi). This different time frame used to examine liver pathology may explain the different results. A recent report by Chang and coworkers observed increases in

autophagy in the small intestine of *Shigella*-infected mice after 6 hours of infection (Chang *et al.* 2013). Taken together, these reports illustrate the difficulties of pinpointing the temporal and spatial conditions that cause illness in animal models of infection.

Proinflammatory cytokine levels in colon and blood serum of infected mice were analyzed with ELISAs however this did not inform the phenotypes observed. There was no significant difference in TNFα observed between the three groups. There was no difference in IL-1 β and IL-6 in WT-infected mice compared to Δ*ipaH9.8*- and Δ*ipaH9.8*Δ*2*-infected mice. This was in contrast to what previous studies had reported when using a pulmonary model of infection. Ashida and coworkers found that MIP-2, IL-6 and IL-1 β were all increased in the absence of WT-IpaH9.8 (Ashida *et al.*, 2010). These differences could be attributed to many things. The mouse experiments done by Ashida *et al.* were performed through intranasal infections, therefore the infection would likely exist in the lung as apposed to oral infection and colonization of the colon (Ashida *et al.*, 2010). Environmental factors alone could account for the differences in cytokines. For example, there are likely to be significant differences in the amounts of antimicrobial peptides in the environment of the mouse lung vs. that of the gut. This is of particular interest given that Sperandio and coworkers have demonstrated that MxiE dependent factors (that include IpaH9.8) are required for *Shigella* to dampen the production of antimicrobial peptides and invade deeper tissues of the gut (Sperandio *et al.*, 2008). As well, the course of infection used by Ashida and coworkers was 1-2 days, compared to my 3 day experiments. Further into the chapter I will discuss my observations of IL-1 β expression in *Shigella*-infected macrophages and how these results are more in line with what was observed by Ashida.

4.2: Confirmation of IpaH9.8 Substrate ZKSCAN3

The search for substrates of bacterial E3 ligases is challenging. While we have a solid understanding of how bacterial E3 ligases behave catalytically, the target proteins of bacterial E3 ligases remain elusive. Substrates of E3 ligases are difficult to identify because they ubiquitinate their substrates, and in many cases ubiquitination leads to degradation (although this is not always the case). Yeast two-hybrid experiments have been used to identify potential substrates of *Shigella* IpaHs, including: glomulin (IpaH7.8 substrate); ABIN-1/NEMO (IpaH9.8 substrate); p65 (IpaH4.5 substrate); and splicing factor U2AF (IpaH9.8 substrate) (Okuda *et al.*, 2005, Ashida *et al.*, 2010, Wang *et al.*, 2013, Suzuki *et al.*, 2014b). Former post-doc, Dr. Jeremy Benjamin, performed a yeast two-hybrid screen with CD-IpaH9.8 as bait. Of the list of potential substrates, one of the top hits with a high level of confidence was also relevant to immune function. This potential substrate of IpaH9.8 was identified as ZKSCAN3.

ZKSCAN3 was originally identified as a novel driver of colon cancer (Yang *et al.*, 2008). There was little information on the function or role of ZKSCAN3 within the cell. During the course of my thesis studies, Boyd and coworkers described a molecular role for ZKSCAN3. ZKSCAN3 was shown to be a transcriptional repressor for genes that govern autophagy (Chauhan *et al.*, 2013). They provided clear evidence through luciferase reporters and qPCR showing the effects ZKSCAN3 has on > 60 autophagy and lysosomal biogenesis associated genes, specifically decreasing expression of *MAP1LC3B* (encodes LC3B) and *WIPI2* (encodes WIPI2). They also observed the shuttling of ZKSCAN3 in and out of the nucleus, dependent upon starvation and stress conditions.

To confirm that ZKSCAN3 is in fact a substrate of IpaH9.8, IpaH9.8 must ubiquitinate ZKSCAN3 *in vitro.* ZKSCAN3 was cloned into a vector designed for GST fusion protein expression and purified with glutathione coated agarose beads. I was able to perform an *in vitro* reaction containing the necessary components for ubiquitination: E1, E2, ubiquitin, IpaH9.8, ZKSCAN3, and reaction buffer containing co-factors for the ubiquitin enzymes. The reaction proceeded at room temperature overnight and was stopped with the addition of 2X PSB with DTT and boiling the samples for 5 minutes. Anti-ZKSCAN3 antibody revealed a unique species 20 kDa above ZKSCAN3 (61 kDa) in the presence of IpaH9.8 within a cell-free system. Previous work on IpaH9.8 had only showed the ability of IpaH9.8 to polymerize polyubiquitin chains on substrates, which normally results in a smearing effect in the space about the normal molecular weight band (Rohde *et al.*, 2007, Ashida *et al.*, 2010). This was not present in my experiments. I hypothesize that the mobility shift is likely due to two monoubiquitin additions to ZKSCAN3, since the HA-tagged ubiquitin used for the reactions has a molecular weight of 9.5 kDa.

Next I set out to support my findings using *in vitro* cell culture. Retroviral and lentiviral transduction systems were used to transduce codon-optimized versions of IpaH9.8 into HEK293T cells and U937 cells, respectively. Cell lysates from HEK293T cells stably expressing WT-IpaH9.8 and CD-IpaH9.8 were examined using SDS-PAGE and Western blot techniques. Probing membranes with anti-ZKSCAN3 antibody did not reveal the 80 kDa ZKSCAN species observed in my previous experiments. Additionally, there was no evidence for increased or decreased expression of ZKSCAN3 in the presence of WT-IpaH9.8. The ZSKCAN3 antibody used was not very specific, as there

was a large amount of background present in the Western blot. The high background hindered my ability to identify possible differences in modifications of ZKSCAN3. There is also the possibility that the effect is very subtle, making it more difficult to identify. It should be noted that E3-substrate modifications may be very difficult to observe in their cellular context. This is demonstrated by the NEL domain SspH1-PKN1 interaction. While this interaction has physiological consequences, it was difficult to demonstrate and required structural analysis and the creation of SspH1-resistant variants of PKN1 to conclusively show an enzyme-substrate interaction (Keszei *et al.*, 2014).

ZKSCAN3 is able to translocate in and out of the nucleus, and so is IpaH9.8. I theorize that the monoubiquitination of ZKSCAN3 results in its inactivation and possible exclusion of ZKSCAN3 from the nucleus. A similar example of such regulation has been described for the RelA (p65) subunit of NF-κB. Hochrainer *et al.* observed that hypo-phosphorylated RelA in the nucleus is monoubiquitinated multiple times and the presence of this modified RelA resulted in decreased NF-κB transcriptional activity (Hochrainer *et al.*, 2012). They also showed that the inactivation of RelA was independent of proteasomal activity, therefore the activity of RelA is regulated independently of degradation. A well-known example of this is the monoubiquination of histones H2A and H2B. Histones are subject to many post-translational modifications, methylation, acetylation, phosphorylation and now ubiquitination as well (Cole *et al.*, 2014). Monoubiquitination of H2B has been implicated in transcription and response to DNA damage (Mueller *et al.*, 1985). Specifically, the ubiquitination of lysine 120 on H2B results in disruption of chromatin strands, leading to a more open conformation (Fierz *et al.*, 2011). There is evidence suggesting that monoubiquitinated H2B also recruits

proteins for transcription (Shema-Yaacoby *et al.*, 2013). Conversely, histone H2A is ubiquitinated at lysine 119 and this modification is associated with the silencing gene expression (Osley *et al.*, 2006, Weake *et al.*, 2008). This exemplifies how diverse monoubiquitination modifications can be and how they can control gene expression. The precise mechanisms by which monoubiquitination alters histone function await structural analysis.

I had the opportunity to travel to Paris, France and collaborate with Dr. Jost Enninga and his group at the Pasteur Institute. While there, I explored my hypothesis that IpaH9.8 ubiquitinates ZKSCAN3 and alters localization of the protein. IpaH9.8 lentiviral transduced U937 cells were differentiated into macrophages, immunostained and examined by fluorescent microscopy. I was unable to determine if ZKSCAN3 was exported out of the nucleus in the presence of IpaH9.8 due to the fact that U937 cells have large nuclei that occupy the majority of the space within the cell. These technical difficulties made it impossible to determine the localization of ZKSCAN3 with any certainty, however I did make an interesting observation. I found that in cells expressing IpaH9.8, there was an increase in the presence of small foci in the ZKSCAN3 channel. Qualification of these foci revealed ~2-fold increase in foci with the expression of IpaH9.8. This data suggest that a functional interaction is occurs between IpaH9.8 and ZKSCAN3. Follow up on this data to see if the localization of the ZKSCAN3 foci is different in cells with IpaH9.8 would be interesting, however a suitable cell type would need to be identified.

4.3: IpaH9.8 and Autophagy

I examined the effect of IpaH9.8 on the autophagy pathway. I observed a striking phenotype; in the presence of IpaH9.8 there was an increase in autophagy marker LC3B. This result was observed consistently within two sets of stable cell lines expressing IpaH9.8 in two different cell types (HEK293T cells and U937 cells). Additionally, U937 cells infected with WT-*Shigella* also had increased levels of LC3B. While infections with Δ*ipaH9.8* and Δ*ipaH9.8*Δ*2* strains had levels of LC3B that were below uninfected cells. This suggests that IpaH9.8 interferes with the regulation of autophagy, potentially through interactions with ZKSCAN3.

To further examine the interaction, RT qPCR was used to assess transcript levels of two ZKSCAN3-controlled genes, *MAP1LC3B* (LC3B) and *WIPI2* (WIPI2). These proteins were both identified as being regulated by ZKSCAN3 and with *WIPI2* expression being almost exclusively subject to ZKSCAN3 control (Pietrocola *et al.*, 2013). Using RNA collected from U937 cells infected with WT, Δ*ipaH9.8* and Δ*ipaH9.8*Δ*2* strains of *Shigella,* I did not observe a change in transcript levels of LC3B or WIPI2 in these cells. I also cloned the *MAP1LC3B* promoter region into a luciferase vector and I measured a decrease in luciferase activity in HEK293T cells infected with Δ*ipaH9.8*Δ*2 Shigella* compared to cells infected WT *Shigella.* The luciferase data provides evidence that IpaH9.8 is initiating autophagy within host cells at the transcriptional level. In regards to the qPCR data, the infection time that was examined was quite short, 1 hour post-infection, and perhaps examining longer time may reveal a more substantial difference between the infection strains.

Previous studies on *Shigella* and autophagy have established that *Shigella* possesses multiple mechanisms to in the evade capture and destruction by autophagy. *Shigella* evades the autophagic machinery with the aid of effector IcsB (Ogawa *et al.*, 2005). IscB binds to IscA on the surface of the bacteria and to Toca-1 (host protein) in the cytosol (Baxt *et al.*, 2014). This prevents recognition of *Shigella* by LRSAM1 and prevents ubiquitin-tagging of *Shigella.* Additionally, Baxt *et al.* proposed that IcsB and Toca-1 binding also facilitates actin-based motility of *Shigella*, which may also deter LRSAM1 from recognizing the bacteria present in the cytosol (Baxt *et al.*, 2014). Many intracellular replicating bacteria employ mechanisms for evasion of xenophagy and some have developed mechanisms that hijack the system for bacterial gain. One example of this is *Legionella pneumophila*; this pathogen inhibits the autophagosome-lysosome fusion event and is contained within the autophagic vacuole where the bacteria can safely replicate (Campoy *et al.*, 2009, Joshi *et al.*, 2011).

It may seem contradictory that *Shigella* is evading and initiating autophagy at the same time; however autophagy has many functions within the cell and is not limited to bacteria clearance. I hypothesize that the induction of autophagy by *Shigella* is a non-selective process aimed at recycling host proteins that may be used to support intracellular growth by *Shigella*. This idea is similar to that proposed by Price and coworkers that showed that the *Legionella* effector LubX (itself a bacterially encoded E3 ubiquitin ligase) provided fuel for the intracellular replication of *Legionella* through proteasome-dependent creation of free amino acids (Price *et al.*, 2011).

Another example of the benefits of autophagy in bacterial growth and replication was reported by Yu and coworkers (2014). Their experiments showed that autophagy

facilitates the replication of cytosolic *Salmonella*. They found that cytosolic bacteria had an increased association with autophagy factors p62 and LC3, which corresponded with increased *Salmonella* replication (hyperreplication). *Salmonella* replication in cells with siRNA knockdowns of autophagy-related proteins was also decreased (Yu *et al.*, 2014). In cells with hyperreplicating *Salmonella* and decreased autophagy, they observed increased activation of caspase-1 and caspase-3/7 leading to cell death. They suggest that the hyperreplication state of cytosolic *Salmonella* may be due to the increase in nutrients made available by the autophagosomes. In comparison, the *Salmonella*-containing vacuole (SCV) is relatively low in nutrient availability and therefore *Salmonella* replication is slow within these vacuoles. This study supports my hypothesis that intracellular bacteria utilize the host autophagy system to obtain nutrients required for intracellular replication and also shows a potential role for autophagy in evading cell death.

4.4: Proposed Mechanism of Action

Shigella is excellent at controlling the host environment. It is able to hijack host actin for motility, induces high levels of inflammation to help with bacterial dissemination and employs mechanisms for down-regulating targeted methods of bacterial clearance, such as xenophagy. It is well known that *Shigella* replicate within and eventually kill macrophages, a cell type that typically is involved with the destruction of bacterial invaders. Macrophages are prepared to deal with pathogens, yet somehow *Shigella* is undetected, or at the very least is able to disable the alarms. One mechanism involved in the immune response in macrophages is the inflammasome. Upon recognition

of pathogen-associated molecular patterns (PAMPs) by NLRs in the cytosol, the inflammasome complex is assembled. This complex is responsible for the major processing of the pro-forms of IL-1 β and IL-18 by caspase-1. Additionally, the inflammasome can mediate pyroptosis, specialized programmed cell death associated with proinflammatory response in immune cells. Pyropotosis of infected macrophages is a means of destroying intracellular bacteria that have invaded the cell. Interestingly, some studies have suggested that the effectiveness of pyroptosis is dependent on the multiplicity of infection (MOI). Lower MOIs lead to pyroptosis that is beneficial to the host, while pyroptosis associated with an MOI > 50 is more beneficial for the bacteria (Suzuki *et al.*, 2007, Willingham *et al.*, 2007, Miao *et al.*, 2010). These data are all based on *in vitro* cell culture studies, so it is difficult to determine if it is reflective of events during infection.

Therefore I propose that IpaH9.8 is inactivating ZKSCAN3 through multiple sites of monoubiquitination. By doing so, IpaH9.8 is turning on autophagy-associated genes (such as *MAP1LC3B* and *WIPI2*) to increase autophagy within the cell. Because autophagy is inherently a mode of recycling overexpressed proteins and has a role in the regulation of immune cascades, specifically the inflammasome, autophagic machinery targets inflammasome machinery for degradation. Therefore, IpaH9.8 is down-regulating the immune response and inhibiting the process of pyroptosis by inducing autophagy. Alternatively, IpaH9.8 is upregulating autophagy to induce non-selective autophagy to degrade abundant proteins and provide free amino acids and nutrients for growth in a similar manner to the function of *Legionella* effector LubX proposed by Price *et al.* (Price *et al.*, 2011). This is outlined in Figure 20. Research by Suzuki *et al.* showed that

inhibition of autophagy promoted cell death in *Shigella*-infected macrophages (Suzuki *et al.*, 2007). This indicates that the interplay between autophagy and the inflammasome are important in mediating pyroptosis. More specifically in regards to *Shigella,* autophagy is important in the protection against pyroptosis of infected macrophages. Since there is evidence supporting the benefits of pyroptosis at high MOIs, it could be possible that IpaH9.8 is just using autophagy to delay the onset of pyroptosis until the amount of bacteria has become sufficiently large to amount a strong survival rate once pyroptosis is initiated.

My theory nicely links all the data observed. I showed that in the presence of IpaH9.8, there is an increase in expression of LC3B at the transcriptional and translational levels, indicating an increase in autophagy. In support of the notion that the increase in autophagy is ZKSCAN3-dependent, I observed increased level of WIPI2 transcripts in the presence of IpaH9.8. Additionally, I show that IL-1 β secretion is decreased in WT-infected cells compared to Δ*ipaH9.8*- and Δ*ipaH9.8*Δ*2*-infected cells, suggesting that the inflammasome is disrupted in the presence of IpaH9.8. This may reflect an induction of autophagy since IL-1 β processing and secretion is regulated by the inflammasome. While this difference in IL-1 β was not observed in the mouse infection model, it could be due to a late time point. Cells are observed secreting IL-1 β early, after 2 hours, whereas cytokines from mouse infections are assessed 3 dpi. Lastly, in a mouse model of infection, I found that mice infected with WT *Shigella* were more ill and experienced higher bacterial burdens than Δ*ipaH9.8*- and Δ*ipaH9.8*Δ*2*-infected mice. In the knockout-infected mice, there is no IpaH9.8, and therefore no autophagy and the inflammasome is intact. Therefore in knockout infected mice, pyroptosis and cytokine

signaling is not delayed or disrupted, leading to normal clearance of bacteria, explaining why these mice are less sick and have lower bacteria burdens.

The large global burden inflicted by *Shigella* has driven research to better understand the pathogen and develop an effective vaccine. Over the last few decades our understanding of the disease progression has greatly expanded but we are still without a vaccine. The rise in antibiotic use worldwide has increased the occurrence of antimicrobial resistance in *Shigella,* making effective prevention measures more desirable. As we study host-pathogen interactions of *Shigella* with more depth we are able to design better treatment options. My research has helped to elucidate the role of IpaH9.8, a NEL-domain enzyme and effector of the T3SS of *Shigella.* The host autophagy-inflammasome interplay and the interference caused by *Shigella* may provide new insight into novel treatment options that help regulate the cross talk between these pathways. As well, studying host-pathogen interactions provides us with new information regarding the host immune response and gives us a better understanding of our own systems.

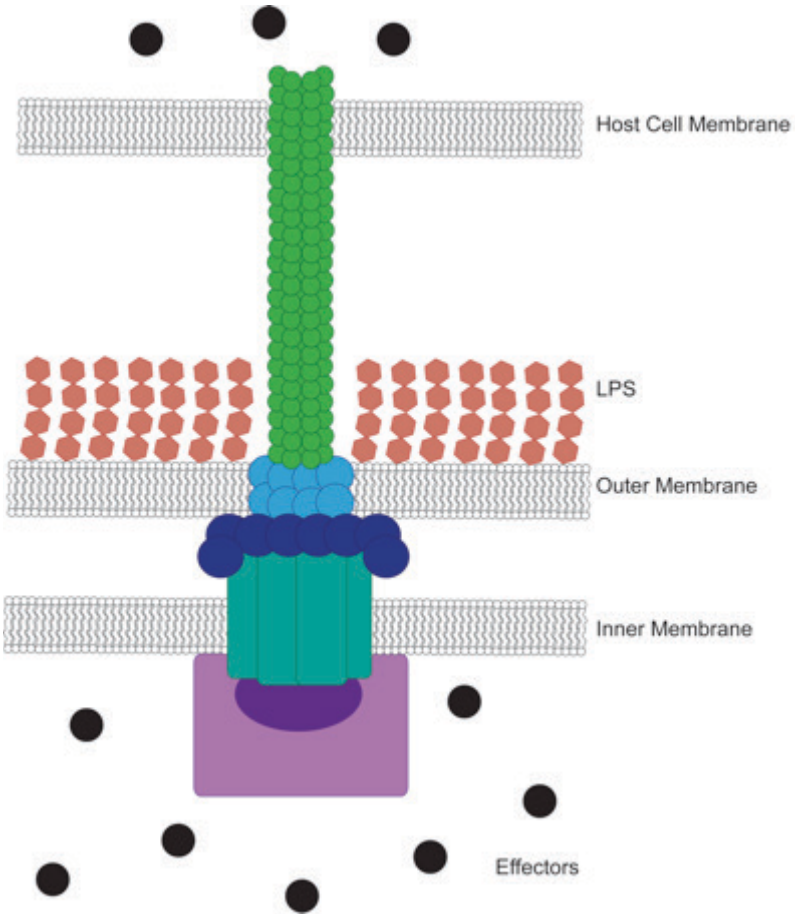

Figure 1: Structural diagram of the T3SS apparatus of *Shigella.*
The T3SS is composed of needle, basal body and C-ring components. The C-ring is the base of the structure and is composed of Spa33 and Spa47. Spanning the inner and outer membranes of the bacteria are MxiG, MxiJ, MxiD and MxiM, composing the basal body. The needle component is made of MxiH and MxiI. Black circles represent the various effectors translocated through the apparatus into the host cell. The needle component is shown protruding through the host cell lipid bilayer.

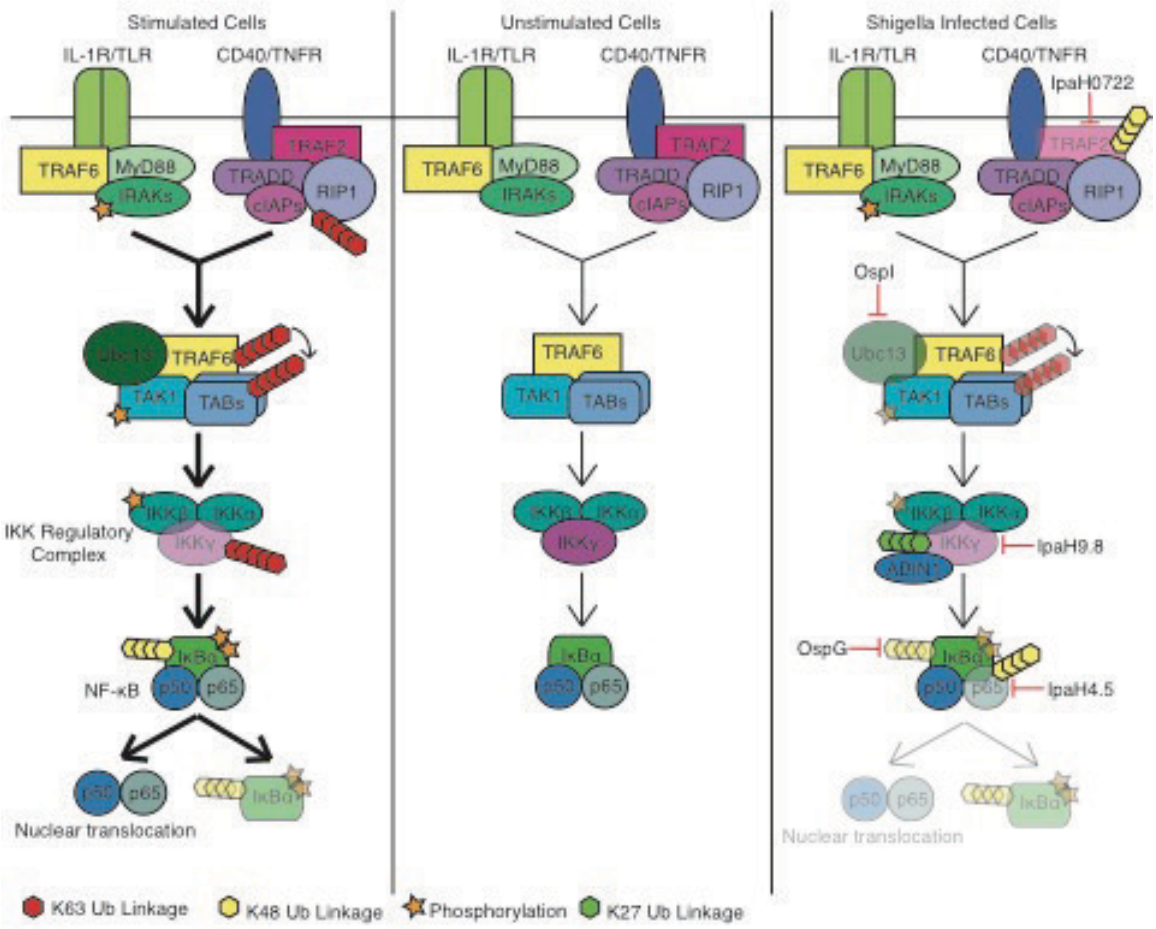

Figure 2: Side-by-side comparison of the NF-κB signaling in unstimulated, extracellular ligand-stimulated and *Shigella*-infected cells.
When unstimulated, the NF-κB pathway is not modified; therefore NF-κB complex remains bound to IκBα, inhibiting translocation into the nucleus. When receptors are stimulated by extracellular ligands, a series of post-translational modifications occur causing a signaling cascade. This results in the degradation of IκBα and nuclear translocation of free NF-κB. When cells are infected with *Shigella*, there are disruptions in the signaling cascade, preventing the NF-κB pathway from functioning properly. IpaH0722 ubiquitinates TRAF2 which targets it for degradation; OspI indirectly inhibits TRAF6 E3 ligase by deamidating Ubc13; OspG prevents degradation of IκBα; IpaH9.8 causes ABIN1-dependent ubiquitination of IKKλ; IpaH4.5 targets p65 subunit for degradation via ubiquitination. Transparency indicates degradation or reduced function.

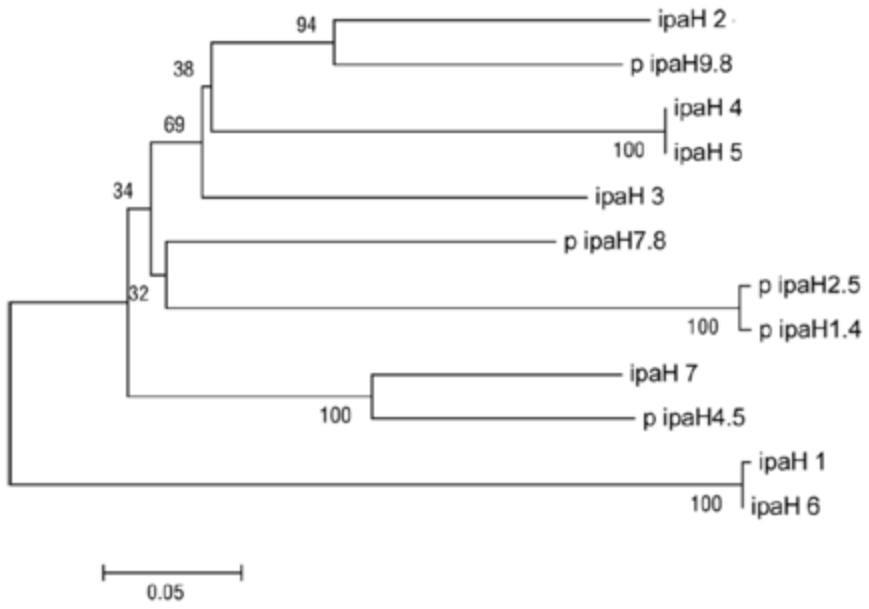

Figure 3: Phylogenetic tree displaying the relatedness of the *ipaH* genes of *S. flexneri* serotype 5a.
"p" found preceding the gene name indicates that it is located on the virulence plasmid. The values at each node on the tree represent the bootstrap value and the genetic distance measurement is located beneath the tree. The figure was created using the neighbor-joining method on a 515 amino acid data set. Credit for the figure belongs to Naoko Onodera.

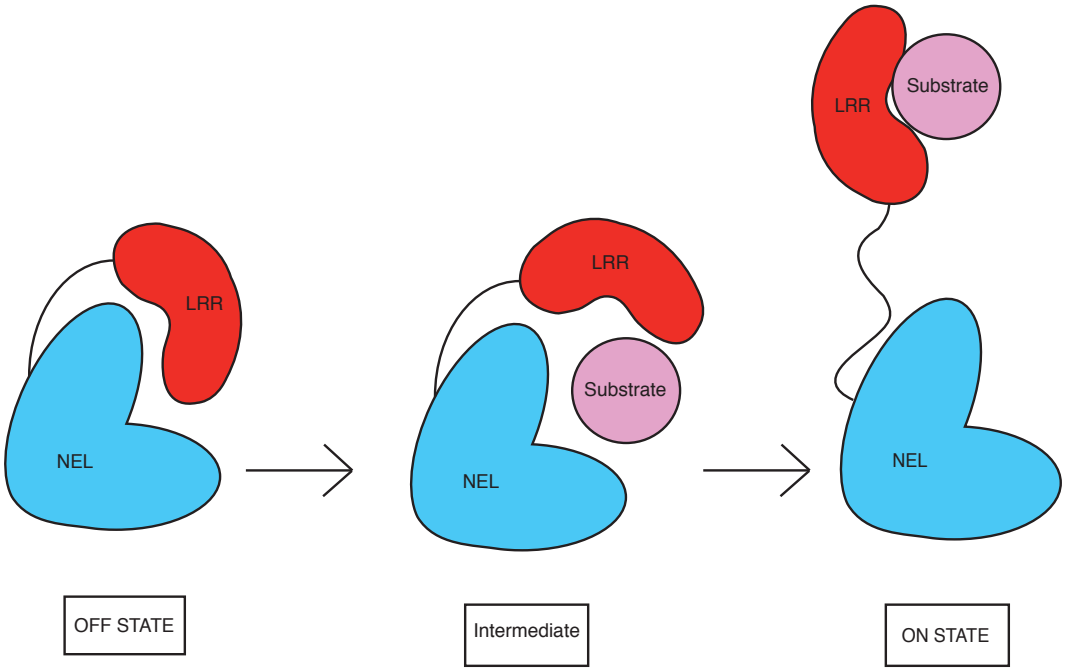

Figure 4: Schematic diagram outlining the ON and OFF states of IpaH proteins. The leucine rich region (LRR) domain folds over the catalytic novel E3 ligase (NEL) domain initiating the "Off" state in IpaHs. An intermediate is formed with the recognition of a substrate and then the confirmation opens fully to the "On" state. Open confirmation allows the substrate to bind to the LRR and activates E3 ligase activity.

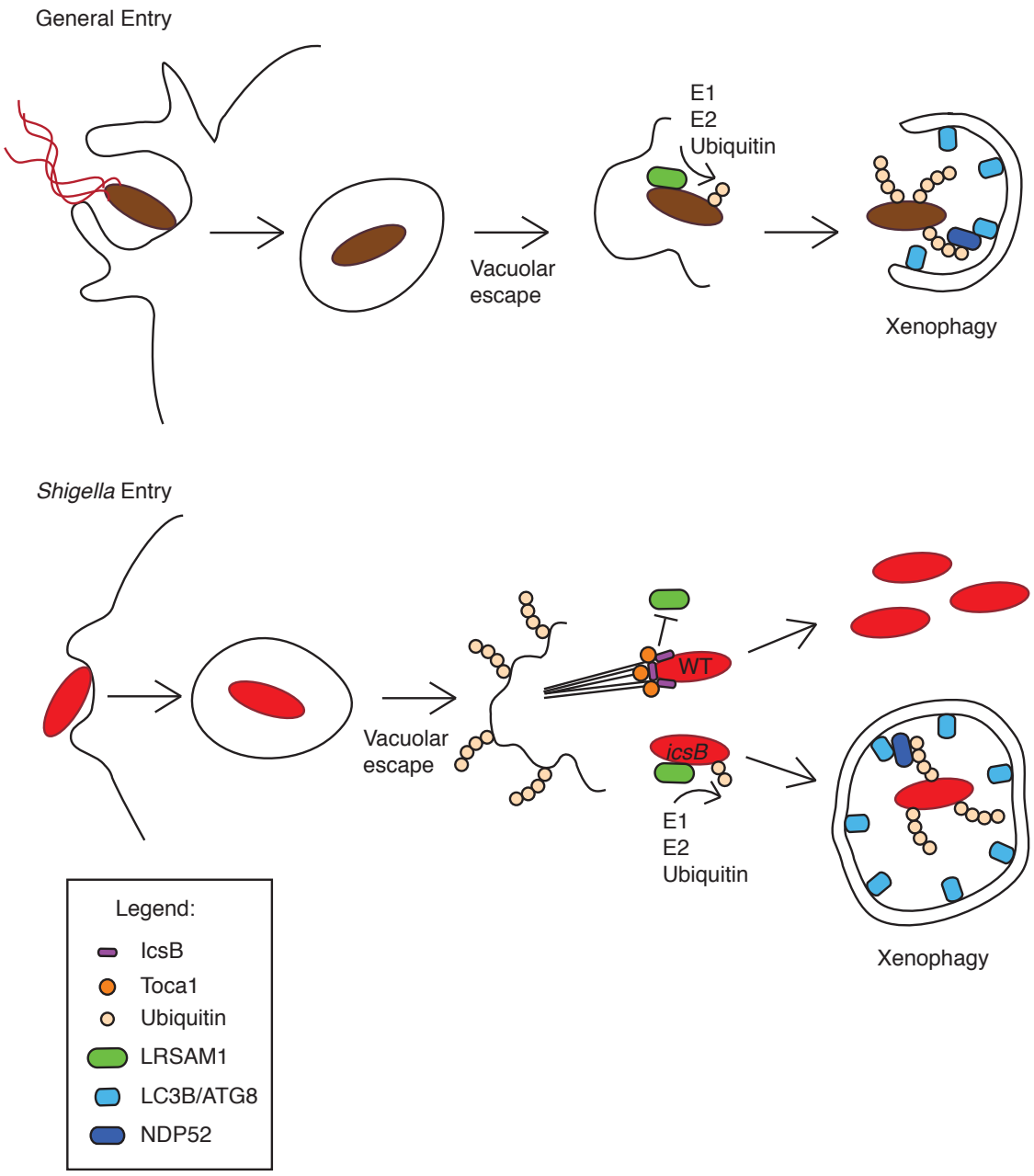

Figure 5: Bacterial clearance by xenophangy and *Shigella* evasion of xenophagy. General bacterial entry: Bacteria are phagocytosed into the mammalian cell. Many bacteria escape from the phagocytic vacuole to gain entry into the cytosol. LRSAM1 recognizes cytosolic bacteria, initiating K27 polyubiquitination of the bacteria. NDP52 recognizes and binds to K27 Ub and LC3 to initialize xenophagy and bacterial clearance. *Shigella* entry: *Shigella* gains entry through phagocytosis. *Shigella* escapes the vacuole and enters the cytosol, leaving behind ubiquitinated vacuolar remnants. IcsB recruits cellular protein Toca-1, inhibiting LRSAM1 recognition and initiates actin-based motility. *Shigella* is not ubiquitinated, thus evading xenophagy. In the absence of IcsB, LRSAM1 ubiquitinates *Shigella,* targeting the bacteria for clearance via xenophagy.

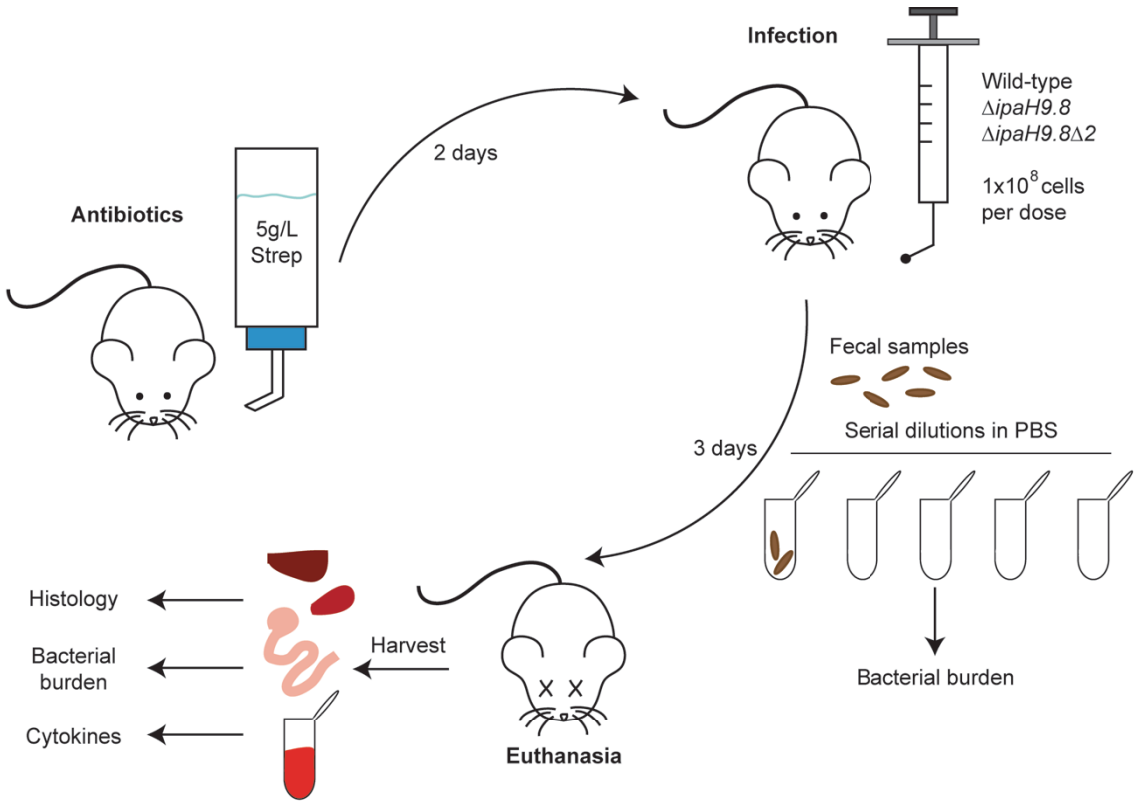

Figure 6: Pictorial representation of the mouse streptomycin model of *Shigella*. Mice are treated with streptomycin two days prior to infection. An oral dose of $1x10^8$ bacteria in 100 µL PBS is given to each mouse. Mice are monitored for three days post-infection, fecal samples are collected and used to assess bacterial burden. Mice are sacrificed on the third day via cardiac puncture and cervical dislocation. Blood, spleens, livers, cecums, and colons are harvested for experimental analysis.

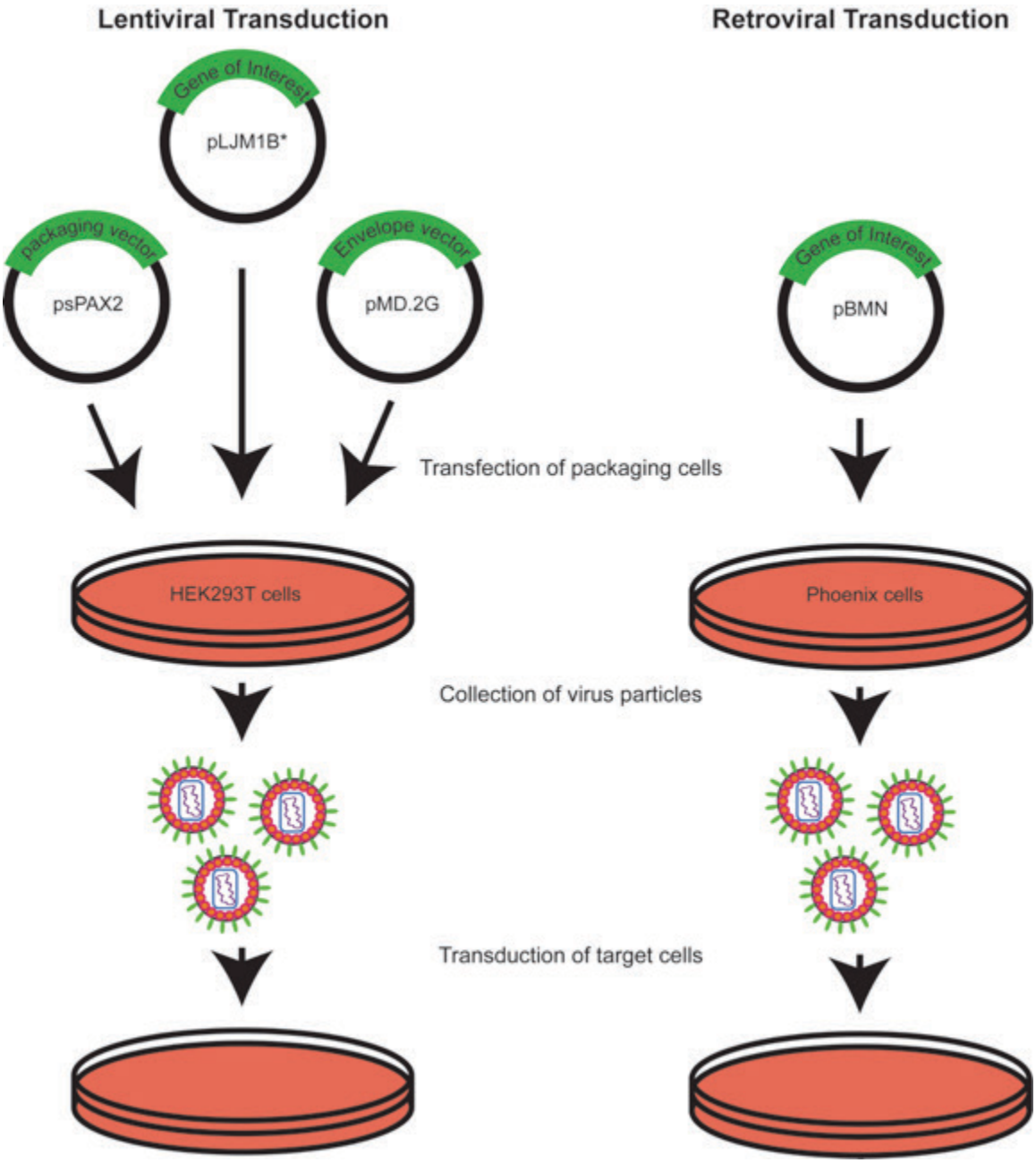

Figure 7: Comparative overview of lentiviral transduction versus retroviral transduction.
Virus packaging cells are transfected with lentiviral or retroviral vectors. One day later, virus is collected and used to transduce the target cell line. Target cells are incubated with virus and then following the recovery period, antibiotic is added to the media for selection.

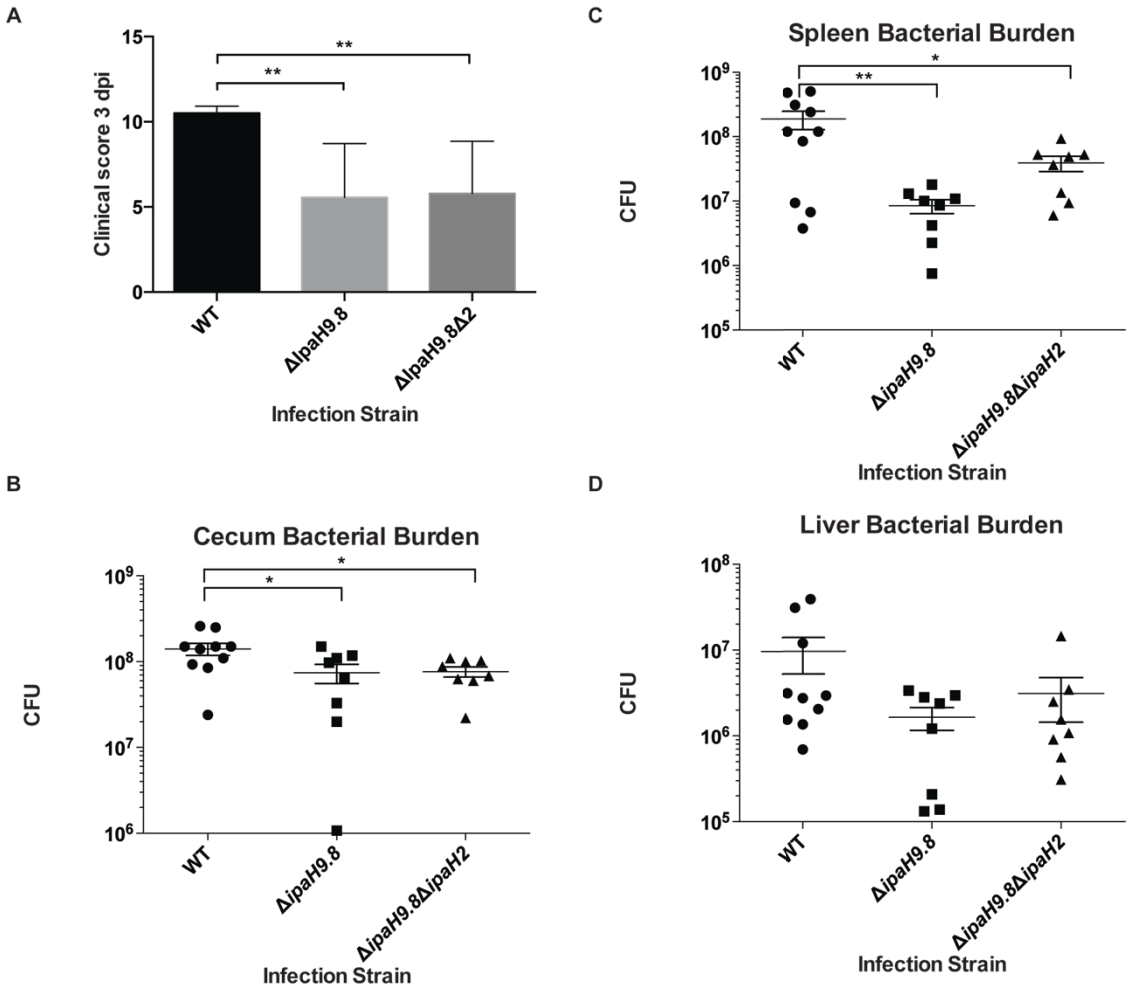

Figure 8: Mice infected with Δ*ipaH9.8* and Δ*ipaH9.8*Δ*2* strains of *Shigella* yield a lower degree of illness and decreased bacterial burdens.

(A) Graph containing clinical scores 3 days post infection (dpi) from mice infected with WT, Δ*ipaH9.8*, and Δ*ipaH9.8*Δ*2* strains of *Shigella*. Values of means ± standard deviation are displayed on each bar (WT *n*=10, Δ*ipaH9.8 n*=8, and Δ*ipaH9.8*Δ*2 n*=8 pooled data from two experiments). *** = P <0.001; ** =P <0.01. (B) Bacterial burden calculated from serial dilutions of the contents of the cecum of mice infected with WT, Δ*ipaH9.8*, and Δ*ipaH9.8*Δ*2* strains of *Shigella* collected 3 dpi. Values of means ± standard deviation are displayed in each column (WT *n*=10, Δ*ipaH9.8 n*=8, and Δ*ipaH9.8*Δ*2 n*=8 pooled data from two experiments). * = P<0.05. (C) Bacterial burden calculated from serial dilutions of homogenized spleen of mice infected with WT, Δ*ipaH9.8*, and Δ*ipaH9.8*Δ*2* strains of *Shigella* collected 3 dpi. * = P<0.05. Values of means ± standard deviation are displayed in each column (WT *n*=10, Δ*ipaH9.8 n*=8, and Δ*ipaH9.8*Δ*2 n*=8 pooled data from two experiments). (D) Bacterial burden calculated from serial dilutions of homogenized liver of mice infected with WT, Δ*ipaH9.8*, and Δ*ipaH9.8*Δ*2* strains of *Shigella* collected 3 dpi. Values of means ± standard deviation are displayed in each column (WT *n*=10, Δ*ipaH9.8 n*=8, and Δ*ipaH9.8*Δ*2 n*=8 pooled data from two experiments).

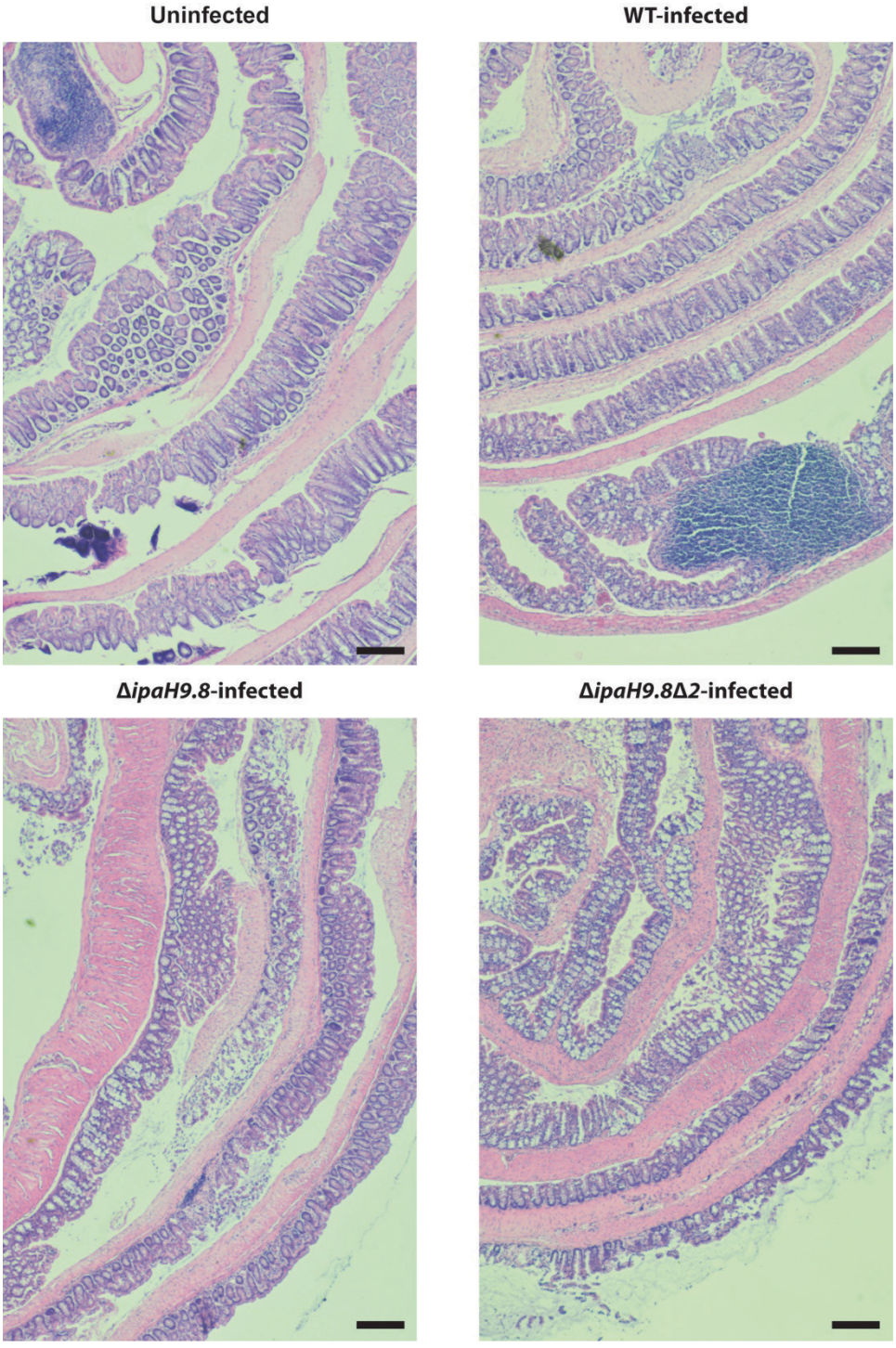

Figure 9: Histology from mice infected with Δ*ipaH9.8* and Δ*ipaH9.8*Δ*2* strains of *Shigella* show signs of cyrpt destruction and thickening of the muscle layer.
Images obtained from H&E stained histology samples from swiss-rolled colons from uninfected, WT-, Δ*ipaH9.8*-, and Δ*ipaH9.8*Δ*2*-infected mice 3 days post-infection. Pink indicates the muscle layer and dark blue areas represent mononuclear cells. Scale bars represent 200 μm.

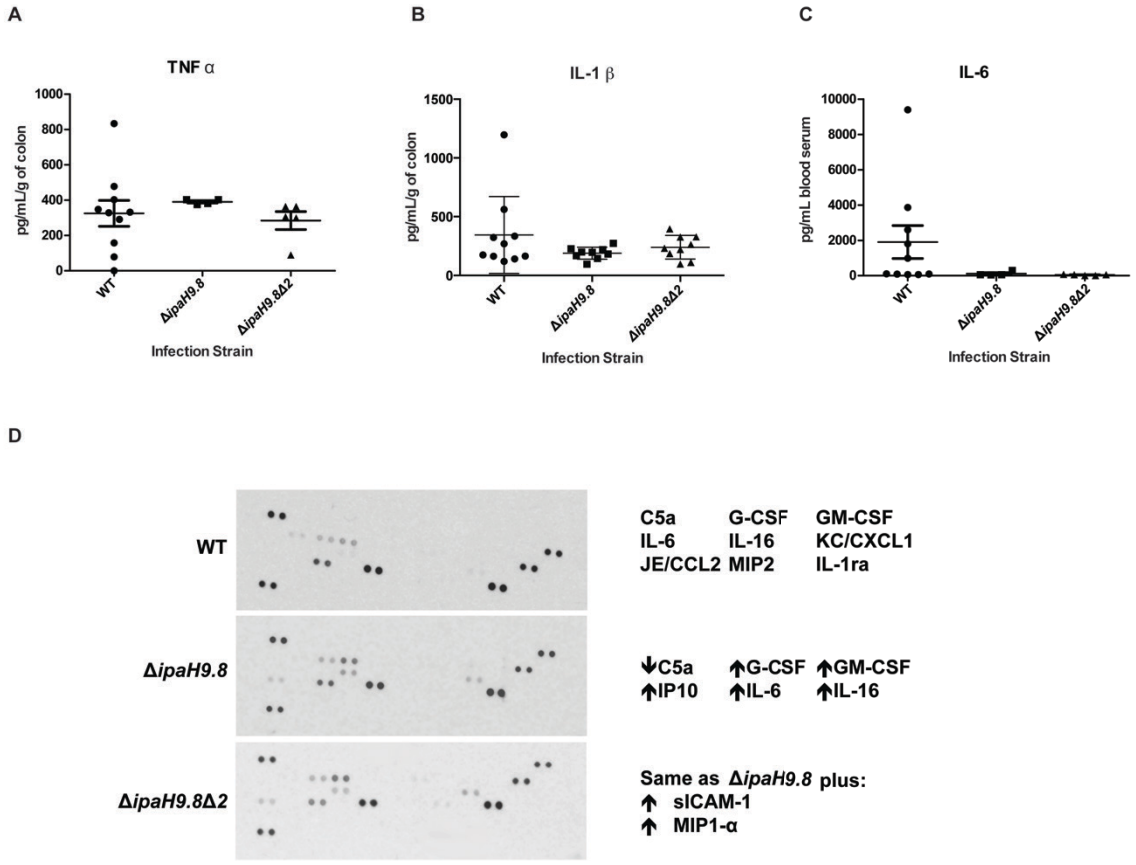

Figure 10: Cytokine levels in the colon and blood appear to have no differences between infection groups.

(A) TNF-α ELISA analysis of supernatant collected from mouse colons infected with WT, Δ*ipaH9.8*, and Δ*ipaH9.8*Δ*2* strains of *Shigella*. Values of means ± standard deviation are displayed in each column (WT *n*=10, Δ*ipaH9.8 n*=8, and Δ*ipaH9.8*Δ*2 n*=8 pooled data from two experiments) (B) IL-1 β ELISA analysis of supernatant collected from mouse colons infected with WT, Δ*ipaH9.8*, and Δ*ipaH9.8*Δ*2* strains of *S. flexneri*. Values of means ± standard deviation are displayed in each column (WT *n*=10, Δ*ipaH9.8 n*=8, and Δ*ipaH9.8*Δ*2 n*=8 pooled data from two experiments) (C) IL-6 ELISA analysis of blood serum collected from mice infected with WT, Δ*ipaH9.8*, and Δ*ipaH9.8*Δ*2* strains of *Shigella*. Values of means ± standard deviation are displayed in each column (WT *n*=10, Δ*ipaH9.8 n*=8, and Δ*ipaH9.8*Δ*2 n*=8 pooled data from two experiments) (D) Cytokine array analysis of supernatant collected from mouse colons infected with WT, Δ*ipaH9.8*, and Δ*ipaH9.8*Δ*2* strains of *Shigella*. To the right of the array panel lists the present cytokines and changes between WT-infected and knockout-infected.

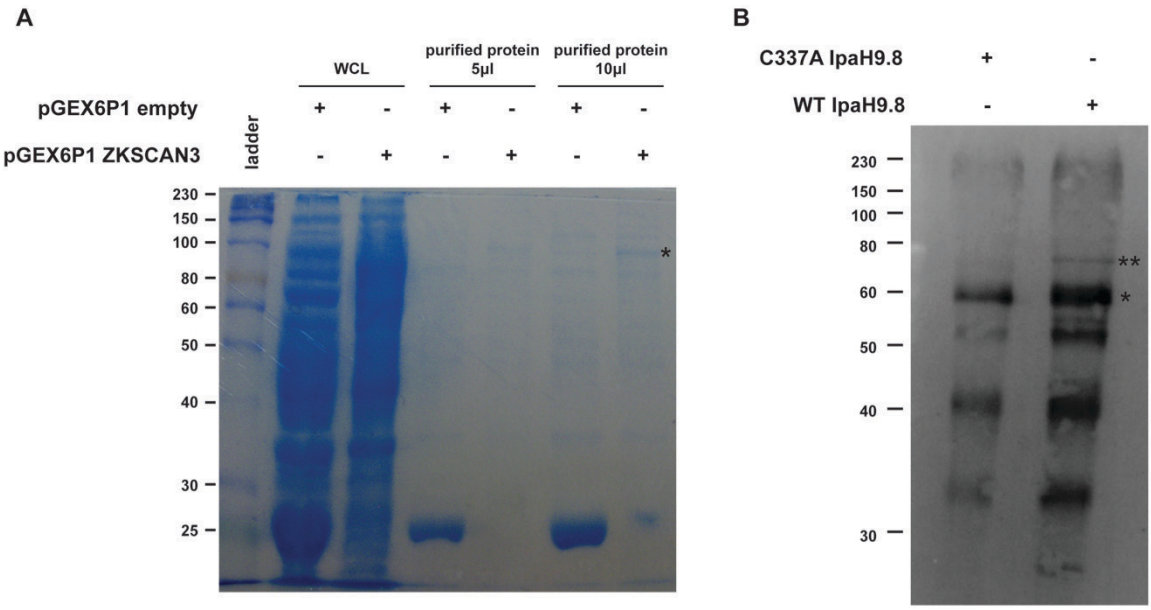

Figure 11: GST-purified ZKSCAN3 is ubiquitinated by IpaH9.8 in a cell free system.

(A) pGEX6P1 empty vector and pGEX6P1-ZKSCAN3 were used to transform BL21 *E. coli.* GST and GST-ZKSCAN3 were purified from cell lysate and examined with SDS-PAGE and stained with Pierce Protein Stain. WCL = whole cell lysate from BL21 *E. coli*. * indicates band belonging to GST-ZKSCAN3 (B) GST-ZKSCAN3 was purified and the GST-fusion protein was cleaved using PreScission Protease. Purified ZKSCAN3 was used as substrate in a cell free ubiquitination assay containing E1, E2, IpaH9.8 (wild-type, WT, or C337A, catalytically dead) and ubiquitin. Samples were separated with SDS-PAGE and then assessed with Western blotting, probing with anti-ZKSCAN3 antibody. * indicates ZKSCAN3 band. ** indicates unique di-ubiquitinated ZKSCAN3 band.

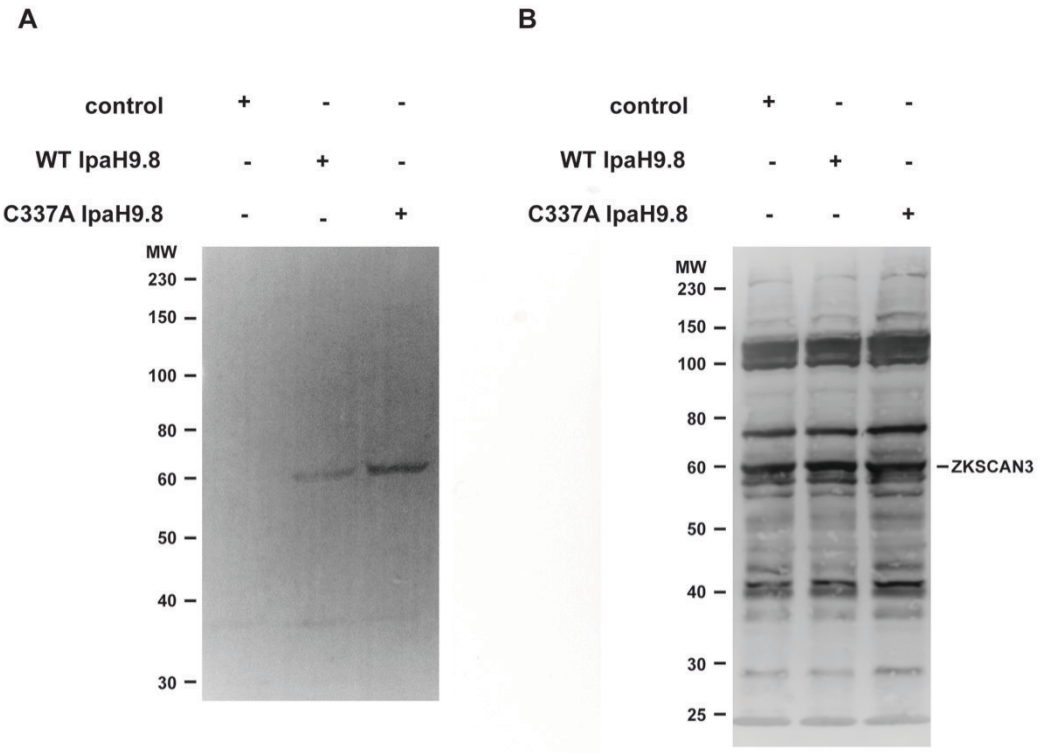

Figure 12: *In vitro* modifications of ZKSCAN3 in HEK293T cells stably expressing IpaH9.8 are inconclusive.
(A) Western blot of cell lysate of HEK293T cells expressing control (empty vector pBMN), WT IpaH9.8 (wild-type), or C337A (catalytically dead) IpaH9.8 probing with anti-IpaH antibody. Cells were treated with MG132 6 hours prior to harvesting. (B) Western blot of cell lysate of HEK293T cells expressing control (empty vector pBMN), WT IpaH9.8, or C337A IpaH9.8 probing with anti-ZKSCAN3 antibody.

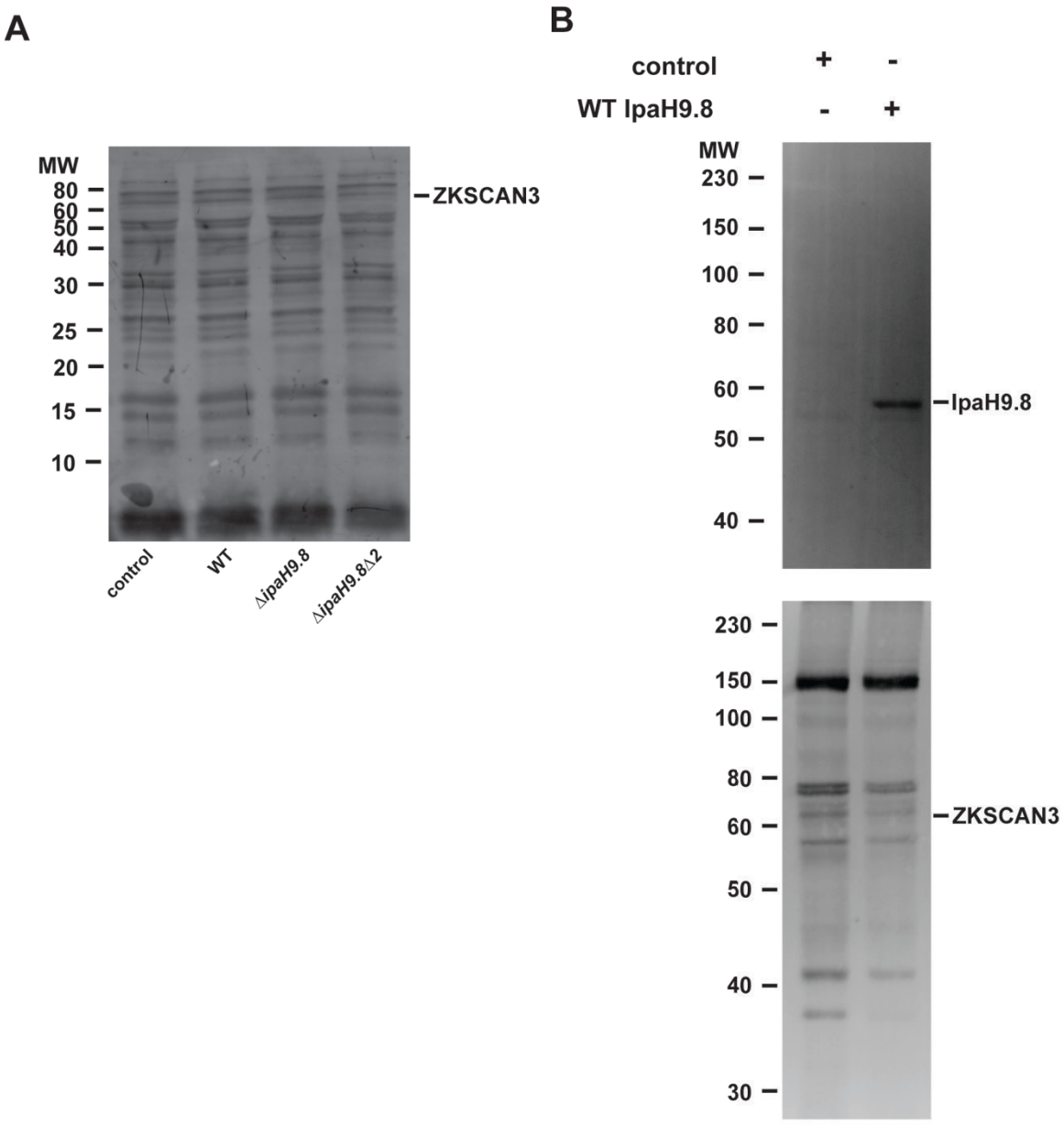

Figure 13: *In vitro* modifications of ZKSCAN3 in U937 cells stably expressing IpaH9.8 are inconclusive.
(A) Western blot of cell lysates 1 hour post-infection from U937 cells infected with WT, Δ*ipaH9.8*, and Δ*ipaH9.8Δ2* strains of *Shigella,* probing for ZKSCAN3. (B) Western blot of cell lysate of U937 cells expressing WT IpaH9.8 or control empty vector probing with anti-IpaH antibody (top). Western blot of cell lysate of U937 cells expressing WT IpaH9.8 or control empty vector probing with anti-ZKSCAN3 antibody (bottom). Cells were treated with MG132 6 hours prior to harvest.

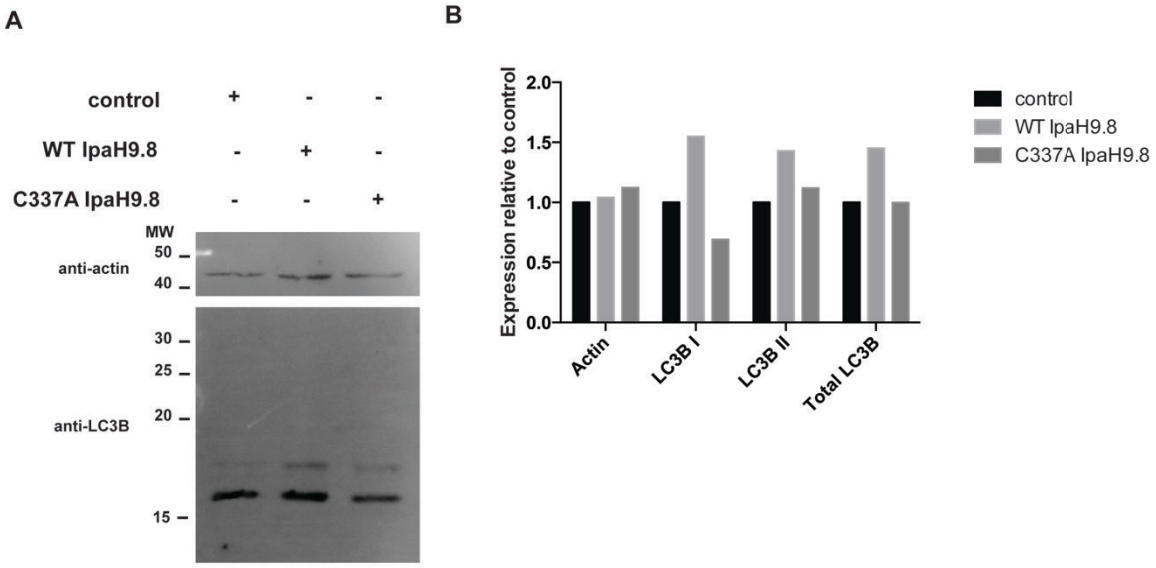

Figure 14: IpaH9.8 increases autophagy in HEK293T cells.
(A) Western blot of cell lysate of HEK293T cells expressing control (empty vector pBMN), WT IpaH9.8, or C337A IpaH9.8 probing with anti-LC3B antibody. (B) Graphical representation of the optical density of LC3B I and II bands in blot (A). Values of means are displayed in each column (*n*=1).

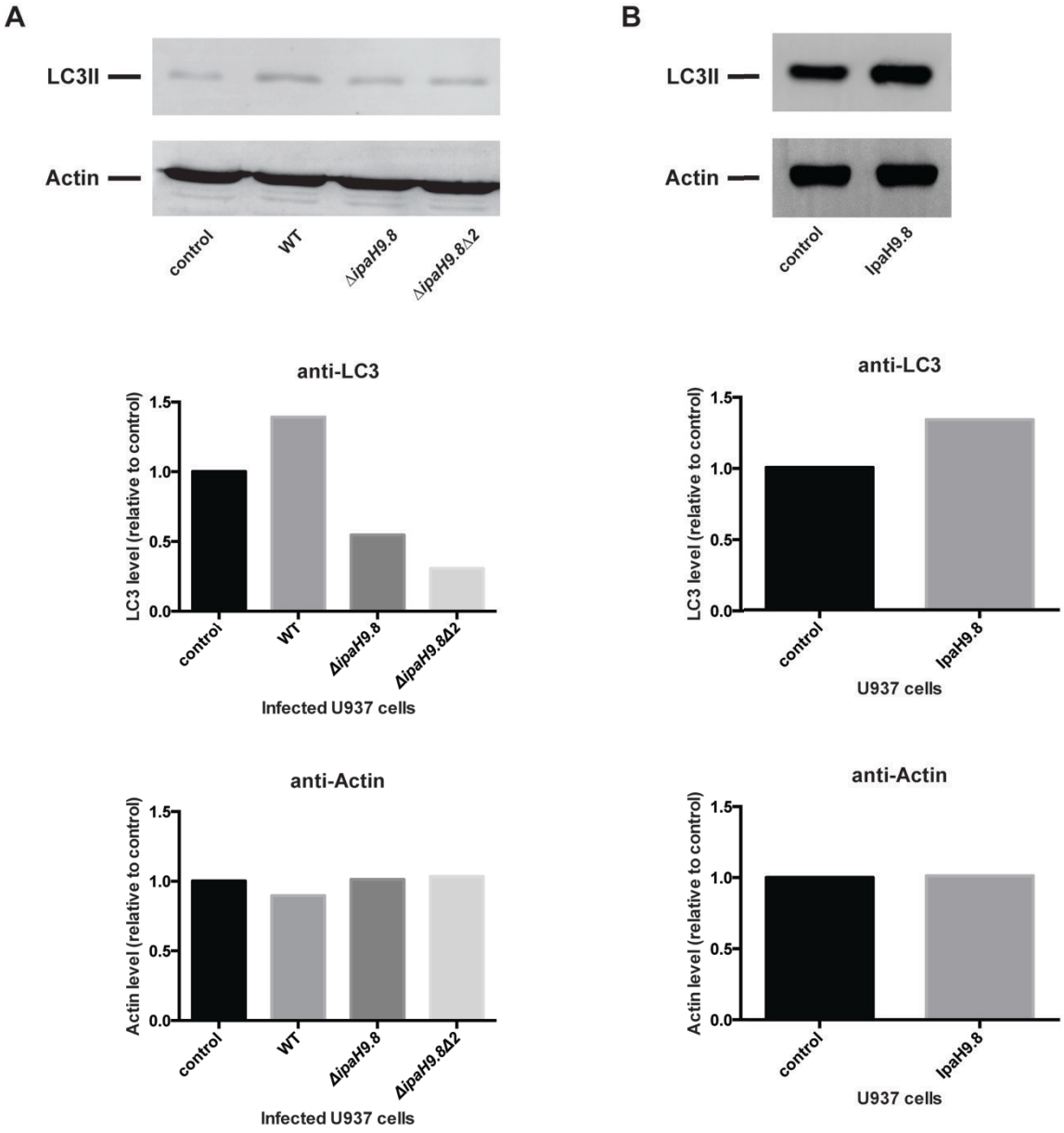

Figure 15: IpaH9.8 increases autophagy in U937 cells.
(A) Western blot of cell lysate 1 hour post-infection of U937 cells infected with WT, Δ*ipaH9.8*, and Δ*ipaH9.8*Δ*2* strains of *Shigella* probing for LC3B and actin. Graphs of the optical density of bands for LC3B and actin are directly below. Values of means are displayed in each column (*n*=1) (B) Western blot of cell lysate of U937 cells expressing WT-IpaH9.8 probing for LC3B and actin. Graphs of the optical density of bands for LC3B and actin are directly below. Values of means are displayed in each column (*n*=1).

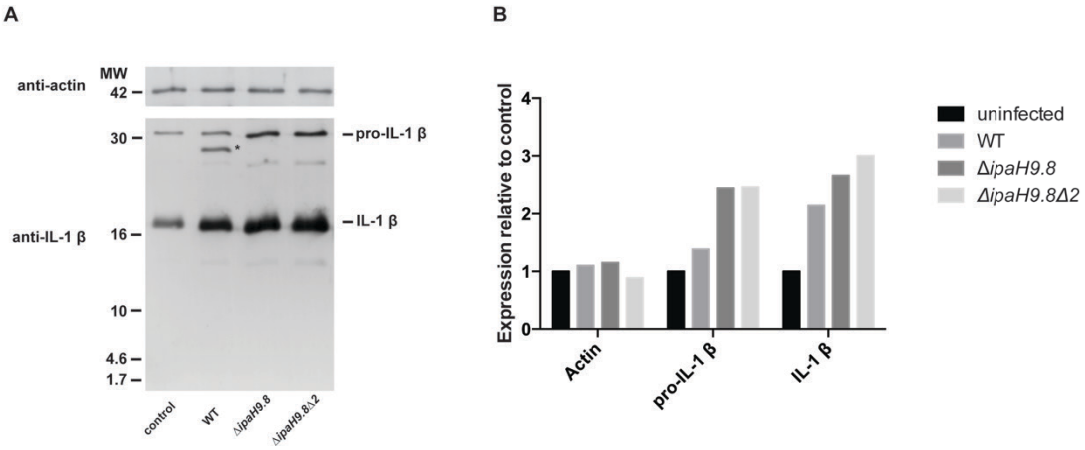

Figure 16: IL-1 β secreted from *Shigella* infected U937 cells is decreased in the presence of IpaH9.8.

(A) Western blot of cell culture supernatant from 1 hour post-infection of U937 cells infected with WT, Δ*ipaH9.8*, and Δ*ipaH9.8*Δ*2* strains of *Shigella* probing for IL-1 β and actin. (B) Graphical representation of band intensity for IL-1 β (pro and mature IL-1 β) and actin for the blots in (A). Values of means are displayed in each column (*n*=1). Asterisk (*) indicates unique 27 kDa IL-1 β intermediate present in the WT-infected cell supernatant.

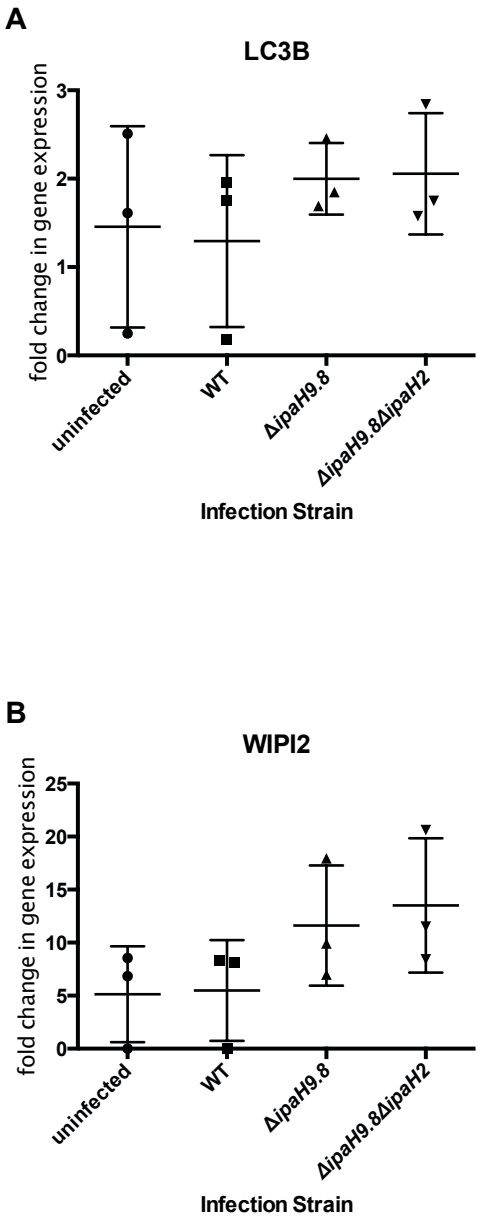

Figure 17: qPCR of ZKSCAN3 controlled transcripts LCB3 and WIPI2 revealed no differences in infected U937 cells.
(A) cDNA from U937 cells infected with WT, Δ*ipaH9.8*, and Δ*ipaH9.8*Δ*2* strains of *S. flexneri* was used for qPCR analysis of WIPI2. Graph represents the fold increase in WIPI2 compared to uninfected U937 cells. Values of means ± standard deviation are displayed in each column (*n*=3). (B) cDNA from U937 cells infected with WT, Δ*ipaH9.8*, and Δ*ipaH9.8*Δ*2* strains of *S. flexneri* was used for qPCR analysis of LC3B. Graph represents the fold increase in WIPI2 compared to uninfected U937 cells. Values of means ± standard deviation are displayed in each column (*n*=3).

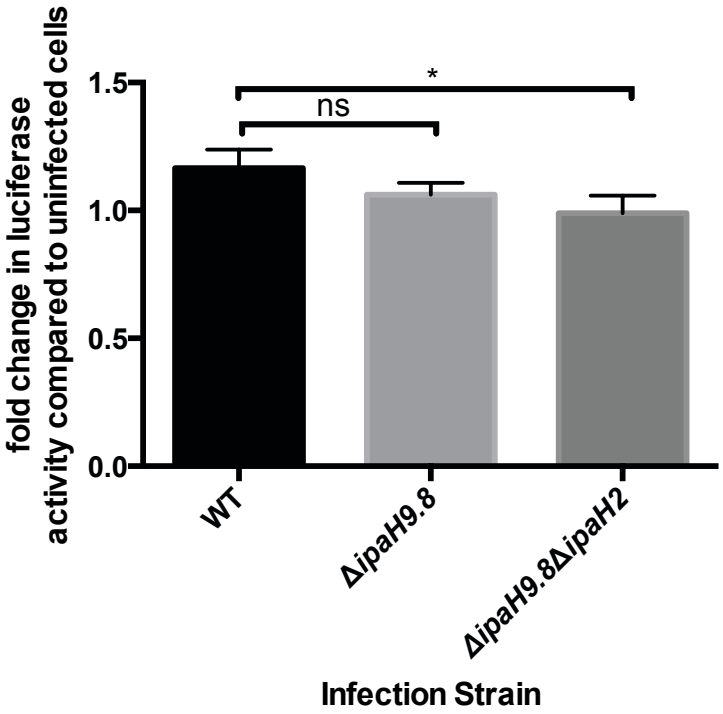

Figure 18: Luciferase activity controlled by LC3B promoter is decreased in cells infected with Δ*ipaH9.8*Δ*2 Shigella.*
Luciferase activity was measured from HEK29T cells transfected with luciferase vector pGL4.26 containing the LC3B promoter region and pcDNA encoding ZKSCAN3 and infected with WT, Δ*ipaH9.8*, and Δ*ipaH9.8*Δ*2* strains of *Shigella*. Graph represents the fold increase in luciferase activity compared to uninfected HEK293T cells. Values of means ± standard deviation are displayed in each column (*n*=3).

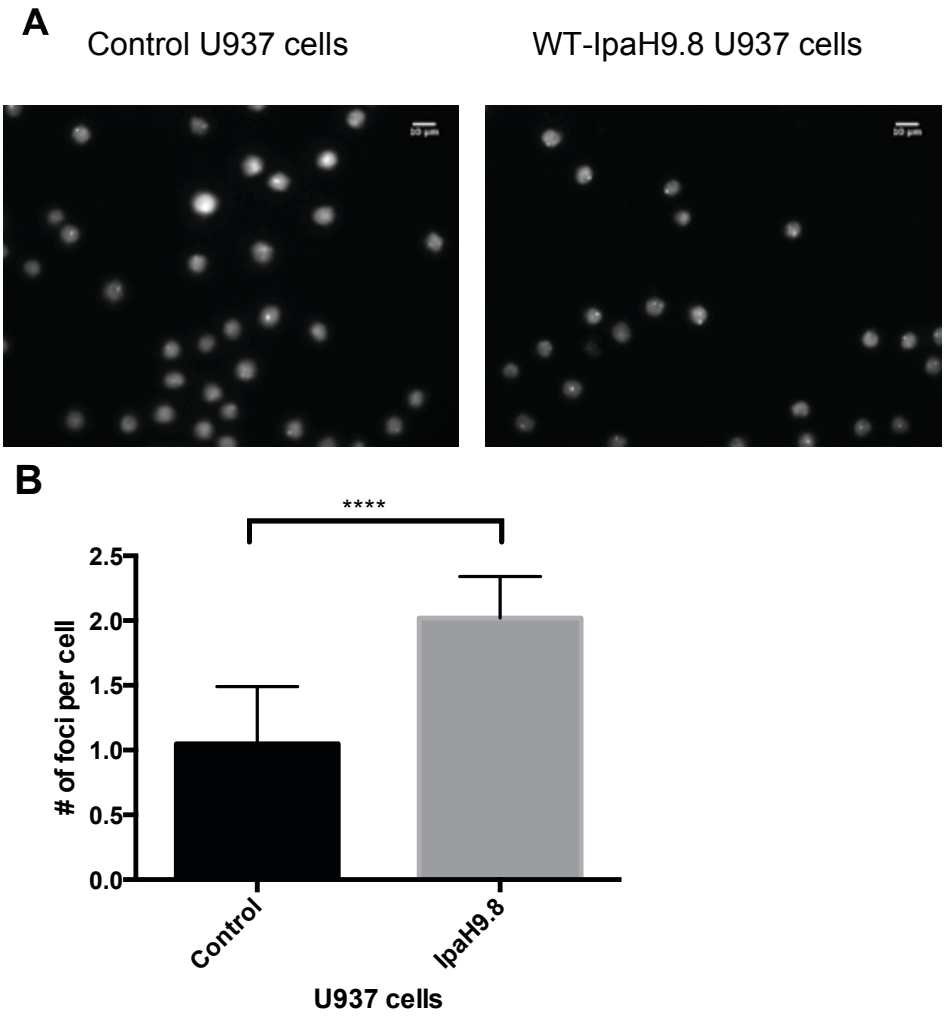

Figure 19: IpaH9.8 increases ZSKCAN3 foci in U937 cells.
(A) Representative images of immunostained U937 cells expressing WT-IpaH9.8 and probing for ZKSCAN3. (B) Graph of total number of foci per cell in immunostained U937 cells expressing WT-IpaH9.8 compared to control U937 cells. Values of means ± standard deviation are displayed in each column (*n*=1).

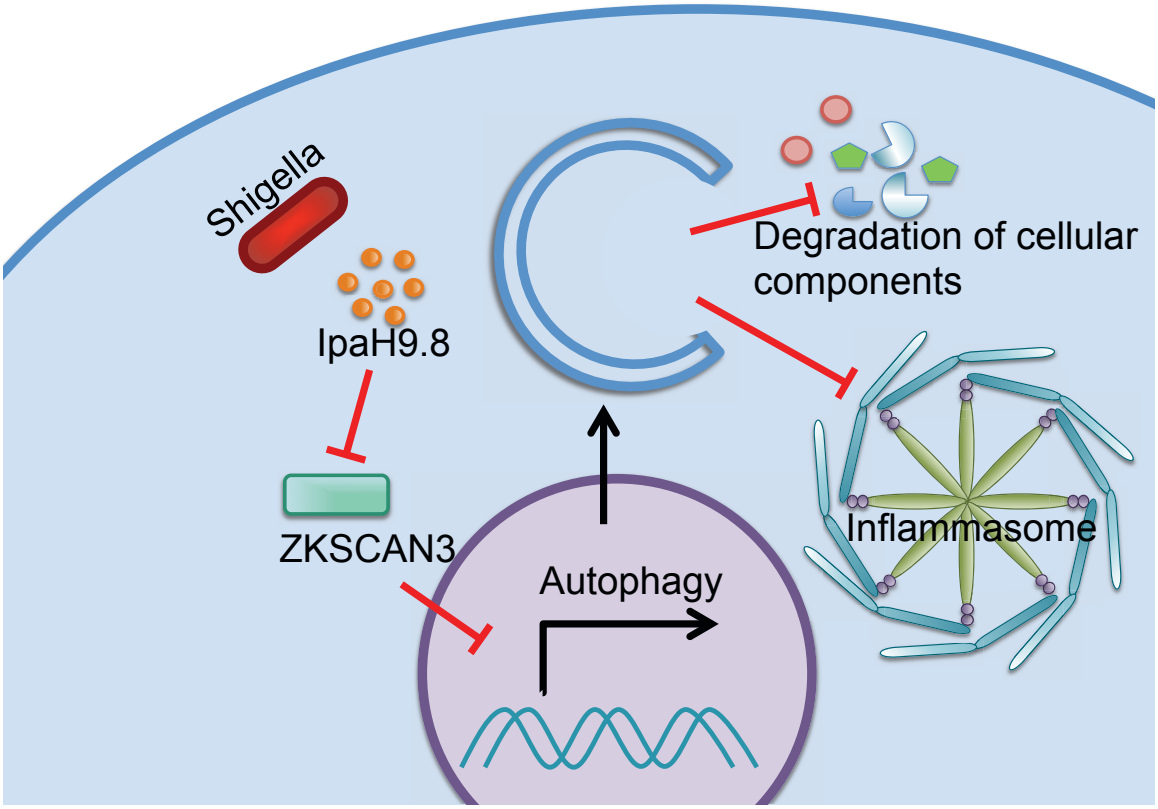

Figure 20: Proposed mechanism of action for IpaH9.8.
Shigella uses the T3SS to inject IpaH9.8 into the host cell, where IpaH9.8 inhibits ZKSCAN3. Due to the inhibition of ZKSCAN3, repressor of autophagy, autophagy is turned on and targets degradation of cellular components to increase nutrients for intracellular growth and downregulates the overstimulated inflammasome, thus decreasing the immune response.

BIBLIOGRAPHY

Abrusci, P., Vergara-Irigaray, M., Johnson, S., Beeby, M.D., Hendrixson, D.R., Roversi, P.*, et al.* (2013). Architecture of the major component of the type III secretion system export apparatus. *Nature structural & molecular biology* **20,** 99-104.

Ashida, H., Kim, M., Schmidt-Supprian, M., Ma, A., Ogawa, M. and Sasakawa, C. (2010). A bacterial E3 ubiquitin ligase IpaH9.8 targets NEMO/IKKgamma to dampen the host NF-kappaB-mediated inflammatory response. *Nature cell biology* **12,** 66-73; sup pp 61-69.

Ashida, H., Nakano, H. and Sasakawa, C. (2013). Shigella IpaH0722 E3 ubiquitin ligase effector targets TRAF2 to inhibit PKC-NF-kappaB activity in invaded epithelial cells. *PLoS pathogens* **9,** e1003409.

Ashida, H., Toyotome, T., Nagai, T. and Sasakawa, C. (2007). Shigella chromosomal IpaH proteins are secreted via the type III secretion system and act as effectors. *Molecular microbiology* **63,** 680-693.

Bals, M. and Leonesco, M. (1961). [Study on the use of the Sereny pathogenicity test in the isolation of Shigella]. *Archives roumaines de pathologie experimentales et de microbiologie* **20,** 365-373.

Baxt, L.A. and Goldberg, M.B. (2014). Host and bacterial proteins that repress recruitment of LC3 to Shigella early during infection. *PloS one* **9,** e94653.

Behrends, C. and Harper, J.W. (2011). Constructing and decoding unconventional ubiquitin chains. *Nature structural & molecular biology* **18,** 520-528.

Bergan, J., Dyve Lingelem, A.B., Simm, R., Skotland, T. and Sandvig, K. (2012). Shiga toxins. *Toxicon : official journal of the International Society on Toxinology* **60,** 1085-1107.

Bernardini, M.L., Mounier, J., d'Hauteville, H., Coquis-Rondon, M. and Sansonetti, P.J. (1989). Identification of icsA, a plasmid locus of Shigella flexneri that governs bacterial intra- and intercellular spread through interaction with F-actin. *Proceedings of the National Academy of Sciences of the United States of America* **86,** 3867-3871.

Blocker, A., Jouihri, N., Larquet, E., Gounon, P., Ebel, F., Parsot, C.*, et al.* (2001). Structure and composition of the Shigella flexneri "needle complex", a part of its type III secreton. *Molecular microbiology* **39,** 652-663.

Bongrand, C., Sansonetti, P.J. and Parsot, C. (2012). Characterization of the promoter, MxiE box and 5' UTR of genes controlled by the activity of the type III secretion apparatus in Shigella flexneri. *PloS one* **7,** e32862.

Brough, D. and Rothwell, N.J. (2007). Caspase-1-dependent processing of pro-interleukin-1β is cytosolic and precedes cell death. *J. Cell Sci* **120,** 772-781.

Campoy, E. and Colombo, M.I. (2009). Autophagy subversion by bacteria. *Current topics in microbiology and immunology* **335,** 227-250.

Chang, S.Y., Lee, S.N., Yang, J.Y., Kim, D.W., Yoon, J.H., Ko, H.J., Ogawa, M., Sasakawa, C. and Kweon, M.N. (2013). Autophagy controls an intrinsic host defense to bacteria by promoting epithelial cell surivival: a murine model. PLoS One **11,** e81095.

Chauhan, S., Goodwin, J.G., Chauhan, S., Manyam, G., Wang, J., Kamat, A.M. and Boyd, D.D. (2013). ZKSCAN3 is a master transcriptional repressor of autophagy. *Molecular cell* **50,** 16-28.

Chen, Z.J. (2012). Ubiquitination in signaling to and activation of IKK. *Immunological reviews* **246,** 95-106.

Chou, Y.C., Keszei, A.F., Rohde, J.R., Tyers, M. and Sicheri, F. (2012). Conserved structural mechanisms for autoinhibition in IpaH ubiquitin ligases. *The Journal of biological chemistry* **287,** 268-275.

Cole, A.J., Clifton-Bligh, R.J. and Marsh, D.J. (2014). Ubiquitination and cancer: Histone H2B monoubiquitination - roles to play in human malignancy. *Endocrine-related cancer*.

Das, R., Liang, Y.H., Mariano, J., Li, J., Huang, T., King, A.*, et al.* (2013). Allosteric regulation of E2:E3 interactions promote a processive ubiquitination machine. *The EMBO journal* **32,** 2504-2516.

Das, R., Mariano, J., Tsai, Y.C., Kalathur, R.C., Kostova, Z., Li, J.*, et al.* (2009). Allosteric activation of E2-RING finger-mediated ubiquitylation by a structurally defined specific E2-binding region of gp78. *Molecular cell* **34,** 674-685.

Datsenko, K.A. and Wanner, B.L. (2000). One-step inactivation of chromosomal genes in Escherichia coli K-12 using PCR products. *Proceedings of the National Academy of Sciences of the United States of America* **97,** 6640-6645.

Donovan, P. and Poronnik, P. (2013). Nedd4 and Nedd4-2: ubiquitin ligases at work in the neuron. *The international journal of biochemistry & cell biology* **45,** 706-710.

Dupont, N., Jiang, S., Pilli, M., Ornatowski, W., Bhattacharya, D. and Deretic, V. (2011). Autophagy-based unconventional secretory pathway for extracellular delivery of IL-1beta. *The EMBO journal* **30,** 4701-4711.

Dupont, N., Lacas-Gervais, S., Bertout, J., Paz, I., Freche, B., Van Nhieu, G.T.*, et al.* (2009). Shigella phagocytic vacuolar membrane remnants participate in the cellular response to pathogen invasion and are regulated by autophagy. *Cell host & microbe* **6,** 137-149.

Fernandez-Prada, C.M., Hoover, D.L., Tall, B.D., Hartman, A.B., Kopelowitz, J. and Venkatesan, M.M. (2000). Shigella flexneri IpaH(7.8) facilitates escape of virulent bacteria from the endocytic vacuoles of mouse and human macrophages. *Infection and immunity* **68,** 3608-3619.

Fierz, B., Chatterjee, C., McGinty, R.K., Bar-Dagan, M., Raleigh, D.P. and Muir, T.W. (2011). Histone H2B ubiquitylation disrupts local and higher-order chromatin compaction. *Nature chemical biology* **7,** 113-119.

Fink, S.L. and Cookson, B.T. (2005). Apoptosis, pyroptosis, and necrosis: mechanistic description of dead and dying eukaryotic cells. *Infection and immunity* **73,** 1907-1916.

Finley, D. (2009). Recognition and processing of ubiquitin-protein conjugates by the proteasome. *Annual review of biochemistry* **78,** 477-513.

Fisher, M.L., Sun, W. and Curtiss, R., 3rd (2014). The route less taken: pulmonary models of enteric Gram-negative infection. *Pathogens and disease* **70,** 99-109.

Fontaine, A., Arondel, J. and Sansonetti, P.J. (1988). Role of Shiga toxin in the pathogenesis of bacillary dysentery, studied by using a Tox- mutant of Shigella dysenteriae 1. *Infection and immunity* **56,** 3099-3109.

Girardin, S.E., Boneca, I.G., Carneiro, L.A., Antignac, A., Jehanno, M., Viala, J.*, et al.* (2003). Nod1 detects a unique muropeptide from gram-negative bacterial peptidoglycan. *Science* **300,** 1584-1587.

Grishin, A.M., Condos, T.E., Barber, K.R., Campbell-Valois, F.X., Parsot, C., Shaw, G.S. and Cygler, M. (2014). Structural basis for the inhibition of host protein ubiquitination by Shigella effector kinase OspG. *Structure* **22,** 878-888.

Haraga, A. and Miller, S.I. (2006). A Salmonella type III secretion effector interacts with the mammalian serine/threonine protein kinase PKN1. *Cellular microbiology* **8,** 837-846.

Harris, J. (2011). Autophagy and cytokines. *Cytokine* **56,** 140-144.

He, C. and Klionsky, D.J. (2009). Regulation mechanisms and signaling pathways of autophagy. *Annual review of genetics* **43,** 67-93.

Hentschke, M., Berneking, L., Belmar Campos, C., Buck, F., Ruckdeschel, K. and Aepfelbacher, M. (2010). Yersinia virulence factor YopM induces sustained RSK activation by interfering with dephosphorylation. *PloS one* **5**.

Hershko, A. and Ciechanover, A. (1998). The ubiquitin system. *Annual review of biochemistry* **67,** 425-479.

Hilbi, H., Moss, J.E., Hersh, D., Chen, Y., Arondel, J., Banerjee, S.*, et al.* (1998). Shigella-induced apoptosis is dependent on caspase-1 which binds to IpaB. *The Journal of biological chemistry* **273,** 32895-32900.

Hochrainer, K., Racchumi, G., Zhang, S., Iadecola, C. and Anrather, J. (2012). Monoubiquitination of nuclear RelA negatively regulates NF-kappaB activity independent of proteasomal degradation. *Cellular and molecular life sciences : CMLS* **69,** 2057-2073.

Hofling, S., Scharnert, J., Cromme, C., Bertrand, J., Pap, T., Schmidt, M.A. and Ruter, C. (2014). Manipulation of pro-inflammatory cytokine production by the bacterial cell-penetrating effector protein YopM is independent of its interaction with host cell kinases RSK1 and PRK2. *Virulence* **5**.

Huang, L., Kinnucan, E., Wang, G., Beaudenon, S., Howley, P.M., Huibregtse, J.M. and Pavletich, N.P. (1999). Structure of an E6AP-UbcH7 complex: insights into ubiquitination by the E2-E3 enzyme cascade. *Science* **286,** 1321-1326.

Hueck, C.J., Hantman, M.J., Bajaj, V., Johnston, C., Lee, C.A. and Miller, S.I. (1995). Salmonella typhimurium secreted invasion determinants are homologous to Shigella Ipa proteins. *Molecular microbiology* **18,** 479-490.

Huett, A., Heath, R.J., Begun, J., Sassi, S.O., Baxt, L.A., Vyas, J.M.*, et al.* (2012). The LRR and RING domain protein LRSAM1 is an E3 ligase crucial for ubiquitin-dependent autophagy of intracellular Salmonella Typhimurium. *Cell host & microbe* **12,** 778-790.

Huibregtse, J. and Rohde, J.R. (2014). Hell's BELs: bacterial E3 ligases that exploit the eukaryotic ubiquitin machinery. *PLoS pathogens* **10,** e1004255.

Huibregtse, J.M., Scheffner, M., Beaudenon, S. and Howley, P.M. (1995). A family of proteins structurally and functionally related to the E6-AP ubiquitin-protein ligase. *Proceedings of the National Academy of Sciences of the United States of America* **92,** 2563-2567.

Ingham, R.J., Gish, G. and Pawson, T. (2004). The Nedd4 family of E3 ubiquitin ligases: functional diversity within a common modular architecture. *Oncogene* **23,** 1972-1984.

Jeong, K.I., Venkatesan, M.M., Barnoy, S. and Tzipori, S. (2013). Evaluation of virulent and live Shigella sonnei vaccine candidates in a gnotobiotic piglet model. *Vaccine* **31,** 4039-4046.

Jessen, D.L., Osei-Owusu, P., Toosky, M., Roughead, W., Bradley, D.S. and Nilles, M.L. (2014). Type III secretion needle proteins induce cell signaling and cytokine secretion via Toll-like receptors. *Infection and immunity* **82,** 2300-2309.

Jo, E.K., Yuk, J.M., Shin, D.M. and Sasakawa, C. (2013). Roles of autophagy in elimination of intracellular bacterial pathogens. *Frontiers in immunology* **4,** 97.

Johnson, S. and Blocker, A. (2008). Characterization of soluble complexes of the Shigella flexneri type III secretion system ATPase. *FEMS microbiology letters* **286,** 274-278.

Joshi, A.D. and Swanson, M.S. (2011). Secrets of a successful pathogen: legionella resistance to progression along the autophagic pathway. *Frontiers in microbiology* **2,** 138.

Kent, T.H., Formal, S.B., LaBrec, E.H., Sprinz, H. and Maenza, R.M. (1967). Gastric shigellosis in rhesus monkeys. *The American journal of pathology* **51,** 259-267.

Keszei, A.F., Tang, X., McCormick, C., Zeqiraj, E., Rohde, J.R., Tyers, M. and Sicheri, F. (2014). Structure of an SspH1-PKN1 complex reveals the basis for host substrate recognition and mechanism of activation for a bacterial E3 ubiquitin ligase. *Molecular and cellular biology* **34,** 362-373.

Kim, D.W., Chu, H., Joo, D.H., Jang, M.S., Choi, J.H., Park, S.M.*, et al.* (2008). OspF directly attenuates the activity of extracellular signal-regulated kinase during invasion by Shigella flexneri in human dendritic cells. *Molecular immunology* **45,** 3295-3301.

Kim, D.W., Lenzen, G., Page, A.L., Legrain, P., Sansonetti, P.J. and Parsot, C. (2005). The Shigella flexneri effector OspG interferes with innate immune responses by targeting ubiquitin-conjugating enzymes. *Proceedings of the National Academy of Sciences of the United States of America* **102,** 14046-14051.

Kim, M., Ogawa, M., Fujita, Y., Yoshikawa, Y., Nagai, T., Koyama, T.*, et al.* (2009). Bacteria hijack integrin-linked kinase to stabilize focal adhesions and block cell detachment. *Nature* **459,** 578-582.

Kofoed, E.M. and Vance, R.E. (2011). Innate immune recognition of bacterial ligands by NAIPs determines inflammasome specificity. *Nature* **477,** 592-595.

Kotloff, K.L., Winickoff, J.P., Ivanoff, B., Clemens, J.D., Swerdlow, D.L., Sansonetti, P.J.*, et al.* (1999). Global burden of Shigella infections: implications for vaccine development and implementation of control strategies. *Bulletin of the World Health Organization* **77,** 651-666.

Kraehenbuhl, J.P. and Neutra, M.R. (2000). Epithelial M cells: differentiation and function. *Annual review of cell and developmental biology* **16,** 301-332.

Levine, M.M., Kotloff, K.L., Barry, E.M., Pasetti, M.F. and Sztein, M.B. (2007). Clinical trials of Shigella vaccines: two steps forward and one step back on a long, hard road. *Nature reviews. Microbiology* **5,** 540-553.

Li, H., Xu, H., Zhou, Y., Zhang, J., Long, C., Li, S.*, et al.* (2007). The phosphothreonine lyase activity of a bacterial type III effector family. *Science* **315,** 1000-1003.

Livak, K.J. and Schmittgen, T.D. (2001). Analysis of Relative Gene Expression Data Using Real-Time Quantitative PCR and the $2^{-\Delta\Delta CT}$ Method. *Methods* **4,** 402-408.

Lorick, K.L., Jensen, J.P., Fang, S., Ong, A.M., Hatakeyama, S. and Weissman, A.M. (1999). RING fingers mediate ubiquitin-conjugating enzyme (E2)-dependent ubiquitination. *Proceedings of the National Academy of Sciences of the United States of America* **96,** 11364-11369.

Marlovits, T.C. and Stebbins, C.E. (2010). Type III secretion systems shape up as they ship out. *Current opinion in microbiology* **13,** 47-52.

Marteyn, B., Gazi, A. and Sansonetti, P. (2012). Shigella: a model of virulence regulation in vivo. *Gut microbes* **3,** 104-120.

Martino, M.C., Rossi, G., Martini, I., Tattoli, I., Chiavolini, D., Phalipon, A.*, et al.* (2005). Mucosal lymphoid infiltrate dominates colonic pathological changes in murine experimental shigellosis. *The Journal of infectious diseases* **192,** 136-148.

Mavris, M., Page, A.L., Tournebize, R., Demers, B., Sansonetti, P. and Parsot, C. (2002a). Regulation of transcription by the activity of the Shigella flexneri type III secretion apparatus. *Molecular microbiology* **43,** 1543-1553.

Mavris, M., Sansonetti, P.J. and Parsot, C. (2002b). Identification of the cis-acting site involved in activation of promoters regulated by activity of the type III secretion apparatus in Shigella flexneri. *Journal of bacteriology* **184,** 6751-6759.

McDonald, C., Vacratsis, P.O., Bliska, J.B. and Dixon, J.E. (2003). The yersinia virulence factor YopM forms a novel protein complex with two cellular kinases. *The Journal of biological chemistry* **278,** 18514-18523.

Menard, R., Prevost, M.C., Gounon, P., Sansonetti, P. and Dehio, C. (1996). The secreted Ipa complex of Shigella flexneri promotes entry into mammalian cells. *Proceedings of the National Academy of Sciences of the United States of America* **93,** 1254-1258.

Metzger, M.B., Hristova, V.A. and Weissman, A.M. (2012). HECT and RING finger families of E3 ubiquitin ligases at a glance. *Journal of cell science* **125,** 531-537.

Metzger, M.B., Pruneda, J.N., Klevit, R.E. and Weissman, A.M. (2014). RING-type E3 ligases: master manipulators of E2 ubiquitin-conjugating enzymes and ubiquitination. *Biochimica et biophysica acta* **1843,** 47-60.

Miao, E.A., Mao, D.P., Yudkovsky, N., Bonneau, R., Lorang, C.G., Warren, S.E.*, et al.* (2010). Innate immune detection of the type III secretion apparatus through the NLRC4 inflammasome. *Proceedings of the National Academy of Sciences of the United States of America* **107,** 3076-3080.

Morita-Ishihara, T., Ogawa, M., Sagara, H., Yoshida, M., Katayama, E. and Sasakawa, C. (2006). Shigella Spa33 is an essential C-ring component of type III secretion machinery. *The Journal of biological chemistry* **281,** 599-607.

Mostowy, S., Boucontet, L., Mazon Moya, M.J., Sirianni, A., Boudinot, P., Hollinshead, M.*, et al.* (2013). The zebrafish as a new model for the in vivo study of Shigella flexneri interaction with phagocytes and bacterial autophagy. *PLoS pathogens* **9,** e1003588.

Mounier, J., Vasselon, T., Hellio, R., Lesourd, M. and Sansonetti, P.J. (1992). Shigella flexneri enters human colonic Caco-2 epithelial cells through the basolateral pole. *Infection and immunity* **60,** 237-248.

Mueller, R.D., Yasuda, H., Hatch, C.L., Bonner, W.M. and Bradbury, E.M. (1985). Identification of ubiquitinated histones 2A and 2B in Physarum polycephalum. Disappearance of these proteins at metaphase and reappearance at anaphase. *The Journal of biological chemistry* **260,** 5147-5153.

Niebuhr, K., Jouihri, N., Allaoui, A., Gounon, P., Sansonetti, P.J. and Parsot, C. (2000). IpgD, a protein secreted by the type III secretion machinery of Shigella flexneri, is chaperoned by IpgE and implicated in entry focus formation. *Molecular microbiology* **38,** 8-19.

Ogawa, M., Yoshimori, T., Suzuki, T., Sagara, H., Mizushima, N. and Sasakawa, C. (2005). Escape of intracellular Shigella from autophagy. *Science* **307,** 727-731.

Okuda, J., Toyotome, T., Kataoka, N., Ohno, M., Abe, H., Shimura, Y.*, et al.* (2005). Shigella effector IpaH9.8 binds to a splicing factor U2AF(35) to modulate host immune responses. *Biochemical and biophysical research communications* **333,** 531-539.

Onodera, N.T., Ryu, J., Durbic, T., Nislow, C., Archibald, J.M. and Rohde, J.R. (2012). Genome sequence of Shigella flexneri serotype 5a strain M90T Sm. *Journal of bacteriology* **194,** 3022.

Osley, M.A., Fleming, A.B. and Kao, C.F. (2006). Histone ubiquitylation and the regulation of transcription. *Results and problems in cell differentiation* **41,** 47-75.

Ouni, I., Flick, K. and Kaiser, P. (2011). Ubiquitin and transcription: The SCF/Met4 pathway, a (protein-) complex issue. *Transcription* **2,** 135-139.

Ozkan, E., Yu, H. and Deisenhofer, J. (2005). Mechanistic insight into the allosteric activation of a ubiquitin-conjugating enzyme by RING-type ubiquitin ligases. *Proceedings of the National Academy of Sciences of the United States of America* **102,** 18890-18895.

Parsot, C. (2009). Shigella type III secretion effectors: how, where, when, for what purposes? *Current opinion in microbiology* **12,** 110-116.

Perdomo, O.J., Cavaillon, J.M., Huerre, M., Ohayon, H., Gounon, P. and Sansonetti, P.J. (1994). Acute inflammation causes epithelial invasion and mucosal destruction in experimental shigellosis. *The Journal of experimental medicine* **180,** 1307-1319.

Phalipon, A. and Sansonetti, P.J. (2007). Shigella's ways of manipulating the host intestinal innate and adaptive immune system: a tool box for survival? *Immunology and cell biology* **85,** 119-129.

Philpott, D.J., Edgeworth, J.D. and Sansonetti, P.J. (2000). The pathogenesis of Shigella flexneri infection: lessons from in vitro and in vivo studies. *Philosophical transactions of the Royal Society of London. Series B, Biological sciences* **355,** 575-586.

Pietrocola, F., Izzo, V., Niso-Santano, M., Vacchelli, E., Galluzzi, L., Maiuri, M.C. and Kroemer, G. (2013). Regulation of autophagy by stress-responsive transcription factors. *Seminars in cancer biology* **23,** 310-322.

Price, C.T., Al-Quadan, T., Santic, M., Rosenshine, I. and Abu Kwaik, Y. (2011). Host proteasomal degradation generates amino acids essential for intracellular bacterial growth. *Science* **334,** 1553-1557.

Pruneda, J.N., Smith, F.D., Daurie, A., Swaney, D.L., Villen, J., Scott, J.D.*, et al.* (2014). E2~Ub conjugates regulate the kinase activity of Shigella effector OspG during pathogenesis. *EMBO J* **33,** 437-449.

Quezada, C.M., Hicks, S.W., Galan, J.E. and Stebbins, C.E. (2009). A family of Salmonella virulence factors functions as a distinct class of autoregulated E3 ubiquitin ligases. *Proceedings of the National Academy of Sciences of the United States of America* **106,** 4864-4869.

Ramanathan, H.N. and Ye, Y. (2012). Cellular strategies for making monoubiquitin signals. *Critical reviews in biochemistry and molecular biology* **47,** 17-28.

Rohde, J.R., Breitkreutz, A., Chenal, A., Sansonetti, P.J. and Parsot, C. (2007). Type III secretion effectors of the IpaH family are E3 ubiquitin ligases. *Cell host & microbe* **1,** 77-83.

Rotin, D. and Kumar, S. (2009). Physiological functions of the HECT family of ubiquitin ligases. *Nature reviews. Molecular cell biology* **10,** 398-409.

Sambrook, J. and Russel, D.W. (2001) Molecular cloning: a laboratory manual (3-volume set) Cold Spring Harbor, New York, Cold Spring Harbor Laboratory Press.

Sanada, T., Kim, M., Mimuro, H., Suzuki, M., Ogawa, M., Oyama, A.*, et al.* (2012). The Shigella flexneri effector OspI deamidates UBC13 to dampen the inflammatory response. *Nature* **483,** 623-626.

Sansonetti, P.J., Arondel, J., Fontaine, A., d'Hauteville, H. and Bernardini, M.L. (1991). OmpB (osmo-regulation) and icsA (cell-to-cell spread) mutants of Shigella flexneri: vaccine candidates and probes to study the pathogenesis of shigellosis. *Vaccine* **9,** 416-422.

Sansonetti, P.J., Kopecko, D.J. and Formal, S.B. (1981). Shigella sonnei plasmids: evidence that a large plasmid is necessary for virulence. *Infection and immunity* **34,** 75-83.

Sansonetti, P.J., Phalipon, A., Arondel, J., Thirumalai, K., Banerjee, S., Akira, S.*, et al.* (2000). Caspase-1 activation of IL-1beta and IL-18 are essential for Shigella flexneri-induced inflammation. *Immunity* **12,** 581-590.

Schnell, J.D. and Hicke, L. (2003). Non-traditional functions of ubiquitin and ubiquitin-binding proteins. *The Journal of biological chemistry* **278,** 35857-35860.

Schnupf, P. and Sansonetti, P.J. (2012). Quantitative RT-PCR profiling of the rabbit immune response: assessment of acute Shigella flexneri infection. *PloS one* **7,** e36446.

Schroeder, G.N. and Hilbi, H. (2008). Molecular pathogenesis of Shigella spp.: controlling host cell signaling, invasion, and death by type III secretion. *Clinical microbiology reviews* **21,** 134-156.

Shema-Yaacoby, E., Nikolov, M., Haj-Yahya, M., Siman, P., Allemand, E., Yamaguchi, Y.*, et al.* (2013). Systematic identification of proteins binding to chromatin-embedded ubiquitylated H2B reveals recruitment of SWI/SNF to regulate transcription. *Cell reports* **4,** 601-608.

Shi, F., Yang, L., Kouadir, M., Yang, Y., Wang, J., Zhou, X.*, et al.* (2012). The NALP3 inflammasome is involved in neurotoxic prion peptide-induced microglial activation. *Journal of neuroinflammation* **9,** 73.

Shibutani, S.T. and Yoshimori, T. (2014). Autophagosome formation in response to intracellular bacterial invasion. *Cellular microbiology* **16,** 1619-1626.

Shim, D.H., Suzuki, T., Chang, S.Y., Park, S.M., Sansonetti, P.J., Sasakawa, C. and Kweon, M.N. (2007). New animal model of shigellosis in the Guinea pig: its usefulness for protective efficacy studies. *Journal of immunology* **178,** 2476-2482.

Sidik, S., Kottwitz, H., Benjamin, J., Ryu, J., Jarrar, A., Garduno, R. and Rohde, J.R. (2014). A Shigella flexneri Virulence Plasmid Encoded Factor Controls Production of Outer Membrane Vesicles. *G3* **12,** 2493-2503.

Singer, A.U., Rohde, J.R., Lam, R., Skarina, T., Kagan, O., Dileo, R.*, et al.* (2008). Structure of the Shigella T3SS effector IpaH defines a new class of E3 ubiquitin ligases. *Nature structural & molecular biology* **15,** 1293-1301.

Sperandio, B., Regnault, B., Guo, J., Zhang, Z., Stanley, S.L., Jr., Sansonetti, P.J. and Pedron, T. (2008). Virulent Shigella flexneri subverts the host innate immune response through manipulation of antimicrobial peptide gene expression. *The Journal of experimental medicine* **205,** 1121-1132.

Suzuki, S., Franchi, L., He, Y., Munoz-Planillo, R., Mimuro, H., Suzuki, T.*, et al.* (2014a). Shigella type III secretion protein MxiI is recognized by Naip2 to induce Nlrc4 inflammasome activation independently of Pkcdelta. *PLoS pathogens* **10,** e1003926.

Suzuki, S., Mimuro, H., Kim, M., Ogawa, M., Ashida, H., Toyotome, T.*, et al.* (2014b). Shigella IpaH7.8 E3 ubiquitin ligase targets glomulin and activates inflammasomes to demolish macrophages. *Proceedings of the National Academy of Sciences of the United States of America* **111,** E4254-4263.

Suzuki, T., Franchi, L., Toma, C., Ashida, H., Ogawa, M., Yoshikawa, Y*., et al.* (2007). Differential regulation of caspase-1 activation, pyroptosis, and autophagy via Ipaf and ASC in Shigella-infected macrophages. *PLoS pathogens* **3,** e111.

Suzuki, T., Nakanishi, K., Tsutsui, H., Iwai, H., Akira, S., Inohara, N*., et al.* (2005). A novel caspase-1/toll-like receptor 4-independent pathway of cell death induced by cytosolic Shigella in infected macrophages. *The Journal of biological chemistry* **280,** 14042-14050.

Toyotome, T., Suzuki, T., Kuwae, A., Nonaka, T., Fukuda, H., Imajoh-Ohmi, S*., et al.* (2001). Shigella protein IpaH(9.8) is secreted from bacteria within mammalian cells and transported to the nucleus. *The Journal of biological chemistry* **276,** 32071-32079.

Tyers, M. and Jorgensen, P. (2000). Proteolysis and the cell cycle: with this RING I do thee destroy. *Current opinion in genetics & development* **10,** 54-64.

van de Verg, L.L., Mallett, C.P., Collins, H.H., Larsen, T., Hammack, C. and Hale, T.L. (1995). Antibody and cytokine responses in a mouse pulmonary model of Shigella flexneri serotype 2a infection. *Infection and immunity* **63,** 1947-1954.

van der Horst, A., de Vries-Smits, A.M., Brenkman, A.B., van Triest, M.H., van den Broek, N., Colland, F*., et al.* (2006). FOXO4 transcriptional activity is regulated by monoubiquitination and USP7/HAUSP. *Nature cell biology* **8,** 1064-1073.

Voino-Yasenetsky, M.V. and Voino-Yasenetskaya, M.K. (1962). Experimental pneumonia caused by bacteria of the Shigella group. *Acta morphologica Academiae Scientiarum Hungaricae* **11,** 439-454.

von Seidlein, L., Kim, D.R., Ali, M., Lee, H., Wang, X., Thiem, V.D*., et al.* (2006). A multicentre study of Shigella diarrhoea in six Asian countries: disease burden, clinical manifestations, and microbiology. *PLoS medicine* **3,** e353.

Wang, F., Jiang, Z., Li, Y., He, X., Zhao, J., Yang, X*., et al.* (2013). Shigella flexneri T3SS effector IpaH4.5 modulates the host inflammatory response via interaction with NF-kappaB p65 protein. *Cellular microbiology* **15,** 474-485.

Weake, V.M. and Workman, J.L. (2008). Histone ubiquitination: triggering gene activity. *Molecular cell* **29,** 653-663.

WHO. (2005) Guidelines for the control of shigellosis, including epidemics due to *Shigella dysenteriae I*. Geneva, Switzerland, World Health Organization.

Willingham, S.B., Bergstralh, D.T., O'Connor, W., Morrison, A.C., Taxman, D.J., Duncan, J.A.*, et al.* (2007). Microbial pathogen-induced necrotic cell death mediated by the inflammasome components CIAS1/cryopyrin/NLRP3 and ASC. *Cell host & microbe* **2,** 147-159.

Xia, Z.P., Sun, L., Chen, X., Pineda, G., Jiang, X., Adhikari, A.*, et al.* (2009). Direct activation of protein kinases by unanchored polyubiquitin chains. *Nature* **461,** 114-119.

Xu, P., Duong, D.M., Seyfried, N.T., Cheng, D., Xie, Y., Robert, J.*, et al.* (2009). Quantitative proteomics reveals the function of unconventional ubiquitin chains in proteasomal degradation. *Cell* **137,** 133-145.

Yang, B. and Kumar, S. (2010). Nedd4 and Nedd4-2: closely related ubiquitin-protein ligases with distinct physiological functions. *Cell death and differentiation* **17,** 68-77.

Yang, L., Hamilton, S.R., Sood, A., Kuwai, T., Ellis, L., Sanguino, A.*, et al.* (2008). The previously undescribed ZKSCAN3 (ZNF306) is a novel "driver" of colorectal cancer progression. *Cancer research* **68,** 4321-4330.

Yi, C.R., Allen, J.E., Russo, B., Lee, S.Y., Heindl, J.E., Baxt, L.A.*, et al.* (2014). Systematic Analysis of Bacterial Effector-Postsynaptic Density 95/Disc Large/Zonula Occludens-1 (PDZ) Domain Interactions Demonstrates Shigella OspE Protein Promotes Protein Kinase C Activation via PDLIM Proteins. *The Journal of biological chemistry* **289,** 30101-30113.

Yu, H.B., Croxen, M.A., Marchiando, A.M., Ferreira, R.B.R., Cadwell, K., Foster, L.J. and Finlay, B.B. (2014). Autophagy Facilitates Salmonella Replication in HeLa Cells. *mBio* **5,** e00865-14.

Yuk, J.M. and Jo, E.K. (2013). Crosstalk between autophagy and inflammasomes. *Molecules and cells* **36,** 393-399.

Zhang, Z., Jin, L., Champion, G., Seydel, K.B. and Stanley, S.L., Jr. (2001). Shigella infection in a SCID mouse-human intestinal xenograft model: role for neutrophils in containing bacterial dissemination in human intestine. *Infection and immunity* **69,** 3240-3247.

Zhao, Y., Yang, J., Shi, J., Gong, Y.N., Lu, Q., Xu, H.*, et al.* (2011). The NLRC4 inflammasome receptors for bacterial flagellin and type III secretion apparatus. *Nature* **477,** 596-600.

Zhu, Y., Li, H., Hu, L., Wang, J., Zhou, Y., Pang, Z.*, et al.* (2008). Structure of a Shigella effector reveals a new class of ubiquitin ligases. *Nature structural & molecular biology* **15,** 1302-1308.

Zurawski, D.V., Mitsuhata, C., Mumy, K.L., McCormick, B.A. and Maurelli, A.T. (2006). OspF and OspC1 are Shigella flexneri type III secretion system effectors that are required for postinvasion aspects of virulence. *Infection and immunity* **74,** 5964-5976.

Zurawski, D.V., Mumy, K.L., Faherty, C.S., McCormick, B.A. and Maurelli, A.T. (2009). Shigella flexneri type III secretion system effectors OspB and OspF target the nucleus to downregulate the host inflammatory response via interactions with retinoblastoma protein. *Molecular microbiology* **71,** 350-368.

Zychlinsky, A., Fitting, C., Cavaillon, J.M. and Sansonetti, P.J. (1994). Interleukin 1 is released by murine macrophages during apoptosis induced by Shigella flexneri. *The Journal of clinical investigation* **94,** 1328-1332.